

**CRC Project AV-20-14**

**DETERMINATION OF HEAT OF  
VAPORIZATION AND CREATING  
ENTHALPY DIAGRAMS FOR  
SEVERAL COMMON JET FUELS**

**Final Report**

**April 2019**



**COORDINATING RESEARCH COUNCIL, INC.**  
5755 NORTH POINT PARKWAY • SUITE 265 • ALPHARETTA, GA 30022

**The Coordinating Research Council, Inc. (CRC) is a non-profit corporation supported by the petroleum and automotive equipment industries. CRC operates through the committees made up of technical experts from industry and government who voluntarily participate. The four main areas of research within CRC are: air pollution (atmospheric and engineering studies); aviation fuels, lubricants, and equipment performance, heavy-duty vehicle fuels, lubricants, and equipment performance (e.g., diesel trucks); and light-duty vehicle fuels, lubricants, and equipment performance (e.g., passenger cars). CRC's function is to provide the mechanism for joint research conducted by the two industries that will help in determining the optimum combination of petroleum products and automotive equipment. CRC's work is limited to research that is mutually beneficial to the two industries involved. The final results of the research conducted by, or under the auspices of, CRC are available to the public.**

**CRC makes no warranty expressed or implied on the application of information contained in this report. In formulating and approving reports, the appropriate committee of the Coordinating Research Council, Inc. has not investigated or considered patents which may apply to the subject matter. Prospective users of the report are responsible for protecting themselves against liability for infringement of patents.**

**The University of Delaware (UDEL) makes no representations extends no warranties, express or implied, concerning the data provided in this report and any resulting information thereof.**

**Further, UDEL makes no representations, extends no warranties, and assumes no responsibilities that the testing method or the use of data in whole or in part will not infringe the claims of any patents or other third party rights.**

**UDEL and CRC are separate and independent entities, and neither is the agent of the other. The users of these data agree to indemnify UDEL and their personnel free and harmless from any and all loss, cost, damage, claim, action, or liability on account of the death of or injury to any person or persons or damage to or destruction of any property resulting from or growing out of any alleged negligence on the part of the user of these data.**

**Determination of Heat of Vaporization  
and Creating Enthalpy Diagrams for  
Several Common Jet Fuels**

**FINAL REPORT**

*Prepared for*  
**Coordinating Research Council, Inc.  
5755 North Point Parkway, Ste. 265  
Alpharetta, GA 30022**

*Prepared by*  
**Steve Sauerbrunn  
Scientist  
University of Delaware  
Center for Composite Materials  
Newark, Delaware**

CRC Project No. AV-20-14

**April 2019**

This page intentionally left blank  
for back-to-back printing

## Executive Summary

This is the Final Report for Project CRC-AV-20-14 “Determination of Heat of Vaporization and Creating Enthalpy Diagrams for Several Common Jet Fuels”. Heat of vaporization (HOV) is not provided for Jet A or Jet A-1 in Figure 2-19 in the current CRC Aviation Fuel Properties Handbook (the Handbook) [1]. There are no Enthalpy Diagrams for these two commercial fuels which are the main-stay of Civil Aviation. This is because the original data were generated in an era when military fuels were the focus of the Council. Enthalpy diagrams are used for determining the state of the fuel in the design of fuel systems for, and performance of, gas turbine augments or afterburner designs and their operability calculations, and in design and performance considerations of fuel systems where fuel will be used as a heat transfer medium. Different types of fuel injectors in engine main combustors and auxiliary power sources generate many different spray droplet sizes and in several different environments, and these design curves help to determine vapor generation for ignition analysis. These curves provide a source of information when trying to understand what has happened in an aircraft accident and aftermath or a fuel spill and fire investigation. HOV is also used in the study of events where fuel vapor production is an important part of an analysis preceding fire initiation, such as in an observed tailpipe fire.

The high-pressure differential scanning calorimeter (HPDSC) is very well suited to the measurement of heat of vaporization (HOV) of these fuels at atmospheric pressure and the production of enthalpy curves, at various pressures, used for the construction of master enthalpy diagrams. This report includes the HOV values for: Jet A, Jet A-1, JP-5, JP-8, JP-TS, FT-SPK, TS-1 and JP-4, as well as a few biojet fuels and blended jet fuels. This report also includes the Enthalpy Diagrams for: JP-8, JP-5, Jet A, JP-8, TS-1 and JP-4.

<b>Table of Contents</b>	<b>Page</b>
1. List of Acronyms and Abbreviations .....	11
2. Background .....	11
3. Scope .....	13
4. Experimental	
4.1. Materials .....	14
4.2. Instrumental .....	14
4.3. Temperature calibration .....	15
4.4. Enthalpy Calibration .....	15
5. HOV Testing	
5.1. Sample Preparation for HOV Testing .....	16
5.2. HOV Testing Method .....	16
5.3. HOV Data Evaluation Procedure .....	16
5.4. Summary of HOV Results .....	18
5.5. Standard Deviation – HOV Results .....	31
6. HOV Quasi-Isothermal (QI) Testing	
6.1. Instrumental .....	33
6.2. Sample Preparation for HOV QI Testing .....	33
6.3. HOV QI Testing Method .....	35
7. HOV Quasi-Isothermal Diagrams	
7.1. QI HOV Data .....	35
7.2. HOV QI Diagram Results .....	37
8. Enthalpy Diagrams	
8.1. Background on Enthalpy Diagrams .....	40
8.2. Sample Preparation for Enthalpy Testing .....	40
8.3. Enthalpy Testing Method .....	40
8.4. Integration of Heat Flow Data .....	41
8.5 Construction of an Enthalpy Diagram .....	43
8.6 Enthalpy Diagram Results .....	49
8.7 How to use Enthalpy Diagrams .....	54
9. Conclusions	
9.1 HOV Conclusions .....	58
9.2 HOV Quasi-Isothermal Conclusions .....	58
9.3 Enthalpy Diagram Conclusions .....	58

## Table of Contents (cont'd)

	Page
10. References .....	59
Appendix A: Enthalpy of Liquid Volumetric Change .....	60
Appendix B: Jet Fuel Enthalpy Equations .....	61
Appendix C: HPDSC Instrumental Details .....	63

## List of Figures

	Page
Figure 1: Enthalpy Diagram for JP-5 .....	13
Figure 2: Example of HOV analysis .....	17
Figure 3: HOV analysis of Jet A, Shell, USA (JF#1) .....	19
Figure 4: HOV analysis of Jet A-1, Shell Netherlands (JF#2) .....	19
Figure 5: HOV analysis of Jet A-1, Dansk Shell, Denmark (JF#3) .....	20
Figure 6: HOV analysis of Jet A-1, T309, Shell, Germany (JF#4) .....	20
Figure 7: HOV analysis of Jet A-1, Q92283, Shell, Germany (JF#5) .....	21
Figure 8: HOV analysis of Biojet, GEVO ATJ, WPAFB, USA (JF#6) .....	21
Figure 9: HOV analysis of Biojet, Test Fld, WPAFB, USA (JF#7) .....	22
Figure 10: HOV analysis of Jet A, WPAFB, USA (JF#8) .....	22
Figure 11: HOV analysis of JP-5, WPAFB, USA (JF#9) .....	23
Figure 12: HOV analysis of JP-8, WPAFB, USA (JF#10) .....	23
Figure 13: HOV analysis of JP-TS, Blend, WPAFB, USA (JF#11) .....	24
Figure 14: HOV analysis of Test Fld, WPAFB, USA (JF#12) .....	24
Figure 15: HOV analysis of HEFA/JP-8, Blend, WPAFB, USA (JF#13) .....	25
Figure 16: HOV analysis of Jet A-1, synthetic, Sasol, S Africa (JF#14) .....	25
Figure 17: HOV analysis of Jet A-1, semi-synthetic, Sasol, S Africa (JF#15) .....	26
Figure 18: HOV analysis of FT-SPK, Sasol, S Africa (JF#18) .....	26
Figure 19: HOV analysis of TS-1, Air BP, UK (JF#17) .....	27
Figure 20: HOV analysis of JP-4 (W), Nova Research, USA, VA (JF#18) .....	27
Figure 21: HOV analysis of Jet A-1, Total, France (JF#19) .....	28
Figure 22: HOV analysis of Jet A-1, hydro-treated, Total, France (JF#20) .....	28
Figure 23: HOV analysis of Jet A-1, meroxed, Total, France (JF#21) .....	29
Figure 24: HOV analysis of JP-4, Nova Research, Chevron, USA (JF#22) .....	29
Figure 25: HOV analysis of JP-5, AVCAT, RNAS Culdrose, UK (JF#23) .....	30
Figure 26: HOV analysis of Jet A-1, with MIL add., Emo-Trans, Germany (JF#24) .....	30
Figure 27: HOV of various hydrocarbons CRC Handbook, Figure 2-19 .....	32
Figure 28: Enthalpy versus QI temperature .....	34
Figure 29: Temperature versus time for a HOV QI HPDSC experiment .....	34
Figure 30: Integration of the vaporization of a JF during the QI HPDSC experiment .....	35
Figure 31: Jet A HOV from a QI HPDSC experiment .....	37
Figure 32: JP-5 HOV from a QI HPDSC experiment .....	38
Figure 33: JP-8 HOV from a QI HPDSC experiment .....	38
Figure 34: TS-1 HOV from a QI HPDSC experiment .....	39
Figure 35: JP-4 HOV from a QI HPDSC experiment .....	39
Figure 36: HPDSC raw data for JP-8 (JF#10) at 1 atm N <sub>2</sub> pressure .....	42

## List of Figures (cont'd)

	Page
Figure 37: Heatflow integral (enthalpy) for JP-8 (JF#10) at 1 atm N <sub>2</sub> pressure.....	42
Figure 38: HPDSC raw data for JP-4 (JF#22) at two atm pressure without purging .....	43
Figure 39: Raw enthalpy curves for JP-8 (JF#10) .....	43
Figure 40: “Mix to Gas” curve, green line, for JP-8 (JF#10) .....	44
Figure 41: JP-8 0.1 atm with no corrections .....	45
Figure 42: JP-8 0.1 atm matching curvature at low temperatures .....	45
Figure 43: JP-8 0.1 atm matching with the 68 atm and ‘Mix to Gas’ lines .....	46
Figure 44: Final enthalpy diagram for JP-8 (JF#10) .....	47
Figure 45: Comparison of the literature enthalpy diagrams for JP-5 .....	48
Figure 46: Enthalpy diagram for jet fuel JP-5 (WPAFB, OH, USA) .....	49
Figure 47: Enthalpy diagram for jet fuel Jet A (WPAFB, OH, USA) .....	50
Figure 48: Enthalpy diagram for jet fuel JP-8 (WPAFB, OH, USA) .....	51
Figure 49: Enthalpy diagram for jet fuel TS-1 (GOST, AirBP, Kent, UK) .....	52
Figure 50: Enthalpy diagram for jet fuel JP-4 (Nova Research, VA, USA) .....	53
Figure 51: Jet A enthalpy at 25 °C is 20 J/g .....	54
Figure 52: Jet A enthalpy at 350 °C is 815 J/g .....	55
Figure 53: Jet A enthalpy at 25 °C is 20 J/g .....	56
Figure 54: Enthalpy of Jet A at 25 °C and 30 psi .....	56
Figure 55: Enthalpy of Jet A at 275 °C and 30 psi .....	57
Figure C1: DSC pan resting on the crimping press lower die .....	63
Figure C2: Micropipette and JF sample .....	63
Figure C3: Micropipette in JF sample .....	64
Figure C4: Micropipette depositing JF sample in DSC pan .....	64
Figure C5: Microscope image of the 50 um laser-drilled hole in the DSC lid .....	65
Figure C6: Laser-drilled lid placed on DSC pan .....	65
Figure C7: DSC pan/lid being pressed in the crimper .....	66
Figure C8: DSC pan/lid after crimping .....	66
Figure C9: Inside of the HPDSC cell, with an empty reference .....	67
Figure C10: Inside of the HPDSC cell, with a JF sample .....	67
Figure C11: Inside of the HPDSC cell, with the inner silver lid installed .....	68
Figure C12: Inside of the HPDSC cell, with the outer silver lid installed .....	68
Figure C13: HPDSC cell, with the water cooled SS lid, photo .....	69
Figure C14: HPDSC cell, ready to run .....	69
Figure C15: Complete HPDSC instrument setup, photo .....	70
Figure C16: QI HPDSC instrument setup, diagram .....	70
Figure C17: QI HPDSC instrument setup, photo .....	71
Figure C18: Typical pressure versus time for a HOV QI HPDSC experiment .....	71

## List of Tables

Table 1:	Sources of Jet Fuels .....	14
Table 2:	Temperature Standards .....	15
Table 3:	Enthalpy Standards .....	15
Table 4:	HOV and Peak Temperature at 1 atm .....	18
Table 5:	Jet A-1 HOV Average and Std. Devi. ....	31
Table 6:	Jet A (JF#8) .....	35
Table 7:	JP-5 (JF#9) .....	36
Table 8:	JP-8 (JF#10) .....	36
Table 9:	TS-1 (JF#17) .....	36
Table 10:	JP-4 (JF#22) .....	37
Table 11:	Critical Temperature of Selected Jet Fuels .....	58
Table A1:	Density of n-Octane and Enthalpy of JP-4 .....	60
Table B1:	Jet-A Enthalpy Curve Equations .....	61
Table B2:	JP-5 Enthalpy Curve Equations .....	61
Table B3:	JP-8 Enthalpy Curve Equations .....	61
Table B4:	TS-1 Enthalpy Curve Equations .....	62
Table B5:	JP4 Enthalpy Curve Equations .....	62

This page intentionally left blank  
for back-to-back printing

## 1. List of Acronyms and Abbreviations

**HPDSC** is a high-pressure differential scanning calorimeter. This instrument measures heat flow during evaporation of a sample at different pressures.

**HOV** or  $\Delta H_{\text{vap}}$  is the heat of vaporization. It is the same as the heat of evaporation. This is the heat (energy) associated with the transition from a liquid to a gas, at a fixed temperature. The Heat of Vaporization is also called the Latent Heat of Vaporization or the Enthalpy of Vaporization. HOV can be expressed in units of J/mol or J/g.

**J/mol** is Joules per mole, the units typically reported for the HOV of a pure substance.

**J/g** is Joules per gram, the units typically reported for the HOV of a mixture.

**PSI** is pressure in pounds per square inch and is relative to absolute vacuum.

**PSIG** is pressure in “pounds per square inch gauge” and is relative to atmospheric pressure.

**T/C** is a thermocouple.

**Quasi-Isothermal (QI) DSC** is a DSC test where the sample is not exactly isothermal and the sample temperature will be changing by a small heating rate, typically less than 0.1 °C/min.

**Critical Point** is the temperature and pressure, above which, the sample is a critical fluid, which has the properties of a gas and a liquid, with no distinction between the two. A sample that is above the critical point in both temperature and pressure does not have a heat of vaporization.

**Critical Temperature ( $T_c$ )** is the temperature where the sample is a critical fluid, which has the properties of a gas and a liquid, with no distinction between the two.

**Critical Pressure ( $P_c$ )** is the pressure where the sample is a critical fluid, which has the properties of a gas and a liquid, with no distinction between the two.

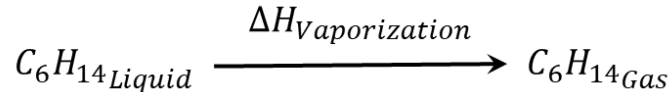
## 2. Background

The Coordinating Research Council (CRC) has sponsored this testing for the “Determination of Heat of Vaporization and Creating Enthalpy Diagram for Several Common Jet Fuels” (CRC Project No. AV-20-14). Enthalpy charts are used for determining the state of the fuel in the design of fuel systems for, and performance of, gas turbine augments or afterburner designs and their operability calculations, and in design and performance considerations of fuel systems where fuel will be used as a heat transfer medium. Different types of fuel injectors in engine main combustors and auxiliary power sources generate many different spray droplet sizes and in several different environments, and these design curves help to determine vapor

generation for ignition analysis. These curves provide a source of information when trying to understand what has happened in an aircraft accident and aftermath or a fuel spill and fire investigation. Heat of Vaporization is also used in the study of events where fuel vapor production is an important part of an analysis preceding fire initiation, such as in an observed tailpipe fire.

### Heat of Vaporization

The heat of vaporization (HOV, also symbolized as  $\Delta H_{\text{vap}}$ ) is the energy that is needed to completely convert a given quantity of a substance from a liquid to a gaseous state at a given temperature and pressure, usually measured at atmospheric pressure. For simple substances (pure chemicals), the HOV can be calculated from the Clausius-Clapeyron equation [2, 3] by measuring the boiling point of a pure substance at several different pressures, or the vapor pressure at several different temperatures. The approach (e.g., used in ASTM E2071 [4]) gives the HOV for the substance in J/mol. Heat of vaporization is the amount of heat required to make a physical change from the liquid phase to the gas phase, shown in the equation below, n-hexane is shown as an example.



Heat of vaporization of liquids has been done by several estimation techniques, most notable being the Clausius-Clapeyron equation,

$$\ln\left(\frac{P}{P_0}\right) = -\frac{\Delta H_{\text{vap}}}{RT} + C$$

Where R = gas constant

T = temperature (K)

C = a constant

P = measured pressure

P<sub>0</sub> = reference pressure

The ASTM standard E2071 [4] uses this technique with a high-pressure DSC. The technique is limited to liquids that boil within a narrow temperature range, usually pure compounds. This technique is an estimation of the heat of vaporization because they all assume an ideal gas behavior, which is the basic assumption of the Clausius-Clapeyron equation.

Engineers that design turbine engines need the HOV in units of energy per mass, such as J/g, in order to improve the fuel efficiency of new engine designs. The HOV of multicomponent, volatile blends, such as jet fuels, must be measured directly and cannot be measured using the Clausius-Clapeyron equation.

The HOV, in J/g, is easily measured with a DSC using aluminum crucibles with a laser drilled 50 um orifice. This technique has been used for many years [5, 6 and 7] to determine the boiling point and HOV of pure liquids. It may also be used to measure these properties of organic mixtures, such as jet fuels.

The heatflow (W/g) measured through the vaporization process can also be integrated to give a single average HOV value for the entire jet fuel blend.

### 3. Scope

The scope of the project is to provide HOV for Jet A and Jet A-1 for the requisite curve, and replicate Figure 2-18 of the Handbook for Jet A and Jet A-1 fuel (see Figure 1 below) [1]. This effort is to provide HOV data for several jet fuels and the enthalpy diagram (and data) for a subset of jet fuels.

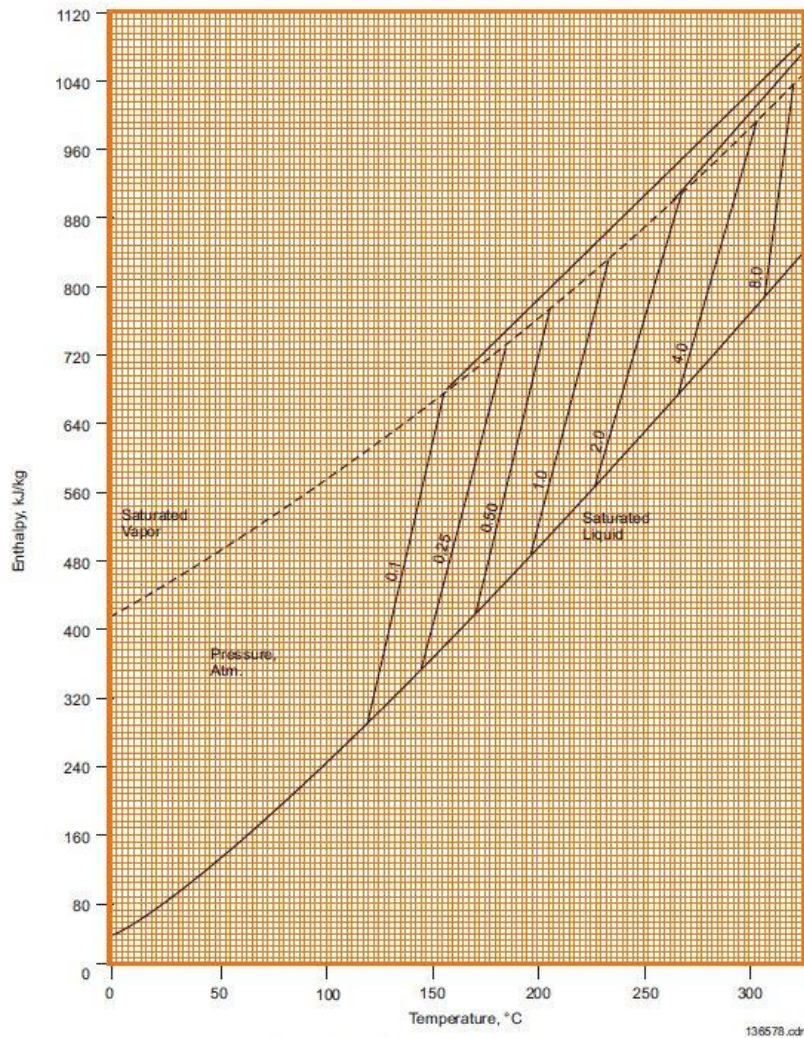


Figure 2-18. Enthalpy Diagram – JP-5

Figure 1: Enthalpy Diagram for JP-5

## 4. Experimental

### 4.1. Materials

Jet fuels were provided by a variety of sources, details are given in Table 1.

**Table 1: Sources of Jet Fuels**

JF#	Type	Marking on container	Company	Country	State	City	Manufacturer
1	Jet A	Jet A	Shell	USA	CA	Martinez	Shell
2	Jet A-1	Jet A-1	Shell	Netherlands		Rotterdam	Shell
3	Jet A-1	Jet A-1	A/S Dansk Shell	Denmark		Fredericia	A/S Dansk Shell
4	Jet A-1	T309 Jet Fuel Nord	Shell	Germany		Koln	Shell
5	Jet A-1	Q92283 Jet Fuel S <sup>d</sup>	Shell	Germany		Koln	Shell
6	GEVO ATJ	11498 Biojet fuel	WPAFB	USA	OH	WPAFB	Gevo
7	Test Fld.	12345 Biojet Fuel, Component Derived, Flat distillation	WPAFB	USA	OH	WPAFB	AFRL/RQTF
8	Jet A	10325 Jet Fuel A	WPAFB	USA	OH	WPAFB	Shell
9	JP-5	10289 Fuel, JP-5	WPAFB	USA	OH	WPAFB	Valero
10	JP-8	10264 Fuel, JP-8	WPAFB	USA	OH	WPAFB	NuStar
11	JP-TS	4527 Fuel, JPTS	WPAFB	USA	OH	WPAFB	Ashland
12	Test Fld.	12223 Fuel, 84/16C14 blend, (C9 + C14 blend), Asymmetric	WPAFB	USA	OH	WPAFB	AFRL/RQTF
13	HEFA/JP-8	12711 HRJ Blend, (50/50 Blend)	WPAFB	USA	OH	WPAFB	AFRL/RQTF
14	Jet A-1	F-T Fully Synthetic	Sasol	S Africa		Sasolburg	Sasol
15	Jet A-1	Semi-Synthetic 48%FT-SPK + 52% Jet A-1	Sasol	S Africa		Sasolburg	Sasol
16	FT-SPK	FT-SPK, Neat Blend Mat'l.	Sasol	S Africa		Sasolburg	Sasol
17	TS-1	IE.Rax, GOST 10227-86 Grade TS-1	Air BP	UK		Kent	Air BP
18	JP-4 (W)	NRL, Patuxent, no Liner in Cap	Nova Research	USA	VA	Alexandria	Chevron USA
19	Jet A-1	Jet A-1 "408-6595 JET straight run"	Total	France		Harfleur	Total
20	Jet A-1	Hydro-treated Jet A-1 "408-65 86"	Total	France		Harfleur	Total
21	Jet A-1	Meroxed Jet A-1 "D111-U32"	Total	France		Harfleur	Total
22	JP-4	JP-4, NRL Patuxent, DLA Alaska	Nova Research	USA	VA	Alexandria	Chevron USA
23	JP-5	AVCAT F-44, MoD Sample	RNAS Culdrose	UK		Helston	
24	Jet A-1 (JF-8)	with MIL additives	Emo-Trans GmbH	Germany		Moerfelden-Walld	BP Australia

Note: The jet fuels were given a unique number "JF#NN", where NN is the sequence of the arrival of the jet fuel to the testing lab.

### 4.2. Instrumental

The NETZSCH HPDSC (model DSC 204 HP) was used for this testing. The HPDSC was also connected to a refrigerated water recirculating temperature controller (Julabo F25) and controlled at 1 °C. The HPDSC was operated under vacuum (Welch model 2014B-01 PTFE diaphragm vacuum pump) for some experiments. The vacuum was measured using a gauge (WIKA PN 20/2556722/1/2) with a range from 0 to -30 inHg with 0.5 inHg divisions. The high-pressure was measured with a 0 to 200 psig pressure gauge (Cecomp Electronics PN F16B200psig-NC). The pressure of the 68 atm (1000 psig) tests for the enthalpy diagrams was measured using the gauge built into the HPDSC. Pictures of the entire HPDSC setup is shown in Figures C15 and C16 in Appendix C. Aluminum crucibles (NETZSCH PN 6.239.2-64.5.01) were used for all experiments. Solid aluminum lids (NETZSCH PN 66.239.2-64.5.02) were used for the 68 atm test for the enthalpy diagrams. Otherwise, laser drilled (50 μm) aluminum lids (NETZSCH PN 6.239.2-54.801) were used. The jet fuel samples received were pipetted into a glass vials with PTFE lined caps (supplier: Discount Vials, PN: CT151760144-C-TEF-N) for more convenient storage. Positive displacement 5 to 10 μL capillary pipets (supplier: Drummond Scientific Company, PN: 5-000-2010) were used to pipet the jet fuel from the storage vial into the DSC crucibles.

### 4.3. Temperature Calibration

The HPDSC calibration materials were supplied by NETZSCH (PN 6.239.2-91.3). All five standards were used to calibrate temperature, per ASTM E967, at each pressure used in this testing. The calibration correction was derived from a straight-line best fit to the corrections for each of the standards. The pressure changes the thermal conductivity between the sample and the DSC sensor. Lower pressure decreases the thermal conductivity and moves the onset of melting to higher temperatures.

**Table 2: Temperature Standards**

<b>Sample</b>	<b>Mass, mg</b>	<b>Melting point, °C</b>
Indium	11.97	156.6
Tin	15.43	231.9
Bismuth	14.94	271.4
Zinc	12.76	419.5
Cesium Chloride	12.31	476.6

### 4.4. Enthalpy Calibration

The DSC was calibrated in order to generate accurate enthalpy results. The DSC enthalpy is calibrated, per ASTM E968, using the known melting point enthalpy of several standards. The HPDSC calibration materials were supplied by NETZSCH (PN 6.239.2-91.3). All five standards were used to calibrate each pressure used in this testing. The enthalpy correction was derived from a straight-line best fit to the corrections for each of the standards. The pressure changes the thermal conductivity between the sample and the DSC sensor. Lower pressures decrease the thermal conductivity and the observed enthalpy of melting and vaporization.

**Table 3: Enthalpy Standards**

<b>Sample</b>	<b>Mass, mg</b>	<b>Enthalpy, J/g</b>
Indium	11.97	28.6
Tin	15.43	60.5
Bismuth	14.94	53.1
Zinc	12.76	107.5
Cesium Chloride	12.31	47.91

## 5. HOV Testing

### 5.1. Sample Preparation for HOV Testing

The crucible and lid were tared on the five-place balance (METTLER TOLEDO model XP205DR). The liquid sample (about 7 to 10  $\mu\text{L}$ ) was pipetted into the aluminum crucible with a 5 to 10  $\mu\text{L}$  capillary pipet. Laser drilled (50  $\mu\text{m}$ ) aluminum lids (NETZSCH PN 6.239.2-54.801) were used and cold welded to the crucible using the NETZSCH crimping press. The sample in the sealed crucible was weighed again until constant mass was achieved. This mass was recorded as the sample mass for the test. Photographs of the sample preparation are in Appendix C.

### 5.2. HOV Testing Method

The HPDSC was cooled using tap water running through the lid of the high-pressure chamber. The sample was placed in the HPDSC as quickly as possible after weighing. The pressure lid was fastened down. The HPDSC cell was filled with nitrogen gas to 50 psi and emptied three times. There was no gas flow through the HPDSC, so the sample was run in static nitrogen. The HPDSC cell was stabilized at 35  $^{\circ}\text{C}$  then heated at 5  $^{\circ}\text{C}/\text{min}$  to 400  $^{\circ}\text{C}$ . Except for JP-4 (JF #22), which was too volatile to begin the test at 35  $^{\circ}\text{C}$ . In this case, the water chiller was used and set to 1  $^{\circ}\text{C}$ . The test was started when the HPDSC cell stabilized at 15  $^{\circ}\text{C}$ .

### 5.3. HOV Data Evaluation Procedure

Region A in Figure 2 shows the endothermic shift in the baseline away from 0 mW/mg. This is due to the heat capacity of the liquid fuel. The region C is after all of the fuel has vaporized, so the baseline is close to 0 mW/mg. Since the fuel has completely vaporized in region C, there is no sample mass and therefore no heat capacity and the heatflow returns to zero. When integrating the area of the HOV peak, one needs to select a baseline type that will simulate the heat capacity of the sample as it is evaporating. The DSC does not measure the mass of the fuel during the experiment, so the baseline is simulated using a mathematically generated sigmoidal curve that follows the integral of the endotherm. This baseline technique is commonly used by all DSC manufacturers.

The vaporization (HOV) endotherm, negative peak shown in Figure 2, was integrated from about 60  $^{\circ}\text{C}$  to about 280  $^{\circ}\text{C}$  using a horizontal sigmoidal baseline. This baseline starts, region A, and stops, region C, with a horizontal slope. The sigmoid baseline, region B, follows the shape of an integral of the heatflow curve. The start and stop region of the baseline were chosen to be flat and nearly zero slope. The peak was analyzed as the lowest point on the heatflow scale. If there were two peaks, then the largest peak was analyzed. The shoulder peak was also analyzed and reported.

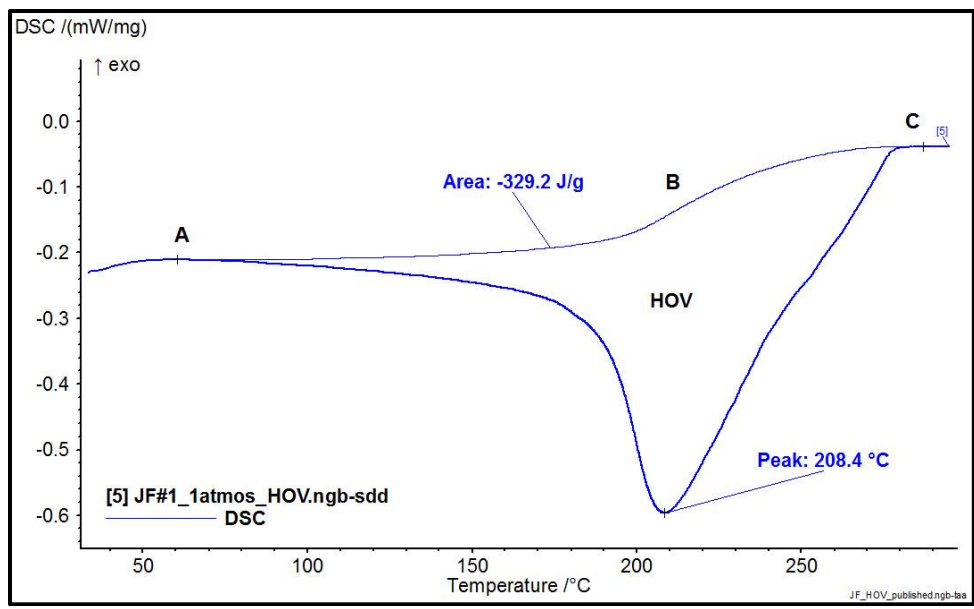


Figure 2: Example of HOV analysis

## 5.4. Summary of HOV Results

Table 4 is a summary of the HOV and the peak temperature for all the samples tested for HOV. JF#12 and JP-4 (JF#18) each had two HOV peaks. The HOV for GEVO ATJ (JF#6) was too small for a proper fit of the sigmoidal baseline. So the curve was analyzed using the tangential baseline. The tangential baseline will give the same results as the sigmoidal baseline provided the start and stop regions have a zero slope. This was the case for GEVO ATJ (JF#6).

**Table 4: HOV and Peak Temperature at One (1) Atm**

JF #	Type	HOV ( J/g )	Peak ( °C )	Comments
1	Jet A	329.2	208.4	
2	Jet A-1	302.3	182.7	
3	Jet A-1	314.5	190.1	
4	Jet A-1	313.8	184.2	
5	Jet A-1	311.8	185.7	
6	GEVO ATJ	179.4	192.2	Tangential base
7	Test Fld.	393.6	171.1	
8	Jet A	301.2	202.1	
9	JP-5	294.5	218.6	
10	JP-8	266.9	185.7	
11	JP-TS	302.2	185.6	
12	Test Fld.	288.1	239.5	2 peaks, 209.6 °C
13	HEFA/JP-8	292.8	203.8	
14	Jet A-1	302.3	194.9	
15	Jet A-1	298.1	190.2	
16	FT-SPK	264.9	185.1	
17	TS-1	268.2	181.6	
18	JP-4 (W)	315.0	159.1	2 peaks, 201.5 °C
19	Jet A-1	294.8	190.2	
20	Jet A-1	310.6	193.6	
21	Jet A-1	302.6	192.3	
22	JP-4	309.7	118.6	
23	JP-5	291.3	216.9	
24	Jet A-1 (JF-8)	291.2	193.1	

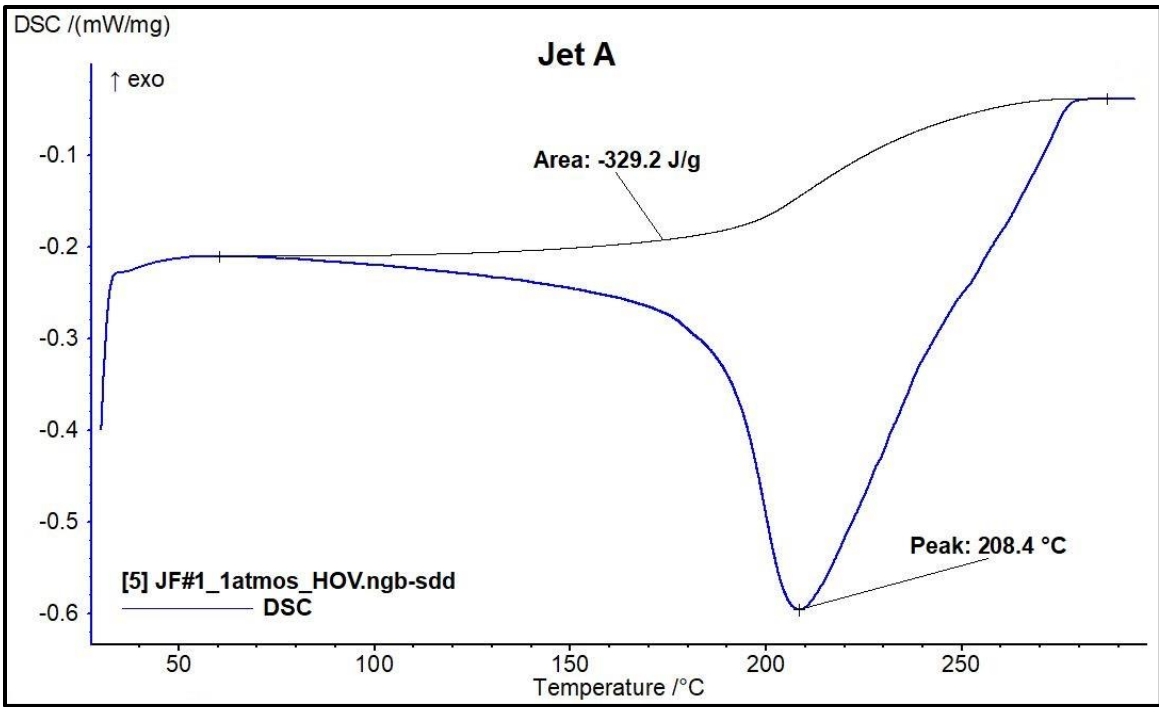


Figure 3: HOV analysis of Jet A, Shell, USA (JF#1).

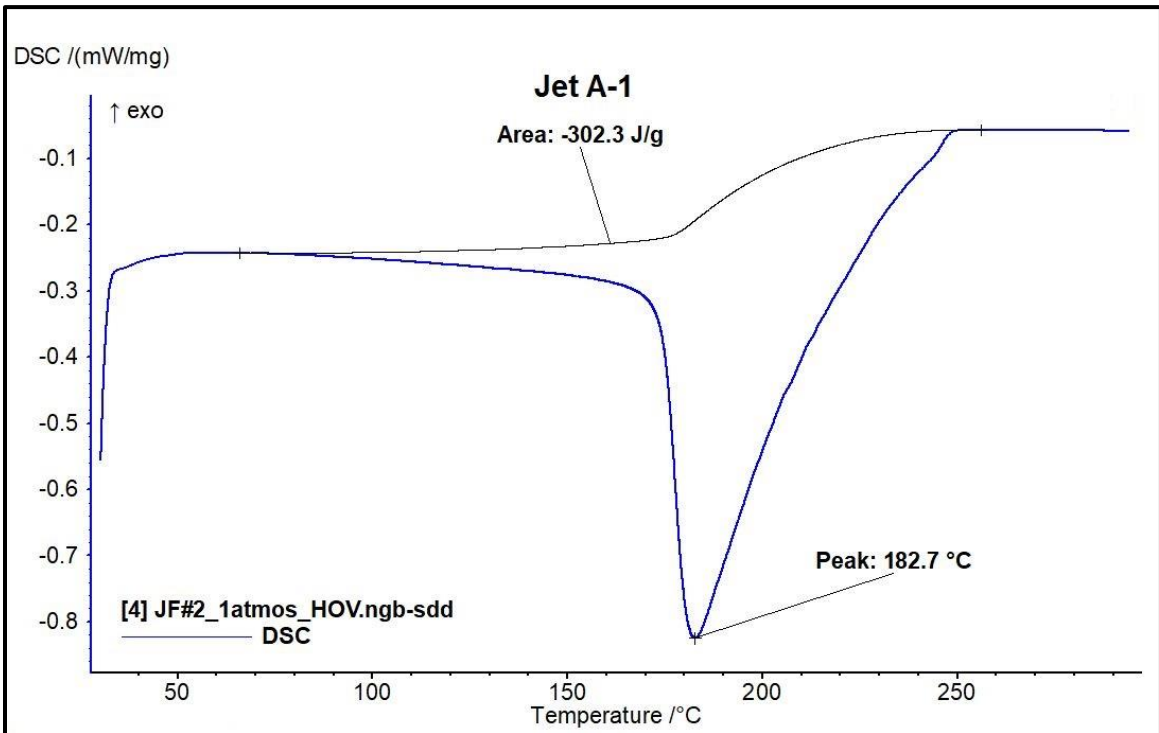


Figure 4: HOV analysis of Jet A-1, Shell Netherlands (JF#2).

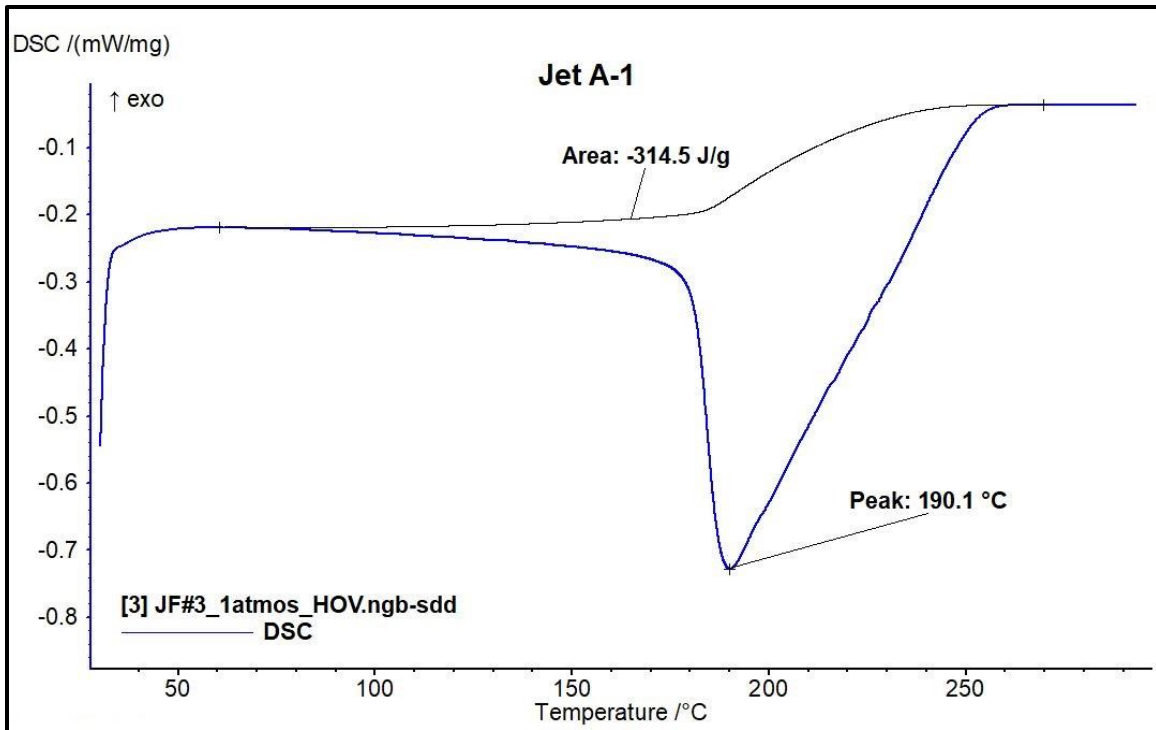


Figure 5: HOV analysis of Jet A-1, Dansk Shell, Denmark (JF#3).

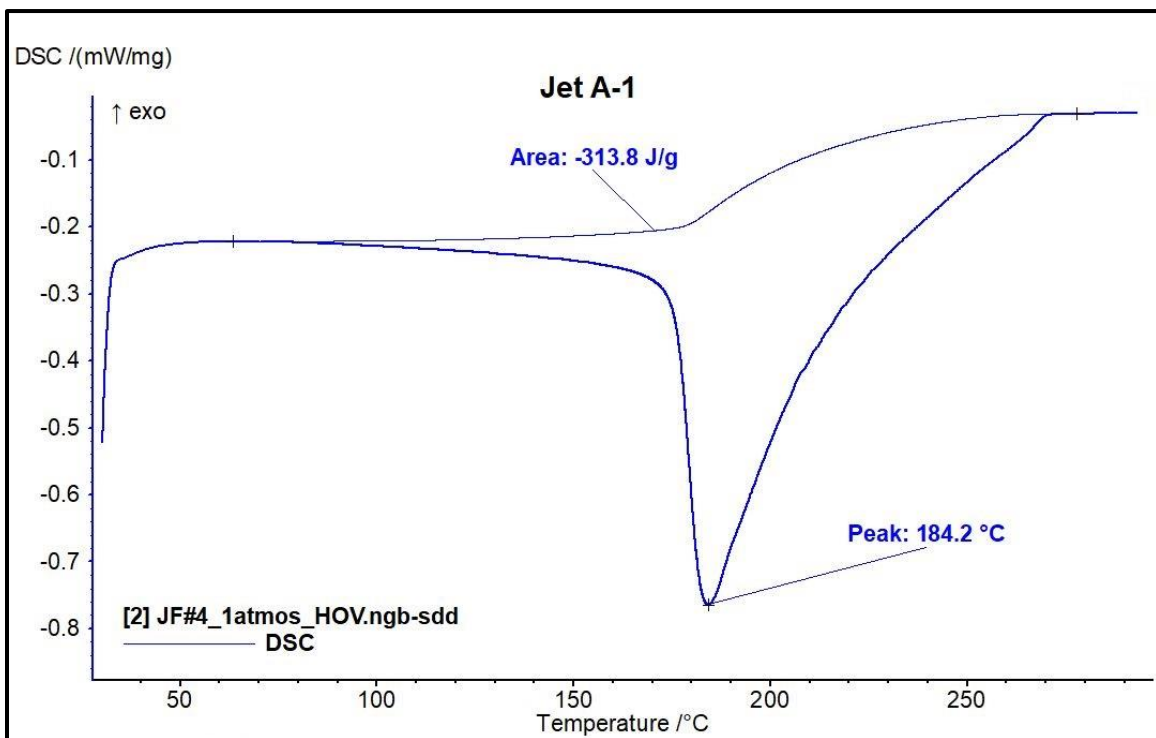


Figure 6: HOV analysis of Jet A-1, T309, Shell, Germany (JF#4).

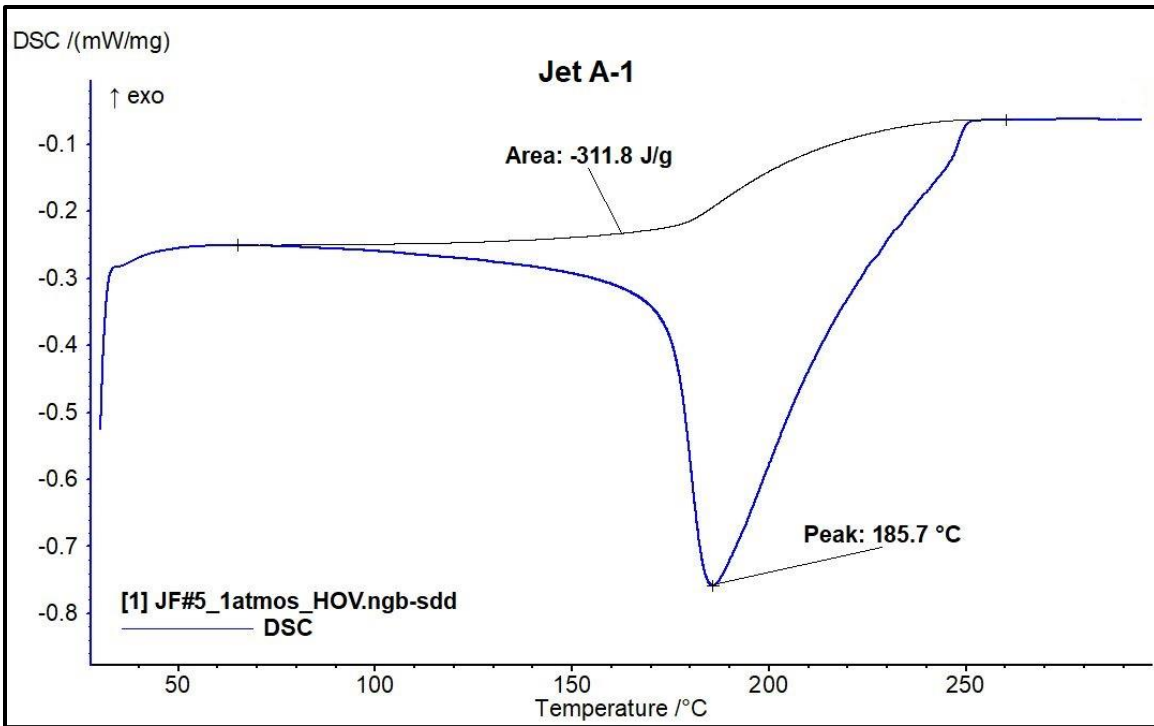


Figure 7: HOV analysis of Jet A-1, Q92283, Shell, Germany (JF#5).

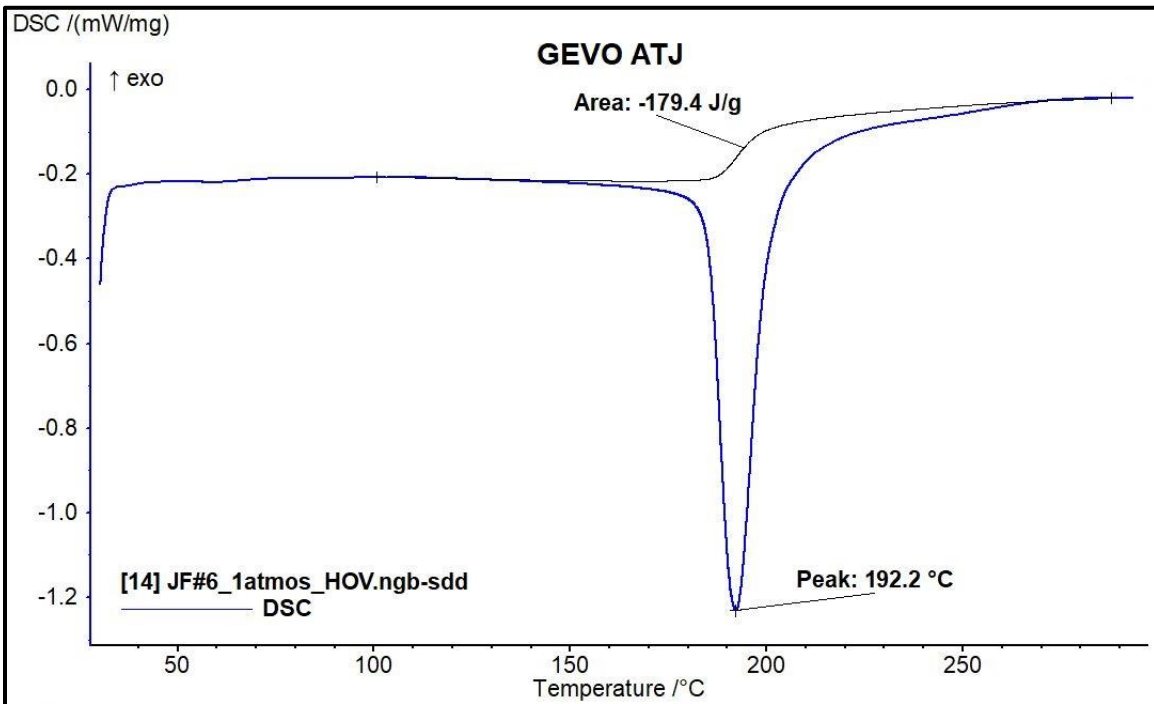


Figure 8: HOV analysis of Biojet, GEVO ATJ, WPAFB, USA (JF#6).

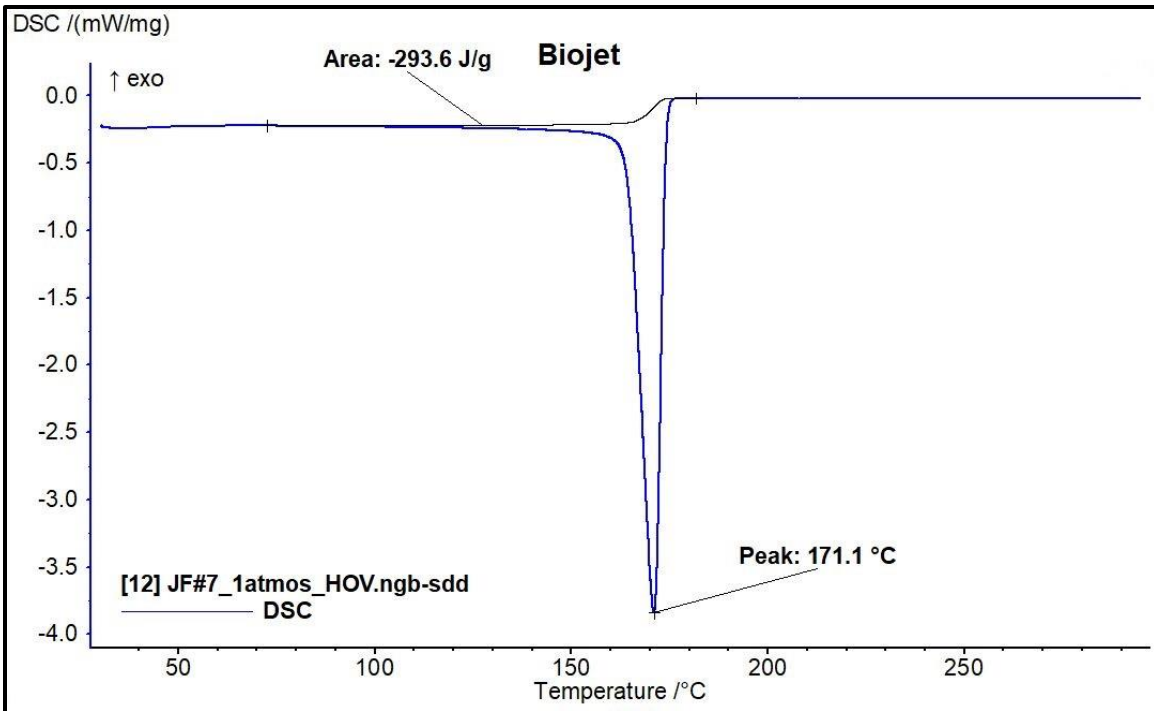


Figure 9: HOV analysis of Biojet, Test Fld, WPAFB, USA (JF#7).

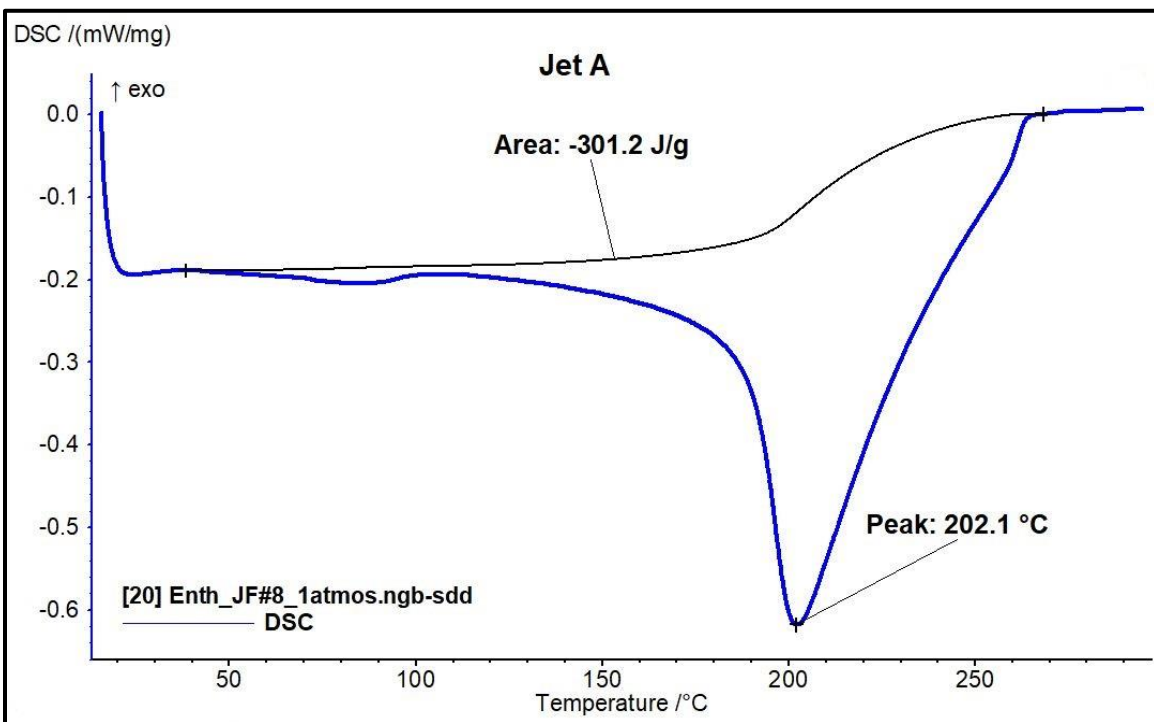


Figure 10: HOV analysis of Jet A, WPAFB, USA (JF#8).

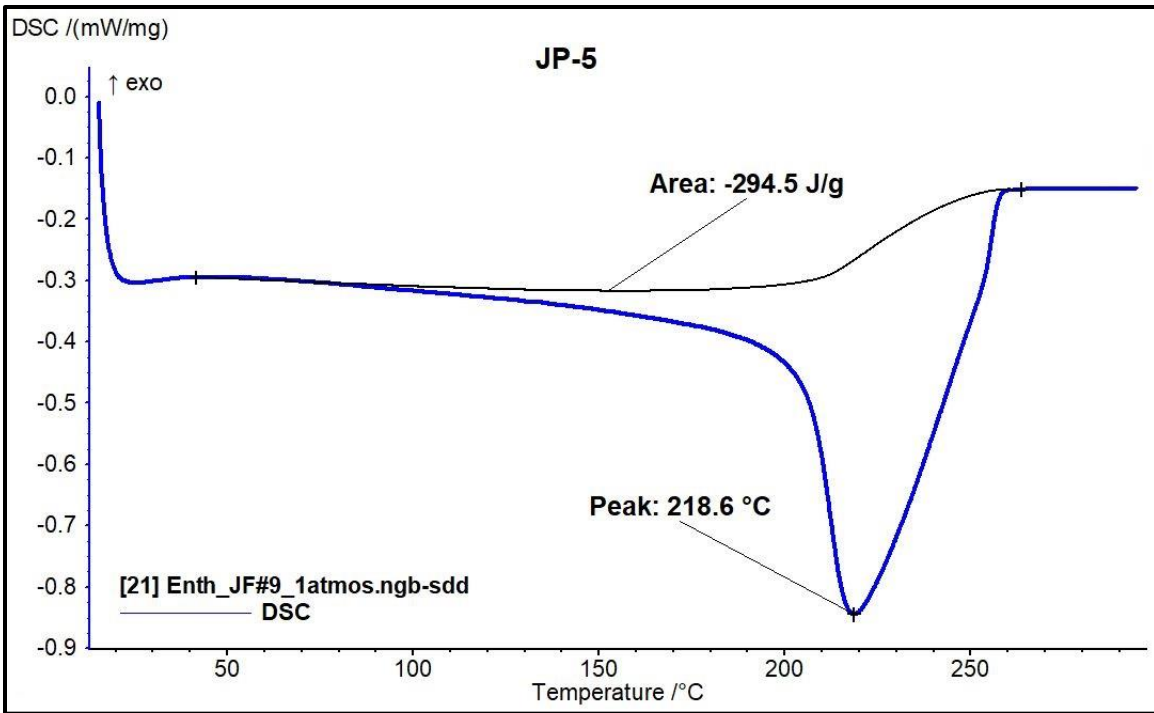


Figure 11: HOV analysis of JP-5, WPAFB, USA (JF#9).

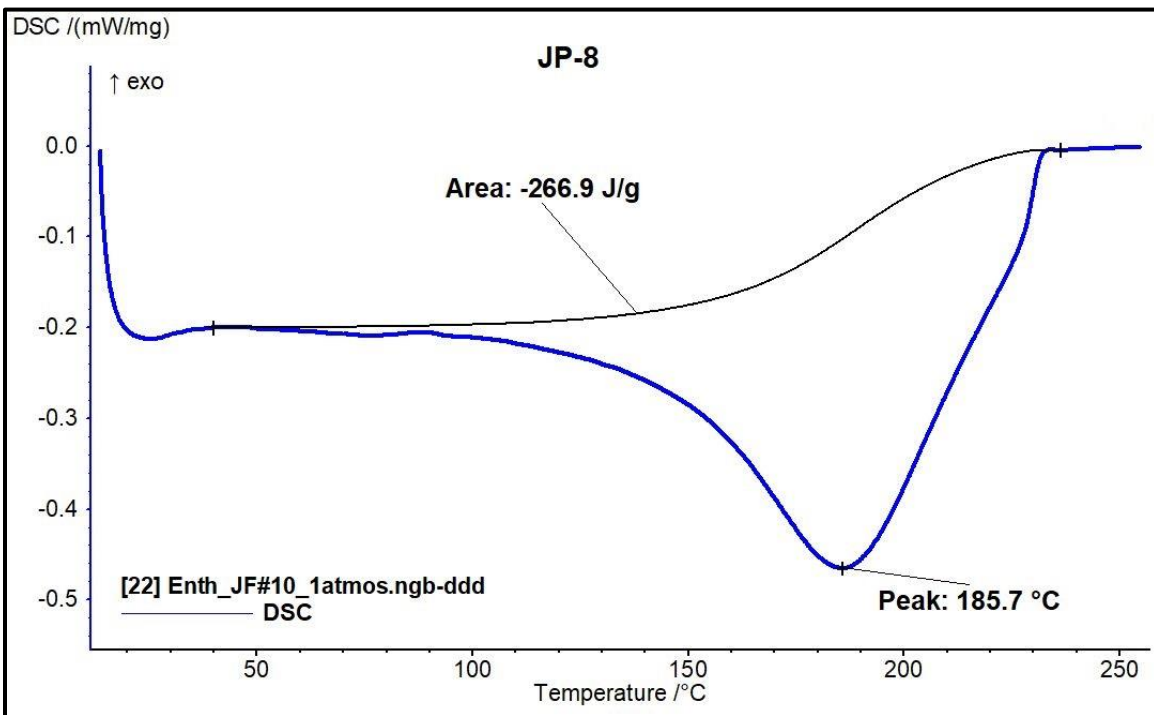


Figure 12: HOV analysis of JP-8, WPAFB, USA (JF#10).

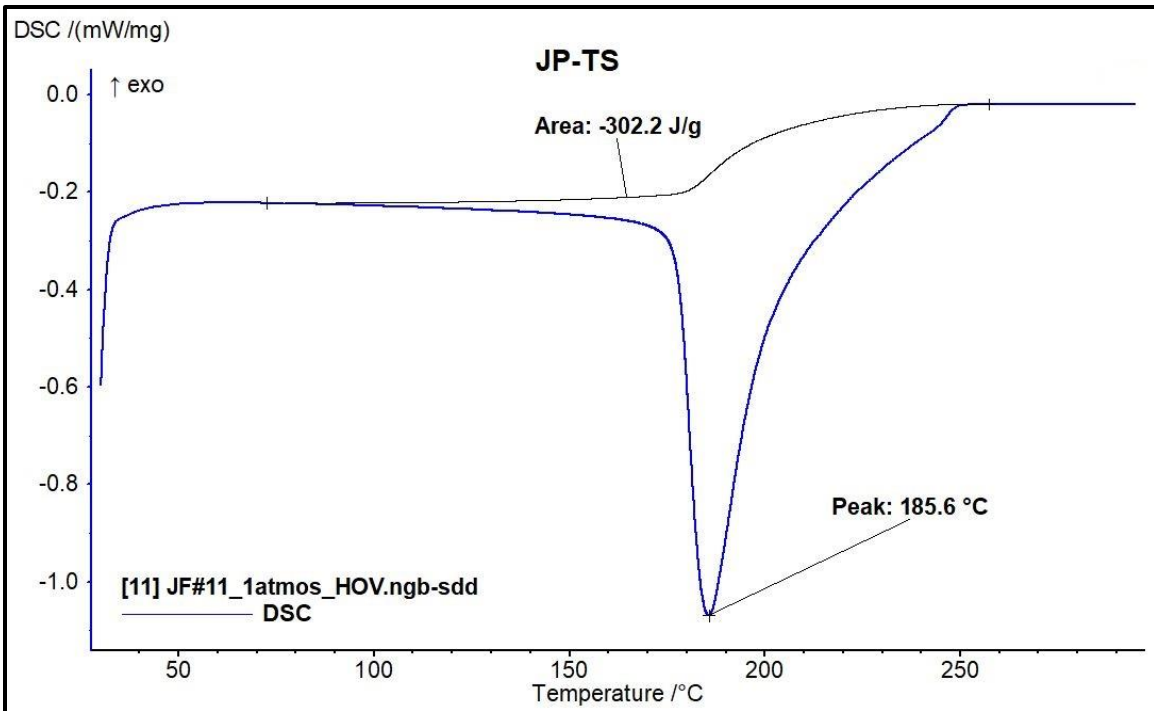


Figure 13: HOV analysis of JP-TS, Blend, WPAFB, USA (JF#11).

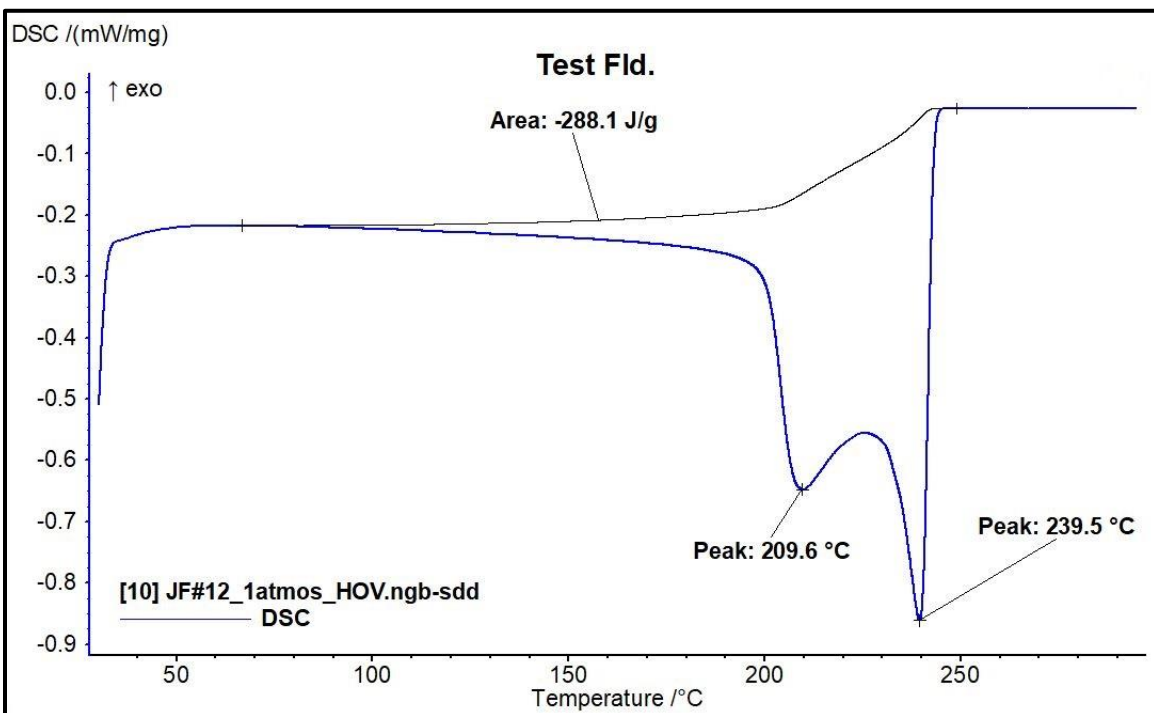


Figure 14: HOV analysis of Test Fld, 12223, WPAFB, USA (JF#12).

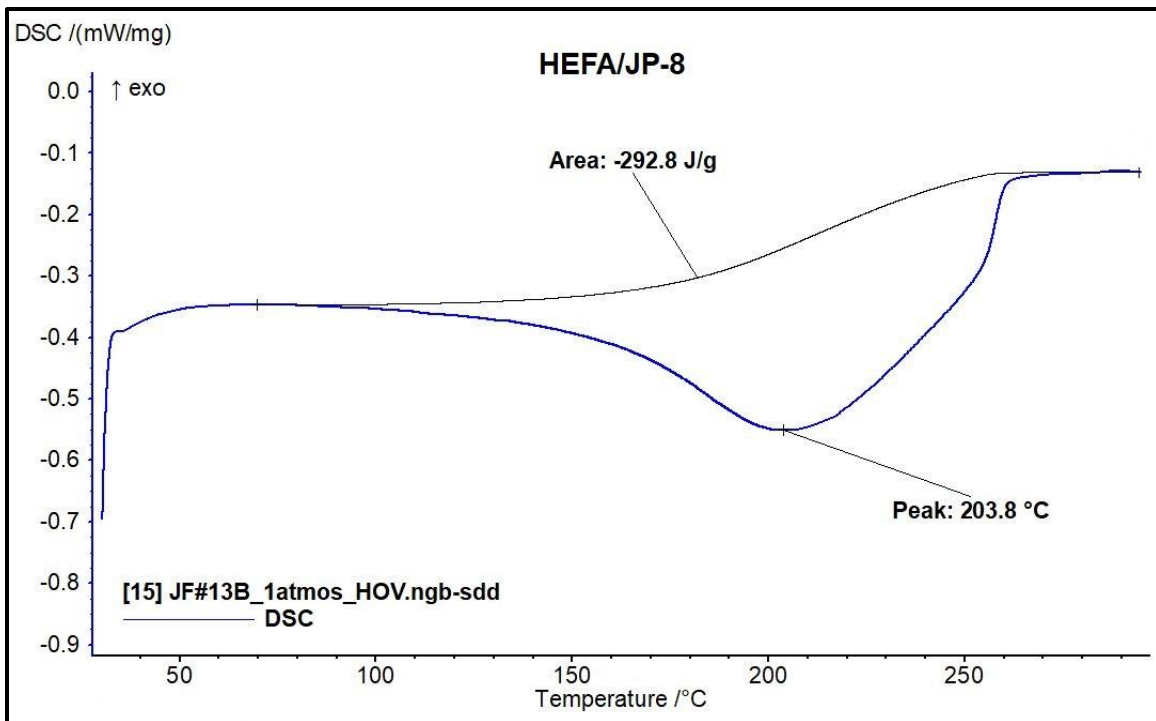


Figure 15: HOV analysis of HEFA/JP-8, Blend, WPAFB, USA (JF#13).

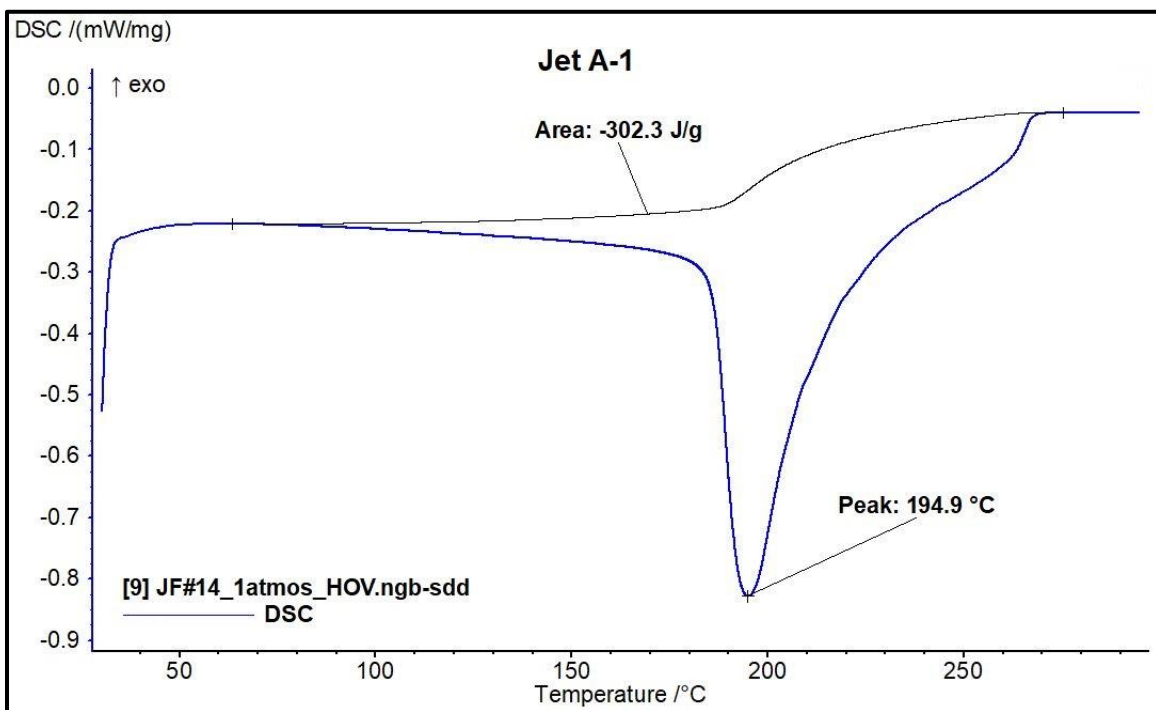


Figure 16: HOV analysis of Jet A-1, synthetic, Sasol, S Africa (JF#14).

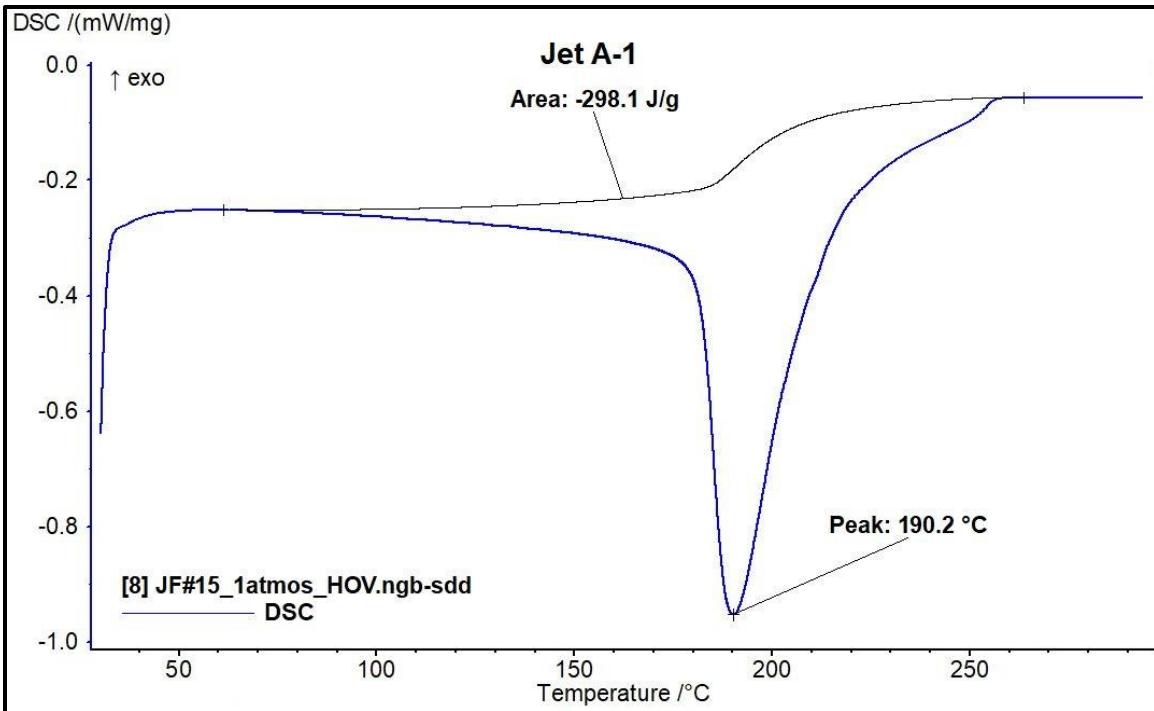


Figure 17: HOV analysis of Jet A-1, semi-synthetic, Sasol, S Africa (JF#15).

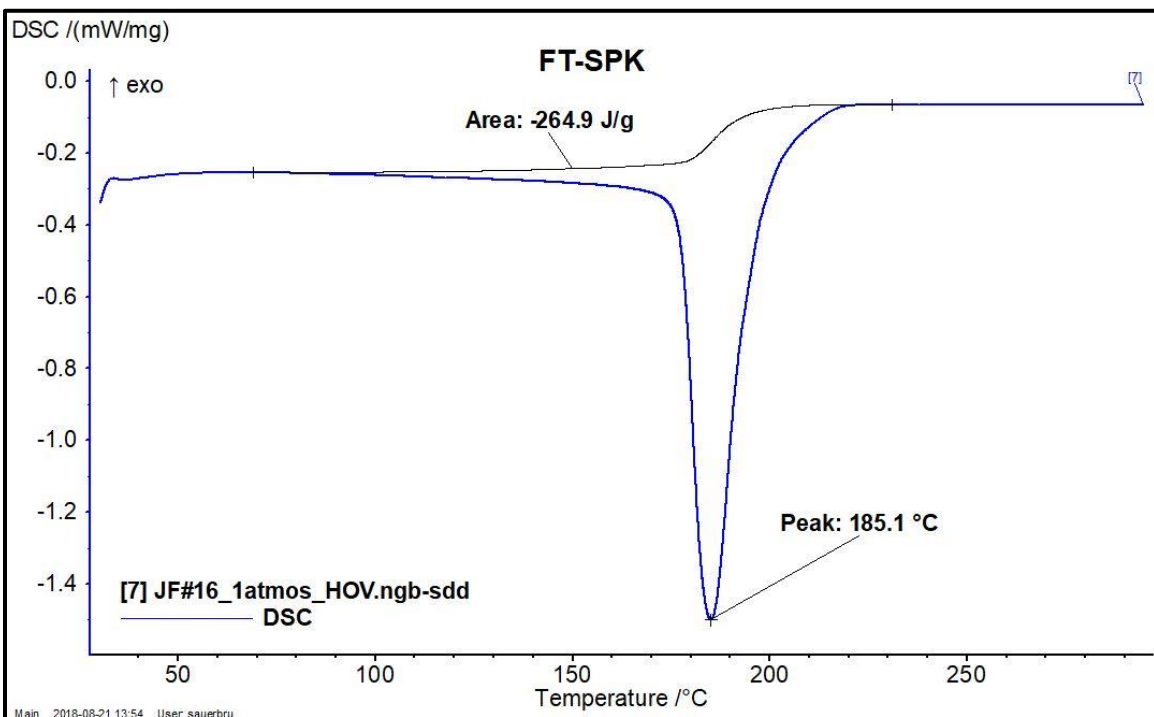


Figure 18: HOV analysis of FT-SPK, Sasol, S Africa (JF#16).

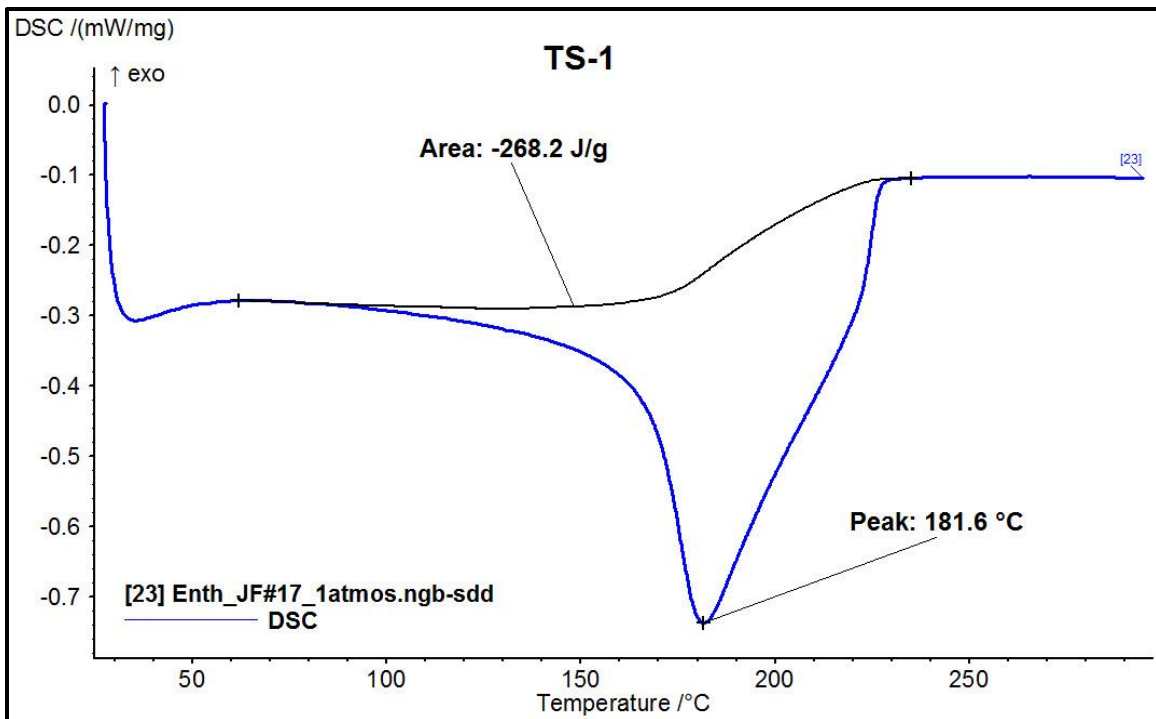


Figure 19: HOV analysis of TS-1, Air BP, UK (JF#17).

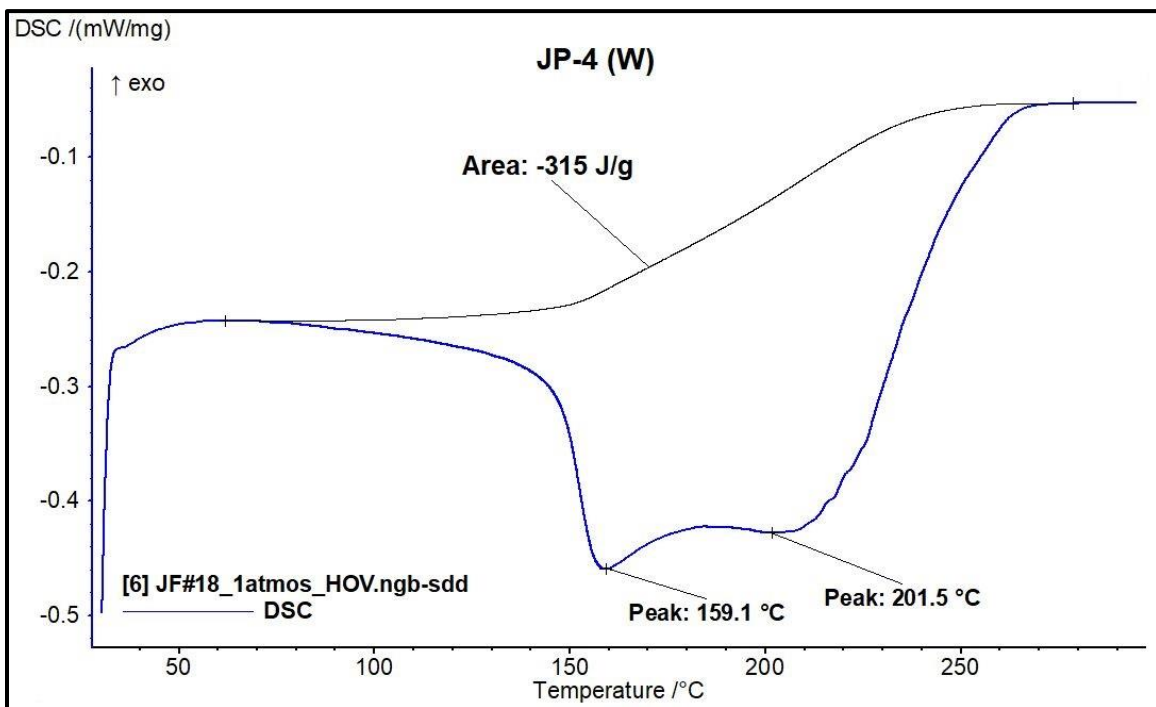


Figure 20: HOV analysis of JP-4 (W), Nova Research, USA, VA (JF#18).

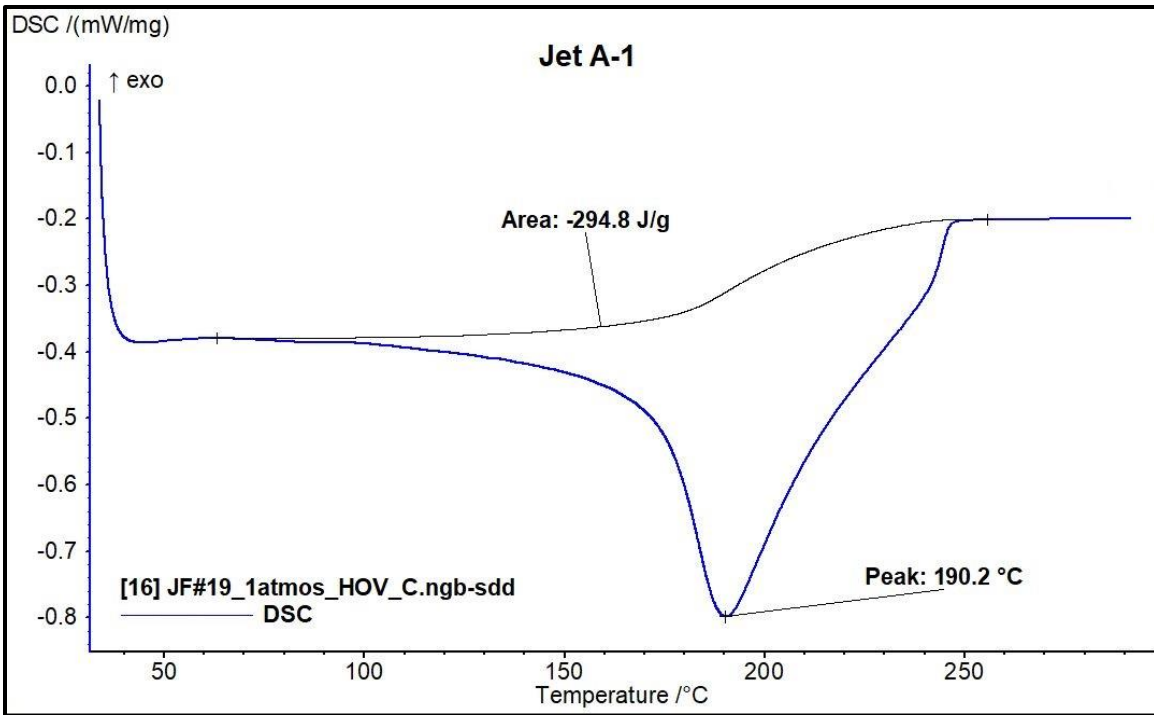


Figure 21: HOV analysis of Jet A-1, Total, France (JF#19).

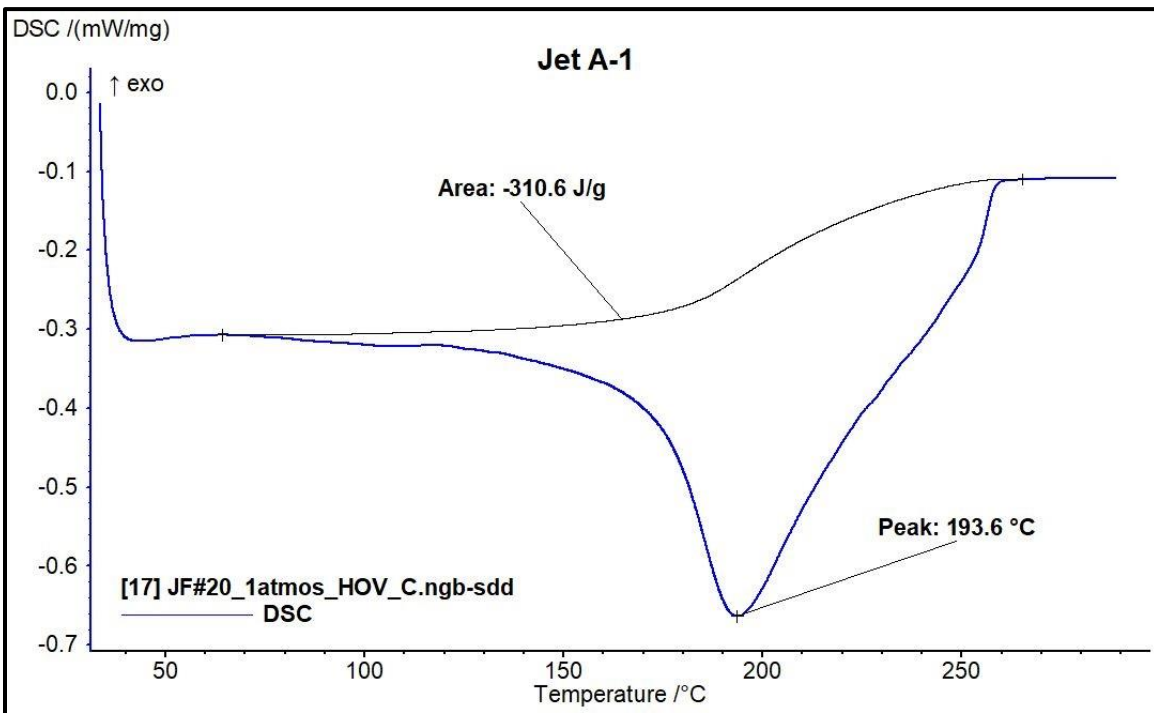


Figure 22: HOV analysis of Jet A-1, hydro-treated, Total, France (JF#20).

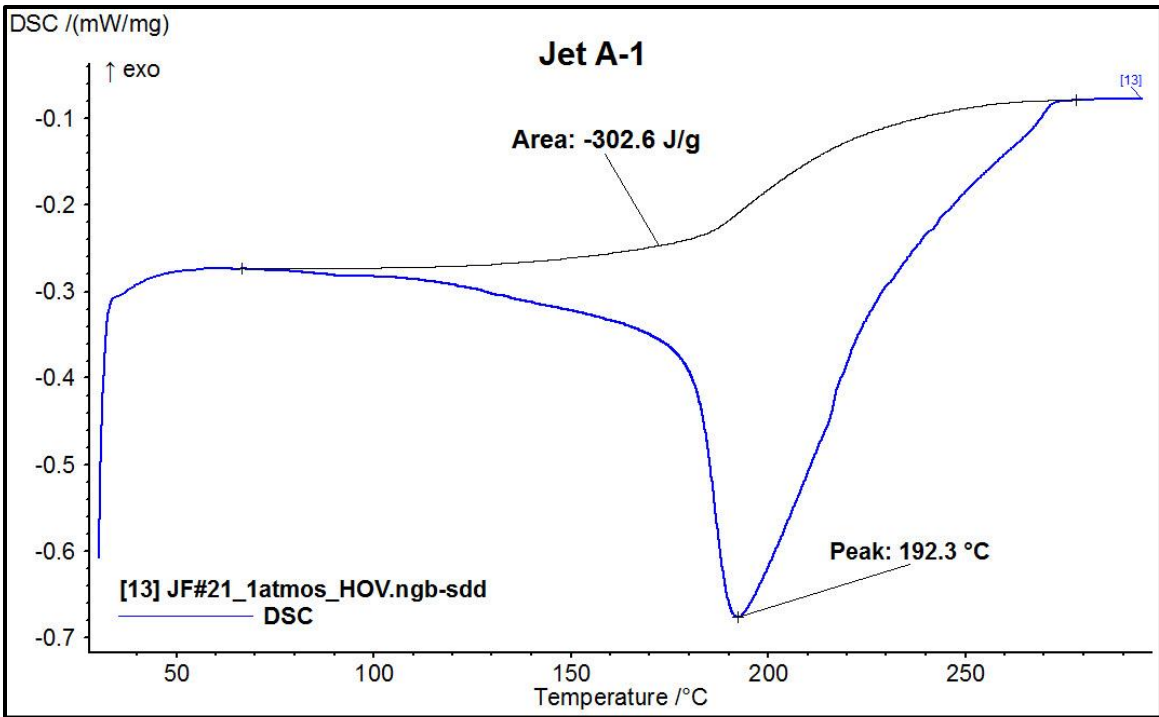


Figure 23: HOV analysis of Jet A-1, meroxed, Total, France (JF#21).

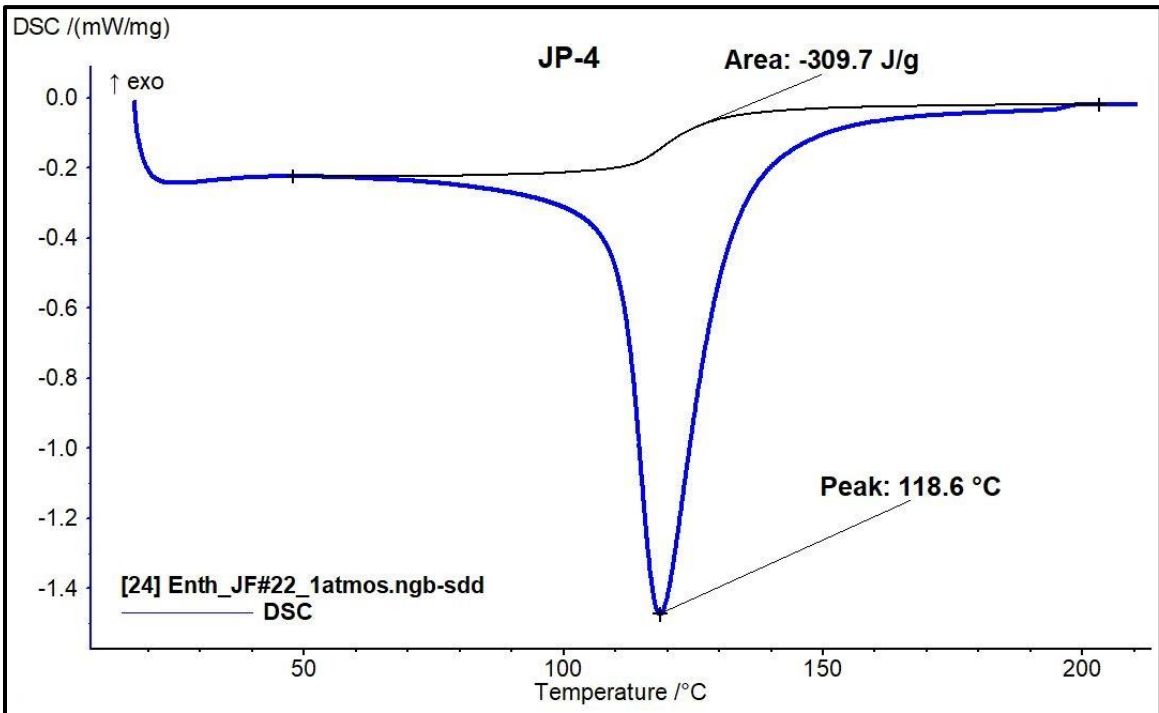


Figure 24: HOV analysis of JP-4, Nova Research, Chevron, USA (JF#22).

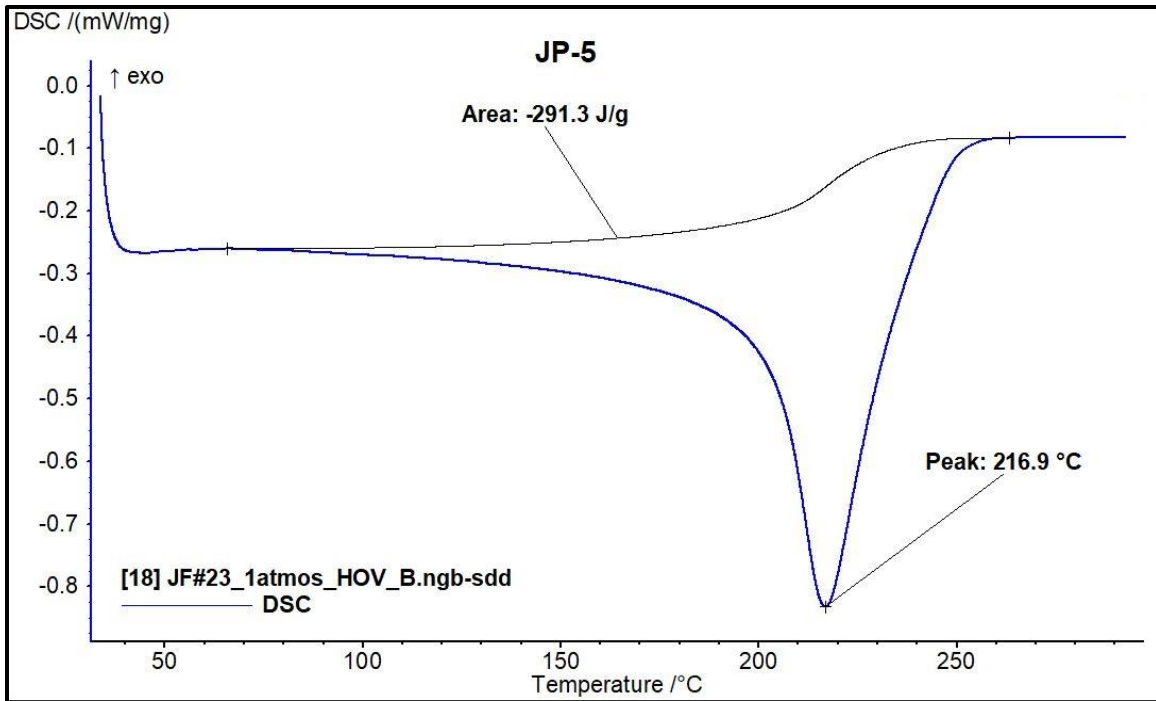


Figure 25: HOV analysis of JP-5, AVCAT, RNAS Culdrose, UK (JF#23).

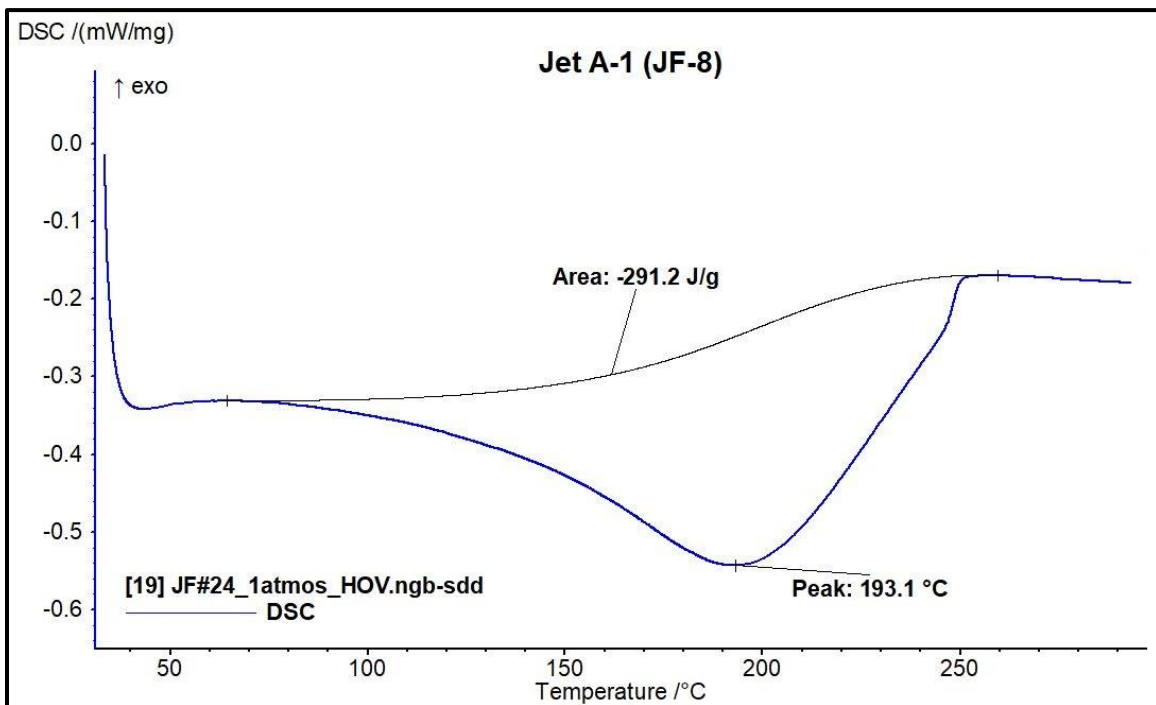


Figure 26: HOV analysis of Jet A-1 (JF-8), with MIL additives, Emo-Trans, Germany (JF#24).

### 5.5. Standard Deviation – HOV Results

No replicates were performed for this report, there was no direct measure of the HOV standard deviation. An indirect measure of HOV standard deviation and average was calculated from all of the Jet A-1 samples shown in Table 5 below. The average is 308.0 +/- 9.6 J/g for a +/- 3.1 % deviation from the average. The MIL spec jet fuels have a higher boiling point and a lower HOV than the commercial Jet A-1.

JF#12 (Blend) and JF#18 (JP-4) each had two peaks. This is not too surprising for a blend. If there two components in a blend that have different boiling points, they will distill at different temperatures in the HPDSC experiment. This will give two HOV peaks or one larger peak and a shoulder. Two other blends JF#13 and JF#16 did not have a second peak. This would happen if the two components of the blend are similar in boiling point.

**Table 5: Jet A-1 HOV Average and Std Devi.**

		<b>HOV</b>	<b>Peak</b>
<b>Number</b>	<b>Type</b>	<b>( J/g )</b>	<b>( °C )</b>
1	Jet A	329.2	208.4
2	Jet A-1	302.3	182.7
3	Jet A-1	314.5	190.1
4	Jet A-1	313.8	184.2
5	Jet A-1	311.8	185.7
14	Jet A-1	302.3	194.9
15	Jet A-1	298.1	190.2
19	Jet A-1	294.8	190.2
20	Jet A-1	310.6	193.6
21	Jet A-1	302.6	192.3
<b>Average</b>		<b>308.0</b>	<b>191.2</b>
<b>Std Devi</b>		<b>9.6</b>	<b>6.9</b>

## 6. HOV Quasi-Isothermal (QI) Testing

The HPDSC needs to be setup differently for the HOV QI testing. The purpose of this test is to determine the HOV of the jet fuel at an isothermal temperature. This test is performed at several temperatures. The HOV will decrease as temperature increases until the HOV is zero at the critical temperature for the jet fuel. The HOV at several temperatures will be used to create a figure similar to Figure 27 [1]. The data will also be used to create the 'mix to gas' line in the enthalpy figures. The NETZSCH High-pressure DSC software can only integrate the area under an evaporation peak when there is a temperature ramp. This is the reason for the quasi-isothermal (QI) HPDSC test. A typical temperature versus time result is shown in Figure 29.

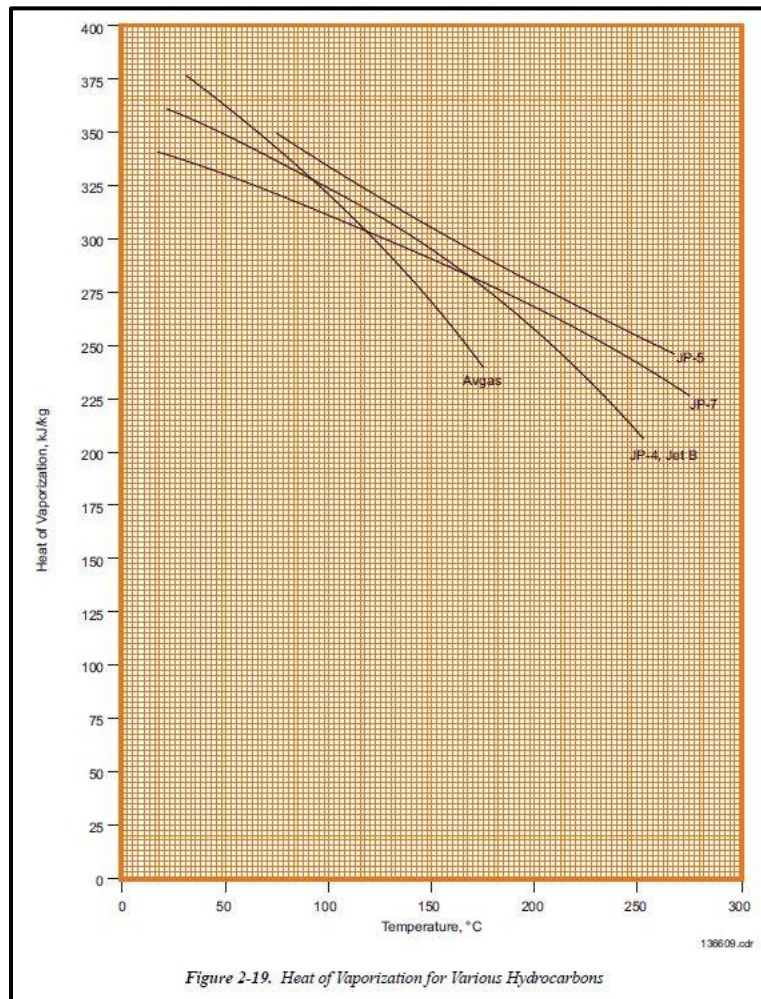


Figure 27: HOV versus temperature. CRC Handbook, Figure 2-19, [1].

## 6.1. Sample Preparation for HOV QI Testing

The crucible and lid were tared on the five-place balance (METTLER TOLEDO model XP205DR). The liquid sample ( about 7 to 10  $\mu\text{L}$ ) was pipetted into the aluminum crucible with a 5 to 10  $\mu\text{L}$  capillary pipet. Laser drilled (50  $\mu\text{m}$ ) aluminum lids (NETZSCH PN 6.239.2-54.801) were used and cold welded to the crucible using the NETZSCH crimping press. The sample in the sealed crucible was weighed again until constant mass was achieved. This mass was entered into the software as the sample mass for the test. Photographs of the sample preparation are in Appendix C.

## 6.2. HOV QI Testing Method

The sample is placed into the HPDSC and the lid was secured. Close the valve to the regulator. The HPDSC was charged with nitrogen gas to 100 psi and released two times using the vent valve. The HPDSC was charged to 800 psi with nitrogen for the test. The heatflow sensitive and temperature calibration at one atm was used. No baseline subtraction was needed for these tests. Flowing tap water was used as the coolant for the HPDSC.

### Test method

Initial Temperature: use the actual temperature as displayed

Ramp temperature: 30  $^{\circ}\text{C}/\text{min}$  to QI test temperature

Ramp temperature: 0.02  $^{\circ}\text{C}/\text{min}$  to 2  $^{\circ}\text{C}$  above the QI test temperature

The method was started. One waits until the temperature reaches the QI temperature. Wait a little longer until the heatflow signal stabilizes close to zero W/g. Turn on the vacuum pump and set it to the maximum vacuum. Open outlet valve to regulator. Wait for method to finish or evaporation endotherm to finish. Turn off the vacuum pump. Open the vent valve to equalize the pressure in the HPDSC to atmospheric pressure. Remove the lid nuts from the HPDSC by hand.

(Safety note: The nuts should be loose enough to remove by hand. If not, there could still be dangerous pressure in the HPDSC. Double check that the vent valve is open and try again.)

This test was repeated for several isothermal temperatures in the region of the enthalpy curve between the intersection of the 0.1 atm, 'Mix-to-Gas' and 68 atm lines, as shown in Figure 28. At least 5 temperatures should be run. In this case, seven tests were run from 175 to 325  $^{\circ}\text{C}$  in steps of 25  $^{\circ}\text{C}$ .

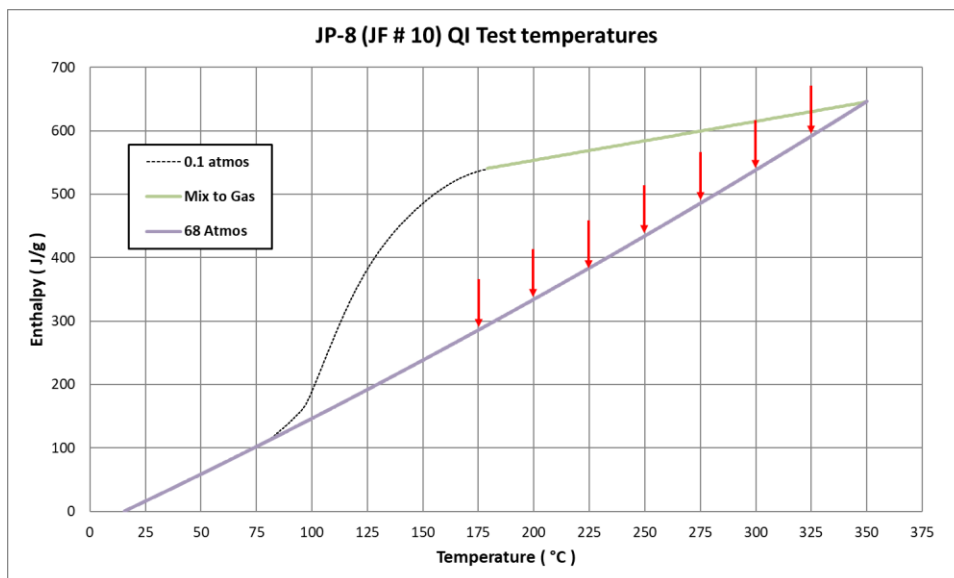


Figure 28: Typical enthalpy versus temperature. The QI temperatures for a HOV QI HPDSC experiment were 175, 200, 225, 250, 275, 300, and 325 °C.

A typical QI temperature ramp is shown in Figure 29. The peak temperature at the evaporation endotherm is used for the temperature of the evaporation which is used for the X value in the HOV versus temperature graphs.

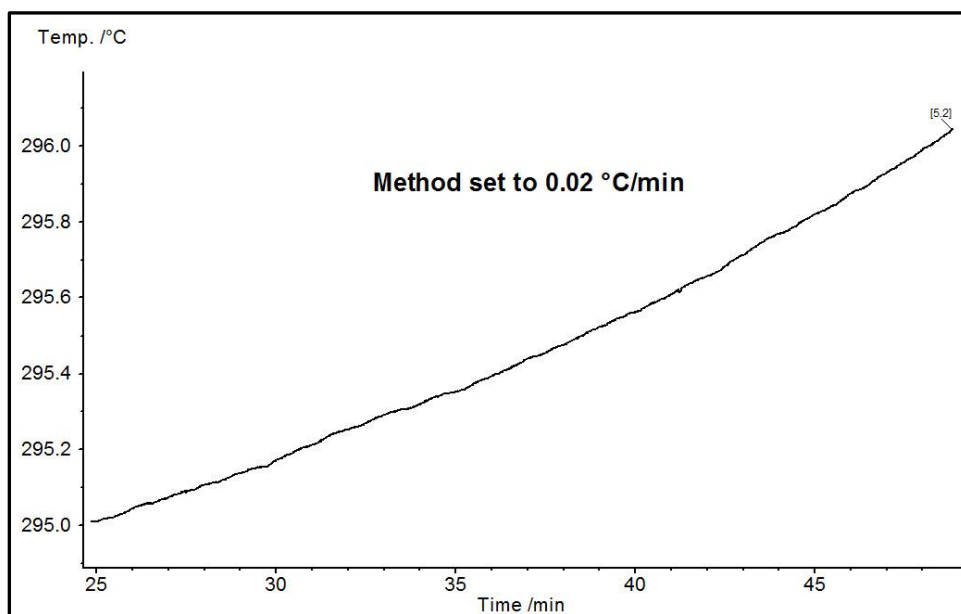


Figure 29: Typical temperature versus time for a HOV QI HPDSC experiment.

### 6.3. HOV QI Data Evaluation Procedure

The evaporation endotherm was integrated, as shown in Figure 30. The area under the peak is the HOV, 51.3 J/g, and the peak temperature, 321.2 °C, is the QI temperature for the evaporation, in this case.

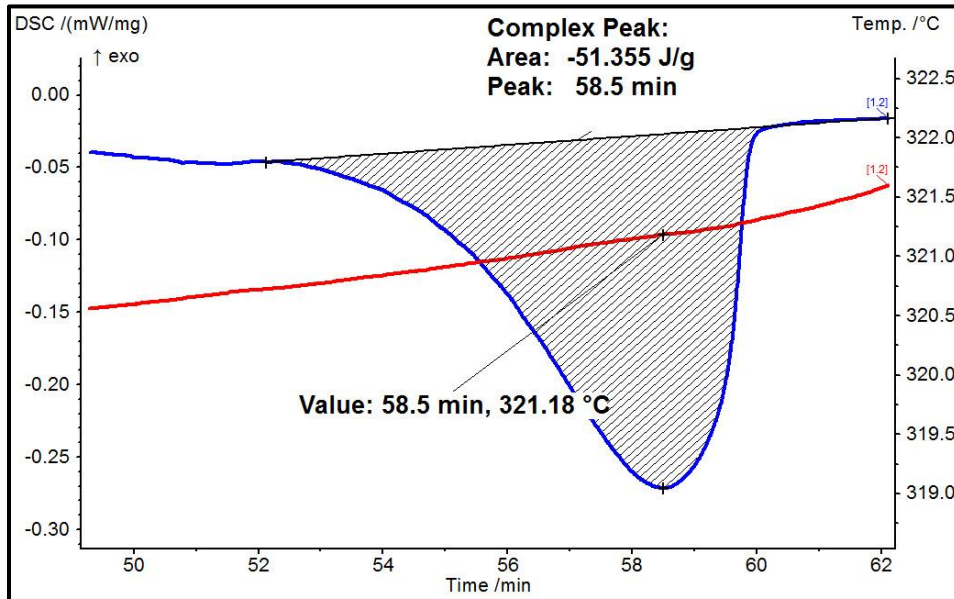


Figure 30: Typical integration of the evaporation of a sample during the QI HPDSC experiment.

## 7. HOV Quasi-Isothermal Diagrams

### 7.1. Tables of QI Heat Flow Data

Tables 6 to 10 show the data for the Peak Temperature and the HOV from the QI HPDSC experiments. The critical temperature,  $T_c$ , was obtained by extrapolating the peak temperature to zero HOV. The critical temperature is where the sample is a critical fluid, which has the properties of a gas and a liquid, with no distinction between the two. Additionally, there is no heat of vaporization because there is no liquid to gas phase change above the critical temperature.

**Table 6: Jet A (JF#8)**

	<b>Peak Temperature</b>	<b>HOV</b>
	( °C )	( J/g )
	196.9	231.34
	221.7	202.56
	247	171.46
	271.6	148.2
	296.4	81.2
	321.2	46.29
	345.7	6.04
$T_{critical}$	346.45	0

**Table 7: JP-5 (JF#9)**

	Peak Temperature	HOV
	( °C )	( J/g )
	172.9	257.74
	197.7	226.83
	222.5	205.35
	247.2	185.05
	271.9	169.19
	297.7	110.62
	321.4	102.74
	346.3	61.81
	370.8	16.56
T <sub>critical</sub>	379.175	0

**Table 8: JP-8 (JF#10)**

	Peak Temperature	HOV
	( °C )	( J/g )
	147.9	257.9
	172.6	259.26
	197.2	226.76
	222	161.25
	246.7	172.43
	271.5	133.46
	296	72.689
	320.9	39.19
	346.1	9.6291
T <sub>critical</sub>	349.15	0

**Table 9: TS-1 (JF#17)**

	Peak Temperature	HOV
	( °C )	( J/g )
	123.4	291.21
	147.8	290.41
	172.8	254.52
	197.6	212.9
	221.8	191.66
	247	151.33
	271.8	77.226
	296.7	85.256
	321.6	15.9131
T <sub>critical</sub>	327.58	0

**Table 10: JP-4 (JF#22)**

	<b>Peak Temperature</b>	<b>HOV</b>
	<b>( °C )</b>	<b>( J/g )</b>
	74.2	292.88
	98.7	280.22
	123.4	193.44
	148	228.3
	172.6	190.27
	197.3	171.97
	221.8	104.74
	246.1	90.509
$T_{critical}$	320.22	0

## 7.2. HOV QI Diagram Results

The tabular data from the table in section 7.1 were used to generate the following Figures 31 to 35. The raw data points are shown as blue circles and the dashed blue line is the 2<sup>nd</sup> order polynomial line fit. The polynomial fit was extrapolated to zero HOV to determine the critical temperature.

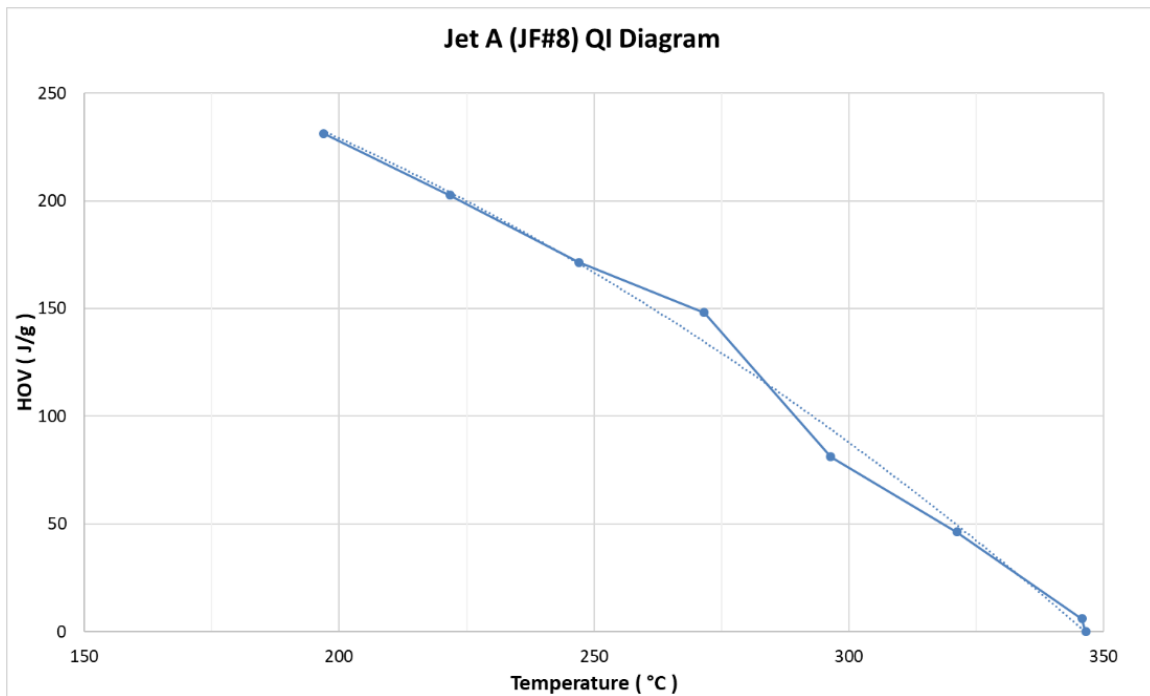


Figure 31: Jet A HOV from a QI HPDSC experiment.

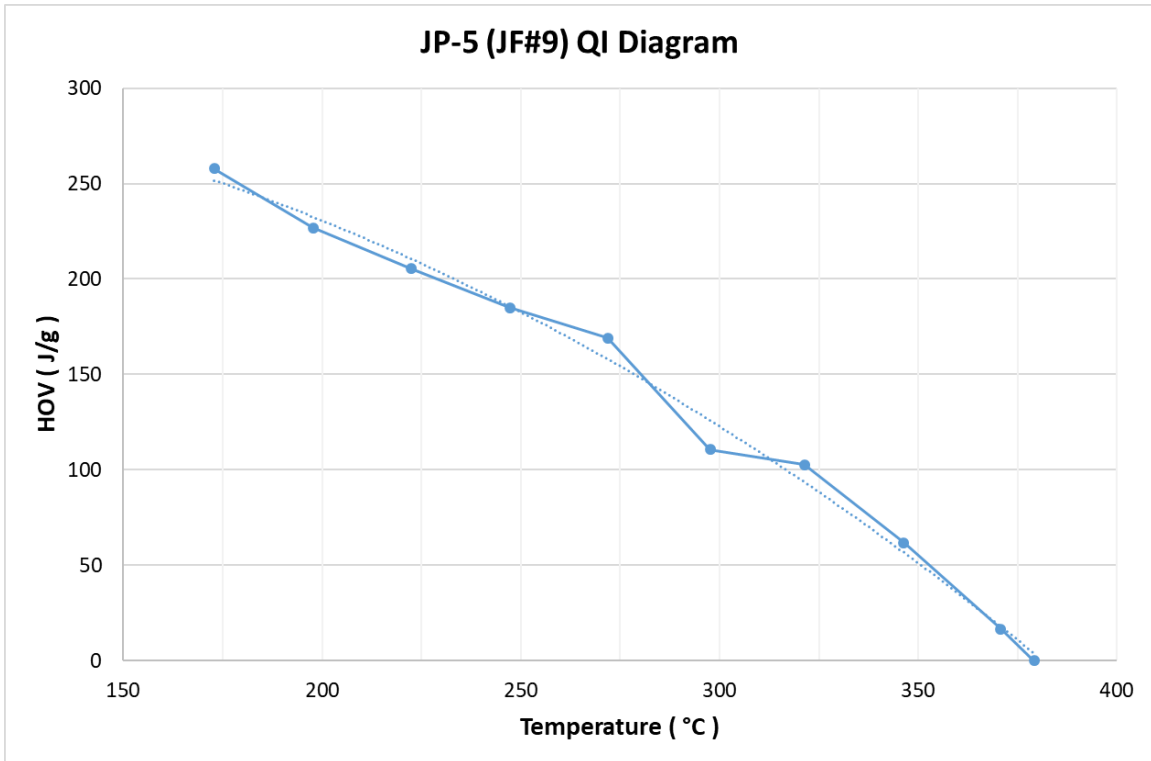


Figure 32: JP-5 HOV from a QI HPDSC experiment.

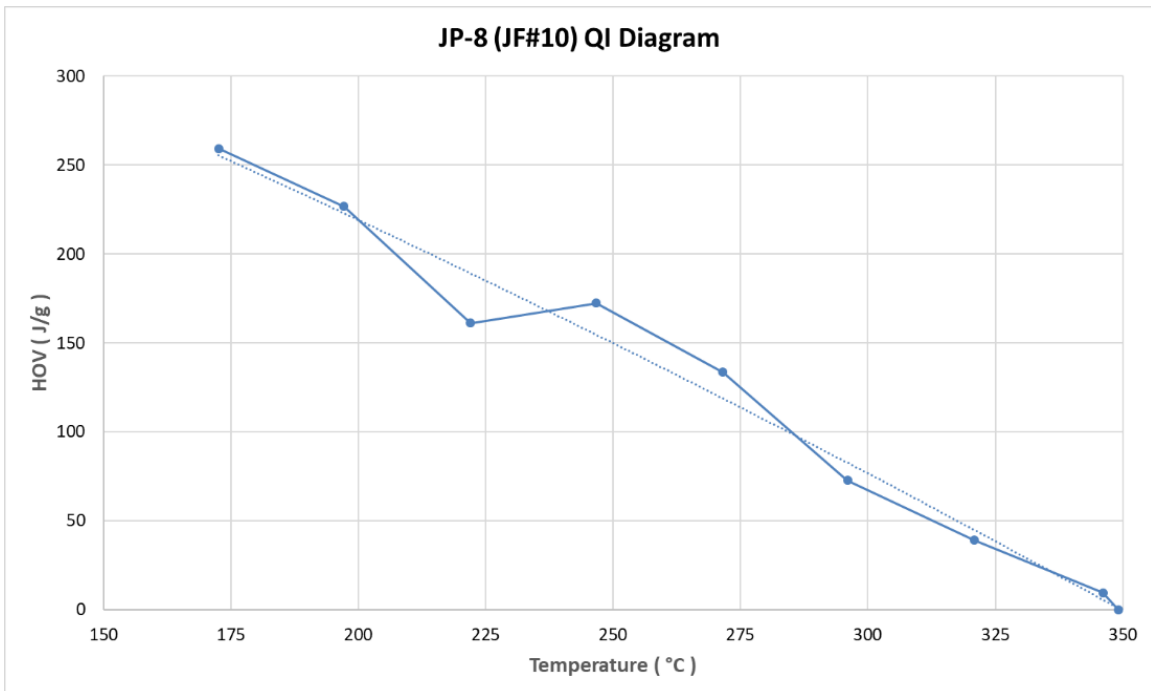


Figure 33: JP-8 HOV from a QI HPDSC experiment.

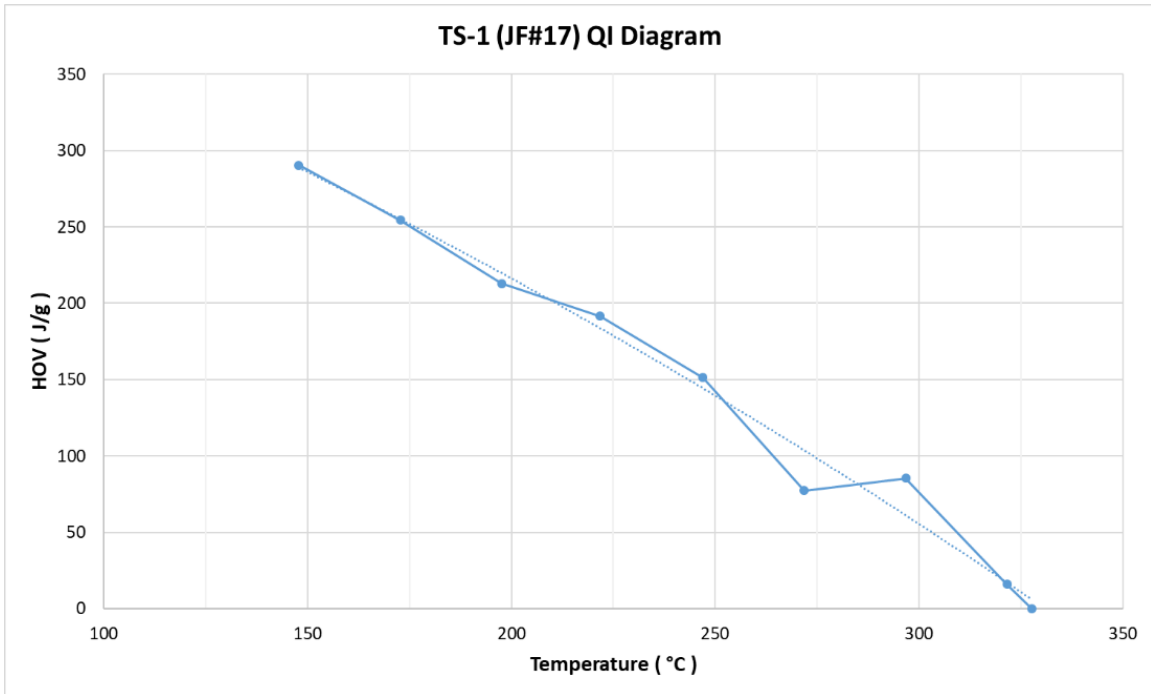


Figure 34: TS-1 HOV from a QI HPDSC experiment.

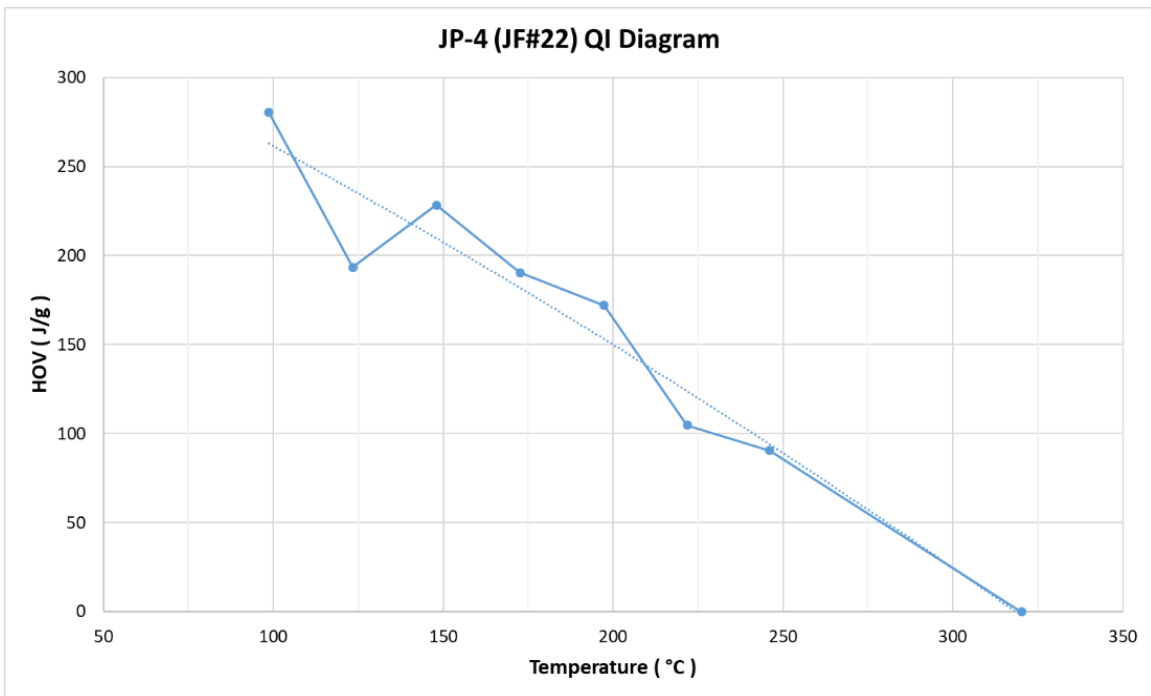


Figure 35: JP-4 HOV from a QI HPDSC experiment.

## 8. Enthalpy Diagram

### 8.1. Background on Enthalpy Diagrams

The HPDSC measures the instantaneous heatflow of the sample in watts per gram (W/g). The enthalpy is the cumulative integral of this heatflow from the beginning to the end of the scan. This integral requires a correct baseline to form one side of the boundary for this integration. The other side is the heatflow curve. The enthalpy calculation requires a baseline curve run under the exact same conditions as the sample will be run. These conditions include: heating rate, type of gas, gas pressure and crucibles. The crucibles all had a 50  $\mu\text{m}$  laser drilled hole in the lid to permit the jet fuel to evaporate. The reference crucible was crimped to the lid and it was used for all future experiments. The sample crucible was not crimped for the blank run and then filled with the jet fuel and crimped shut for the sample test. Since the crimped sample crucible could not be reused, a blank had to be run for each sample/pressure pair that was tested.

### 8.2. Sample Preparation for Enthalpy Testing

The crucible and lid were tared on the five-place balance. The liquid sample (about 7 to 10  $\mu\text{L}$ ) was pipetted into the aluminum crucible with a 5 to 10  $\mu\text{L}$  capillary pipet. Laser drilled (50  $\mu\text{m}$ ) aluminum lids were used and cold-welded to the crucible using the crimping press. The sample in the sealed crucible were weighed again until constant mass. This mass was entered into the software as the sample mass for the test.

### 8.3. Enthalpy Testing Method

The HPDSC was cooled using tap water running through the lid of the high-pressure chamber. The sample was placed in the HPDSC as quickly as possible after weighing. The pressure lid was fastened down. The HPDSC cell was filled with nitrogen gas to 50 psi and emptied three times. There was no gas flow through the HPDSC, so the sample was run in static nitrogen. The HPDSC cell was stabilized at 35  $^{\circ}\text{C}$  then heated at 5  $^{\circ}\text{C}/\text{min}$  to 400  $^{\circ}\text{C}$ .

Except for JP-4 (JF #22), which was too volatile to begin the test at 35  $^{\circ}\text{C}$ . In this case, the water chiller was used and set to 1  $^{\circ}\text{C}$ . The HPDSC was allowed to stabilize at 15  $^{\circ}\text{C}$  +/- 1  $^{\circ}\text{C}$  before the sample is prepared. This reduces the amount of sample evaporation that might happen in the HPDSC while waiting for the temperature to come back to 15  $^{\circ}\text{C}$ . The test was started when the HPDSC cell stabilized at 15  $^{\circ}\text{C}$ .

Two crucibles, one sample and one empty, are used for all HPDSC tests. The reference crucible is crimped shut and can be used for all of the HPDSC experiments. The sample crucible is run first and the lid is not crimped closed. This is the baseline, which the software automatically subtracted for the next test, which is the sample run. The mass of the empty sample crucible was tared. The sample, 10  $\mu\text{L}$ , was pipetted into the sample crucible and promptly crimped shut. The sample was weighed until the mass is stable. The difference between the tare mass and the crucible with the sample is the sample mass. The crucible was put in the HPDSC. For tests  $\geq 1$  atm, the HPDSC is pressurized to 50 psig and released and refilled three times. This removes oxygen from the HPDSC that might react (exothermic combustion) with the jet fuel as it is coming out of the laser drilled hole in the lid. For tests at 68 atm, this purging is not required because the crucible is hermetically sealed, not laser drilled hole. For tests  $< 1$  atm, the vacuum removes enough of the

oxygen so that combustion is not a concern. Then the HPDSC was pressurized, or evacuated, to the test pressure. A sample of JF#9 (JP-5) was pressurized/depressurized between 100 psi and atmospheric pressure three times and there was no mass loss of the JF. This is confirmation that the JF sample does not evaporate during the degassing process. The HPDSC temperature was allowed to settle to 15 °C +/- 0.5 °C. The method was started and heated at 5 °C/min to 350 °C or until the evaporation is complete, whichever happens first. The pressure was released from the HPDSC and the sample/crucible is removed. A new empty sample crucible was placed in the HPDSC and the HPDSC is closed. The HPDSC must be at 15 °C +/- 1 °C before the next sample is prepared. This reduces the amount of sample evaporation that might happen in the HPDSC while waiting for the temperature to come back to 15 °C.

The 68 atm (1000 psi) sample test was prepared differently. A crucible and a solid lid were used to prevent the jet fuel from evaporating during the test. The high pressure was selected so that none of the jet fuel sample would leak from the crucible during the test. This was confirmed by weighing each sample/crucible pair after the test. If the mass changed by more than 0.1 mg, a new sample was prepared and tested. The high pressure caused the crucible to collapse if there is a gas space above the sample. This problem was solved by inverting the lid so the convex side is down toward the liquid sample. The crucible was filled to overflowing with jet fuel. The lid was placed, concave side up, over the liquid such that it was floating on the jet fuel. The sample/crucible was placed in the crimper. The crimper arm was lowered to expel the excess jet fuel and allow the liquid to leave the crimping zone of the crucible and lid. This took about one minute. The crimper arm was lowered to complete the crimp. The sample was weighed several times over about one hour or until the sample mass was stable. This gave time for the excess jet fuel to evaporate from the outside of the crucible. The HPDSC temperature was allowed to settle to 15 °C +/- 0.5 °C. The method was started and heated at 5 °C/min to 350 °C. At the end of the test, the pressure was released from the HPDSC and the sample/crucible was removed.

#### **8.4. Integration of Heat Flow Data**

The enthalpy is the integral of the heatflow curve versus seconds from the beginning to the end of evaporation, or 350 °C, whichever one happens first. The software automatically integrates versus time in seconds even though the curve is plotted versus temperature. The baseline for this integration is a straight line at zero heatflow, Figure 36. The resulting enthalpy curve is shown as the green dash-dot line in Figure 37. One needs to carefully inspect the heatflow curves at this point. If the heatflow signal is oscillating (Figure 38), especially near the end of evaporation, this is an indication of combustion of the jet fuel with residual oxygen in the HPDSC. Data such as this need to be discarded and the sample rerun.

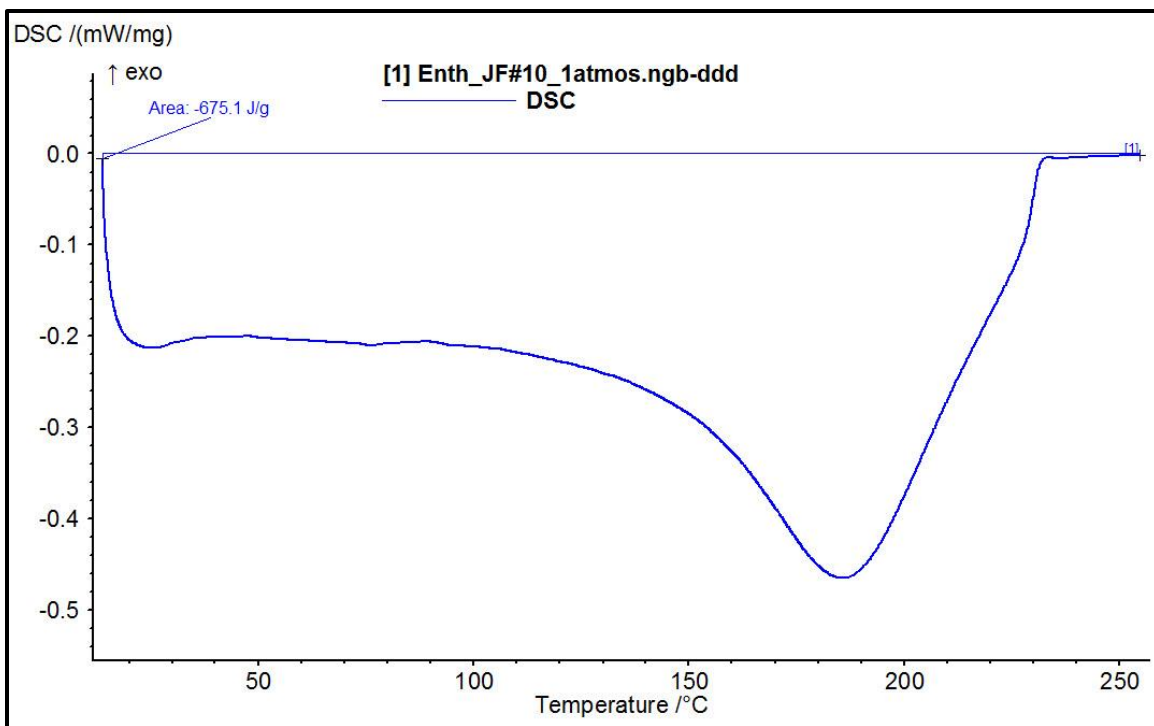


Figure 36: HPDSC raw data for JP-8 (JF#10) at 1 atm nitrogen pressure.

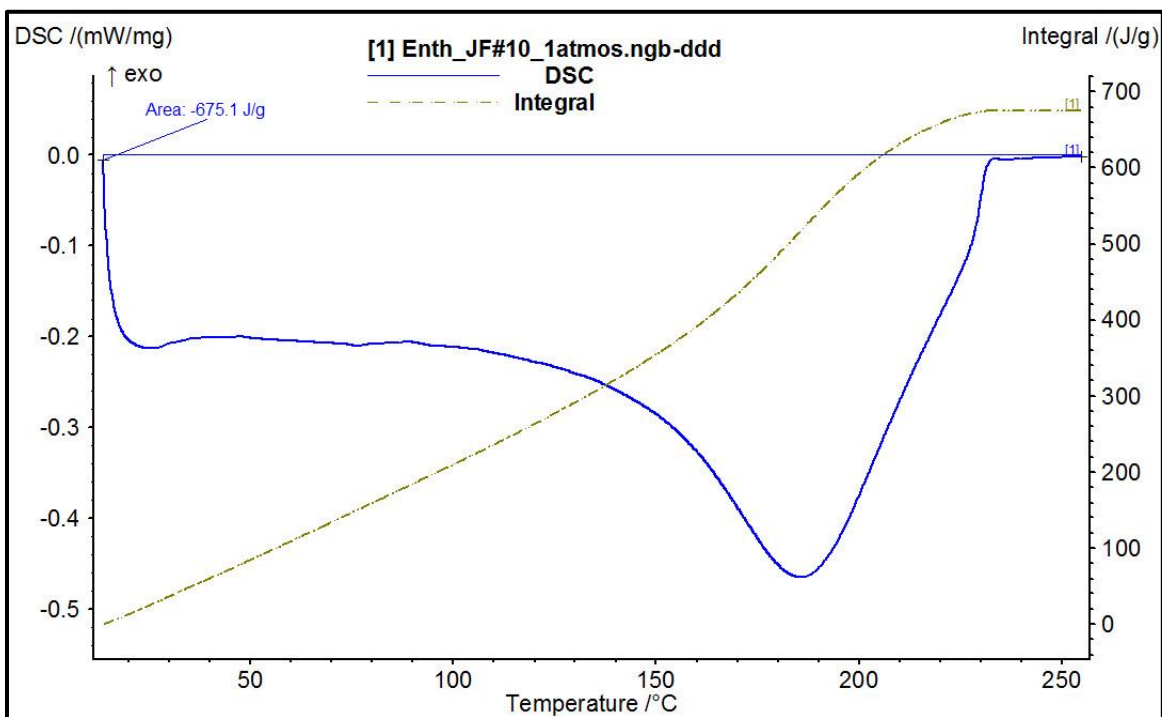


Figure 37: HPDSC heatflow integral (enthalpy) data for JP-8 (JF#10) at 1 atm nitrogen pressure.

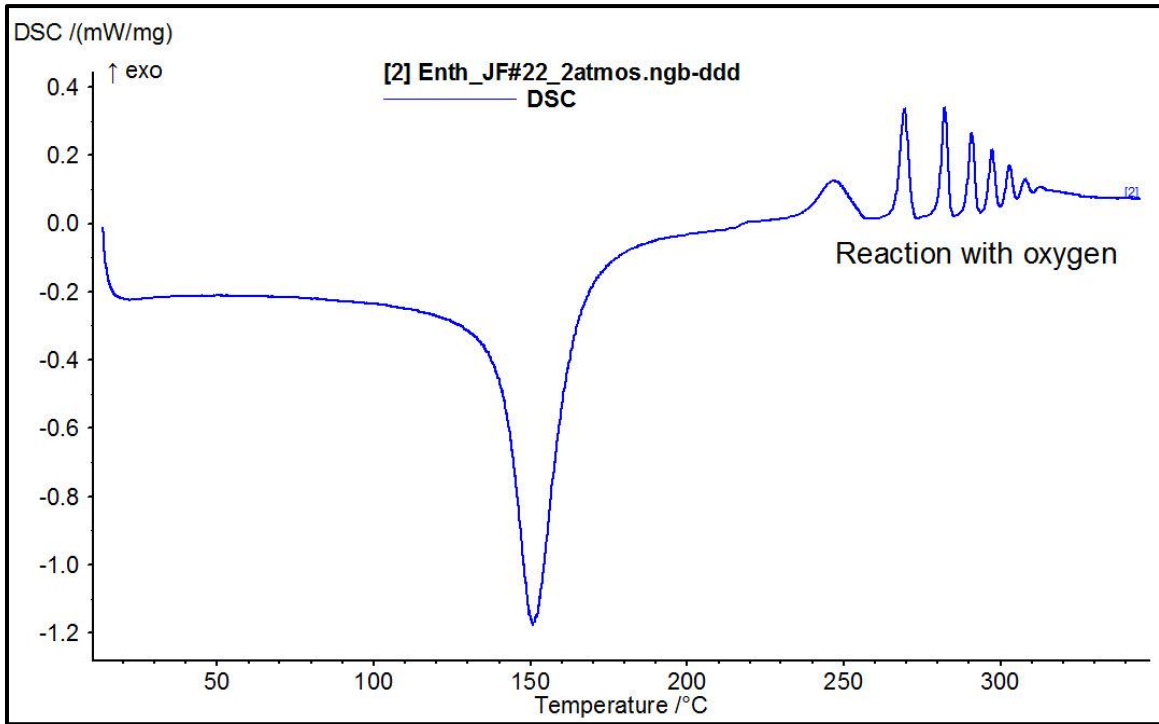


Figure 38: HPDSC raw data for JP-4 (JF#22) at two atm pressure without purging.

## 8.5. Construction of an Enthalpy Diagram

### 8.5.1. Plotting of All Enthalpy Data

The first look at the test results was done by plotting the curves at 68 atm and the QI HOV, as shown in Figure 39.

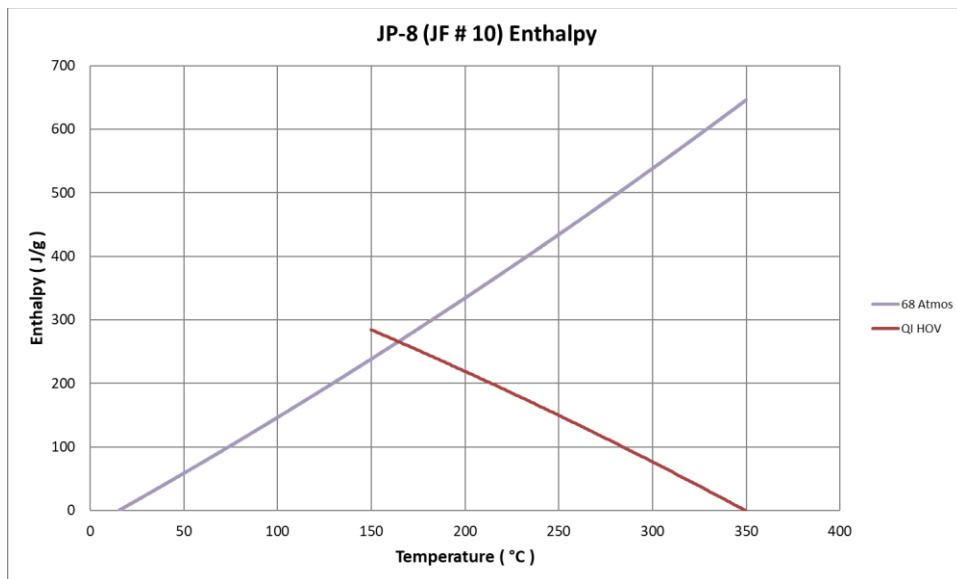


Figure 39: Raw enthalpy curves for JP-8 (JF#10).

The QI HOV and the 68 atm data were added to create the ‘Mix to Gas’ curve, as shown in Figure 40. The 68 atm and “Mix to Gas’ curves were used as the standard curves that all other curves must match, so no adjustments were made to these two curves. This 68 atm curve must be a smooth curve with no sudden shifts in enthalpy. (A sudden shift is an indication of crucible rupture and the test must be rerun.) A mass loss between the start and end of the test was an indication of a slow leak of the jet fuel during the experiment and the test was rerun. Great care was taken in producing the 68 atm results because these data were the standard results that affect the accuracy of the final enthalpy plots. The 68 atm data line is replaced with the 3<sup>rd</sup> order polynomial equation. This removes the signal noise from the 68 atm data and permits a better fit with the lower pressure data.

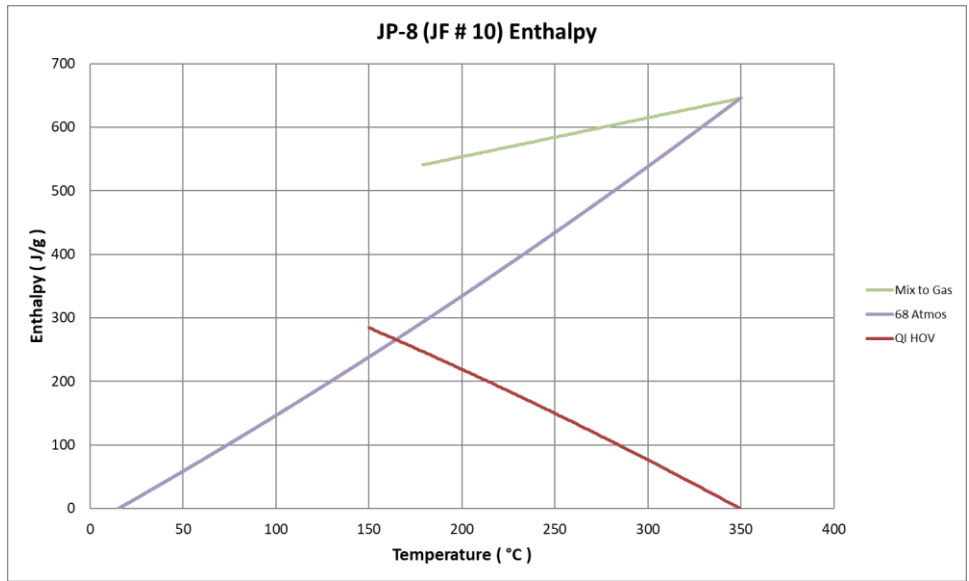


Figure 40: “Mix to Gas” curve, green line, for JP-8 (JF#10).

### 8.5.2. Matching Starting Enthalpies

There are two factors, the slope and offset, that was used to match the starting enthalpies, of different pressure curves, just prior to vaporization. The offset correction is used to correct errors that come from the experiments starting at slightly different temperatures. The raw data for the 0.1 atm curve is shown in Figure 41.

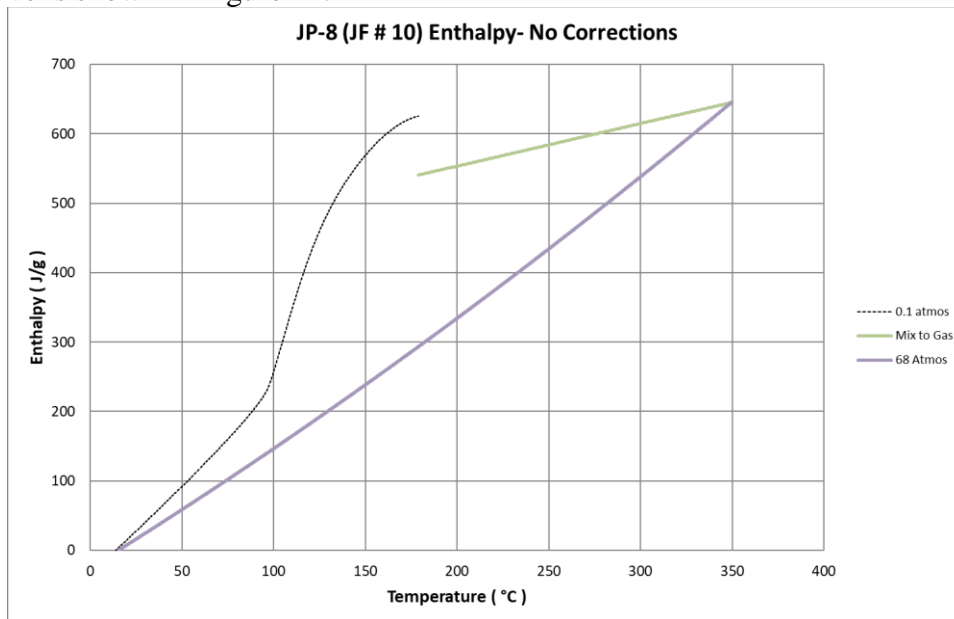


Figure 41: JP-8 0.1 atm with no corrections

At this point in the adjustments, only the slope is adjusted so the 0.1 atm line's curvature matches the 68 atm line's curvature. This determines the starting point of evaporation for the 0.1 atm line, see Figure 42. All data at lower temperatures were deleted.

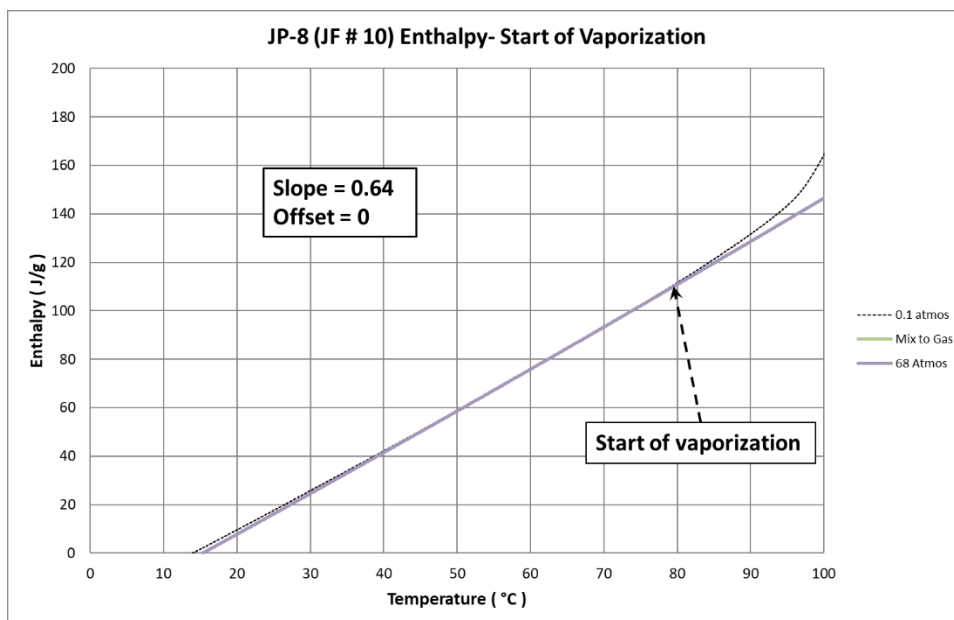


Figure 42: JP-8 0.1 atm matching curvature at low temperatures, near the start of vaporization.

### 8.5.3. Fitting Data to the 68 atm and ‘Mix to Gas’ Lines

The slope and offset of the 0.1 atm curve was adjusted so the 0.1 atm line matched with the 68 atm curve, at low temperature, and with the ‘Mix to Gas’ line at high temperature, the end of vaporization, shown in Figure 43.

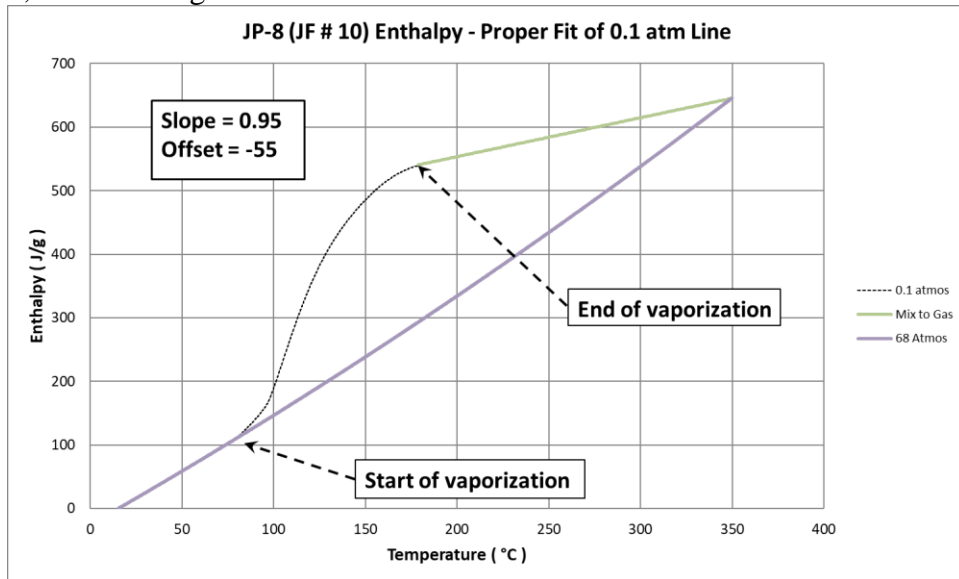


Figure 43: JP-8 0.1 atm matching with the 68 atm curve at low temperature and with the ‘Mix to Gas’ line at high temperature, the end of vaporization.

The steps 8.5.2 and 8.5.3 are repeated from lower pressures to higher pressures. The slope and offset are adjusted for each of the 0.25 to 8 atm data so that the beginning of evaporation matches the 68 atm line, at low temperature, and the ‘Mix to Gas’ line. Data points for the 0.1 to 8 atm lines that are at higher temperature than the ‘Mix to Gas’ line were deleted. This results in the final enthalpy graph for JP-8 shown in Figure 44.

Additionally, one must check to make sure that the lines at different pressures do not cross over each other in the region of about 50% evaporation. If this happens, the sample tests at both of those pressures need to be rerun. The enthalpy plot should look similar to the plot shown in Figure 44.

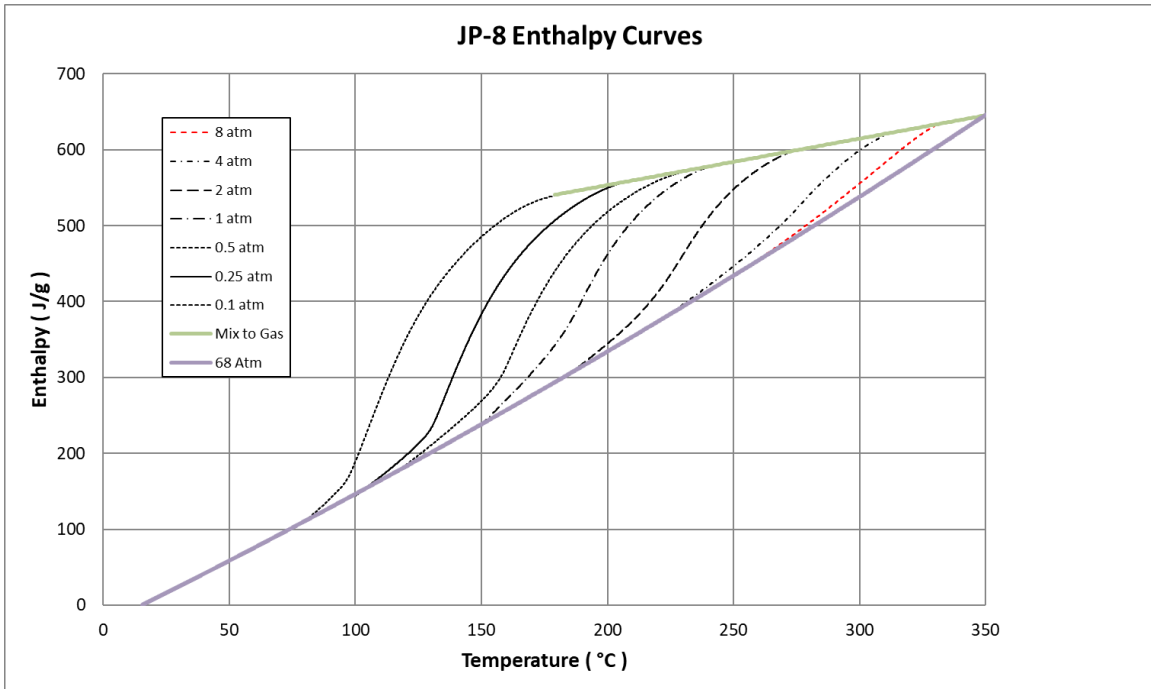


Figure 44: Final enthalpy diagram for JP-8 (JF#10).

### 8.5.4. Comparison of Enthalpy Curves with Literature

The data generated in this work was validated by correlating it to historical data. In this case, the enthalpy plot for JP-5 from this work was compared to CRC Handbook Figure 2-18, the enthalpy plot of JP-5. In Figure 45, the dashed lines are manually digitized from Figure 2-18 in the CRC Handbook [1]. The solid lines, in Figure 45, are data from this work. The two sets of data are very similar below about 225 °C. The ‘Mix to Gas’ lines are shifted in about the same enthalpy through the entire temperature range. The beginning of vaporization for each of the pressure curves, 0.1 to 8 atm, are very similar in both data sets. The temperature of the end of vaporization is different in the two data sets. The vaporization results in this work are probably the most correct since the data was taken from actual jet fuel under pressure in the high-pressure DSC.

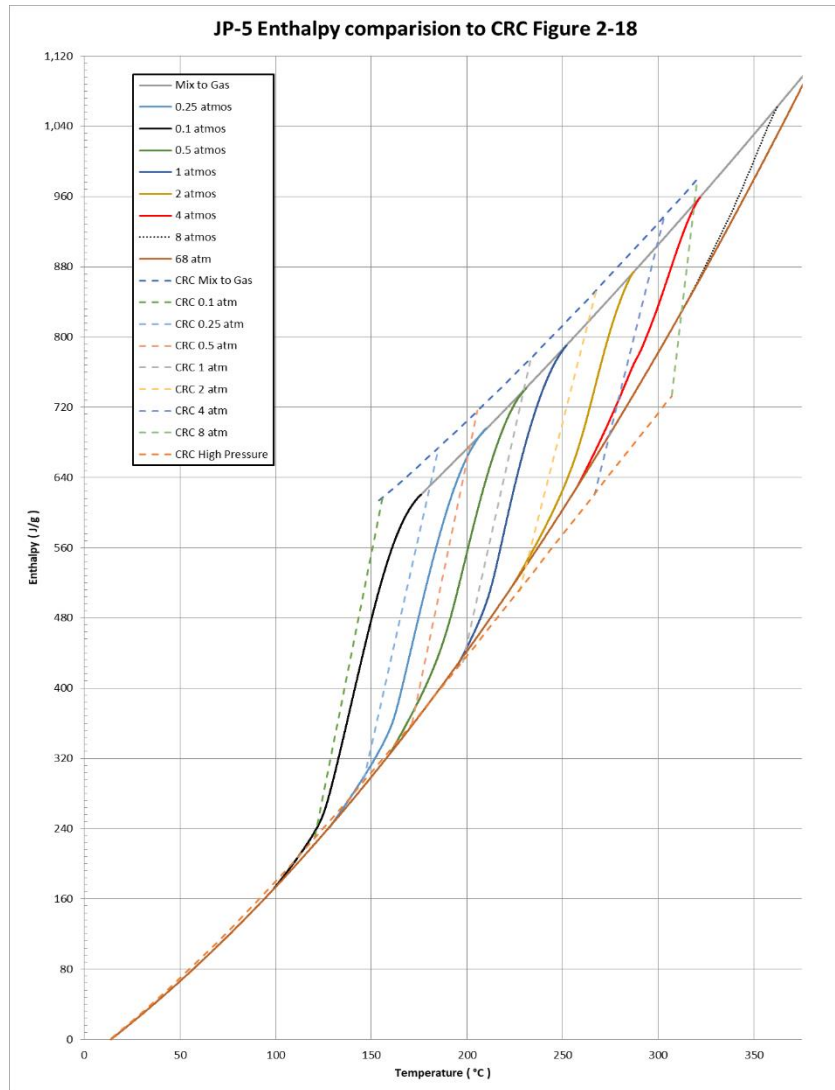


Figure 45: Comparison of the enthalpy diagram for JP-5. The dashed lines are from CRC Handbook [1], Figure 2-18. The solid lines are data from this work.

## 8.6. Enthalpy Diagram Results

The enthalpy diagram plots are shown in Figures 46 to 50. Equations for these enthalpy curves are in Appendix B.

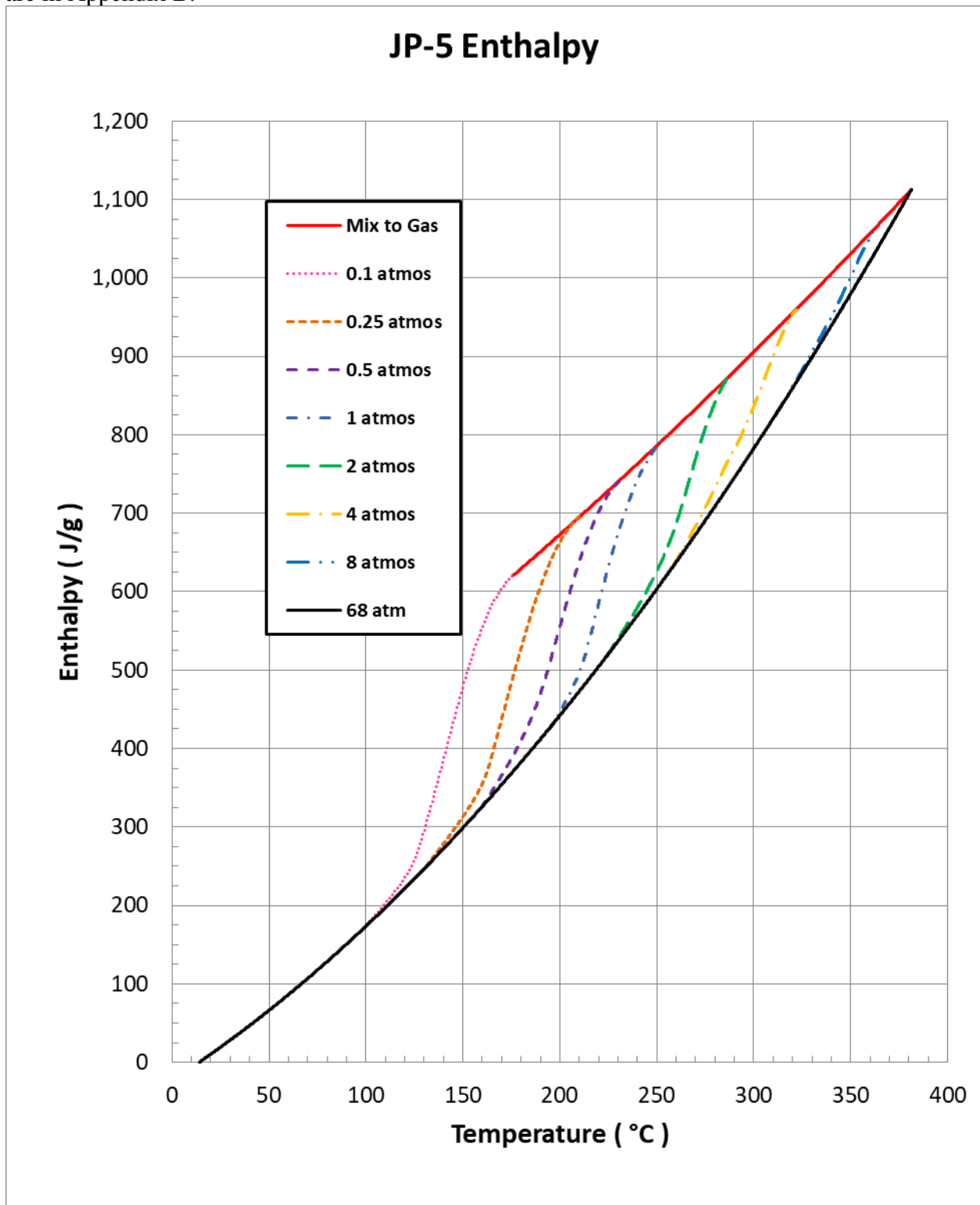


Figure 46: Enthalpy diagram for jet fuel JP-5 (WPAFB, OH, USA).

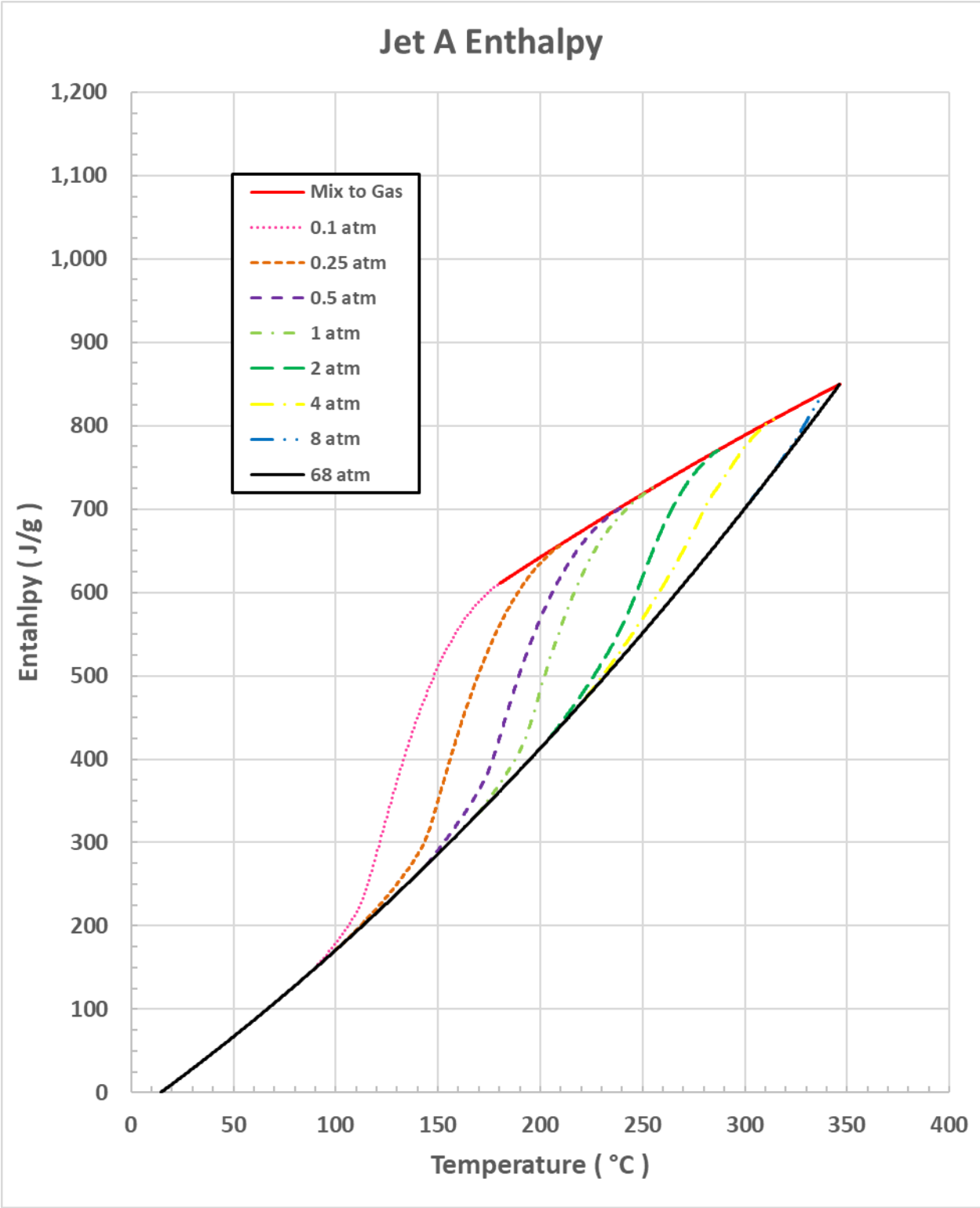


Figure 47: Enthalpy diagram for jet fuel Jet A (WPAFB, OH, USA).

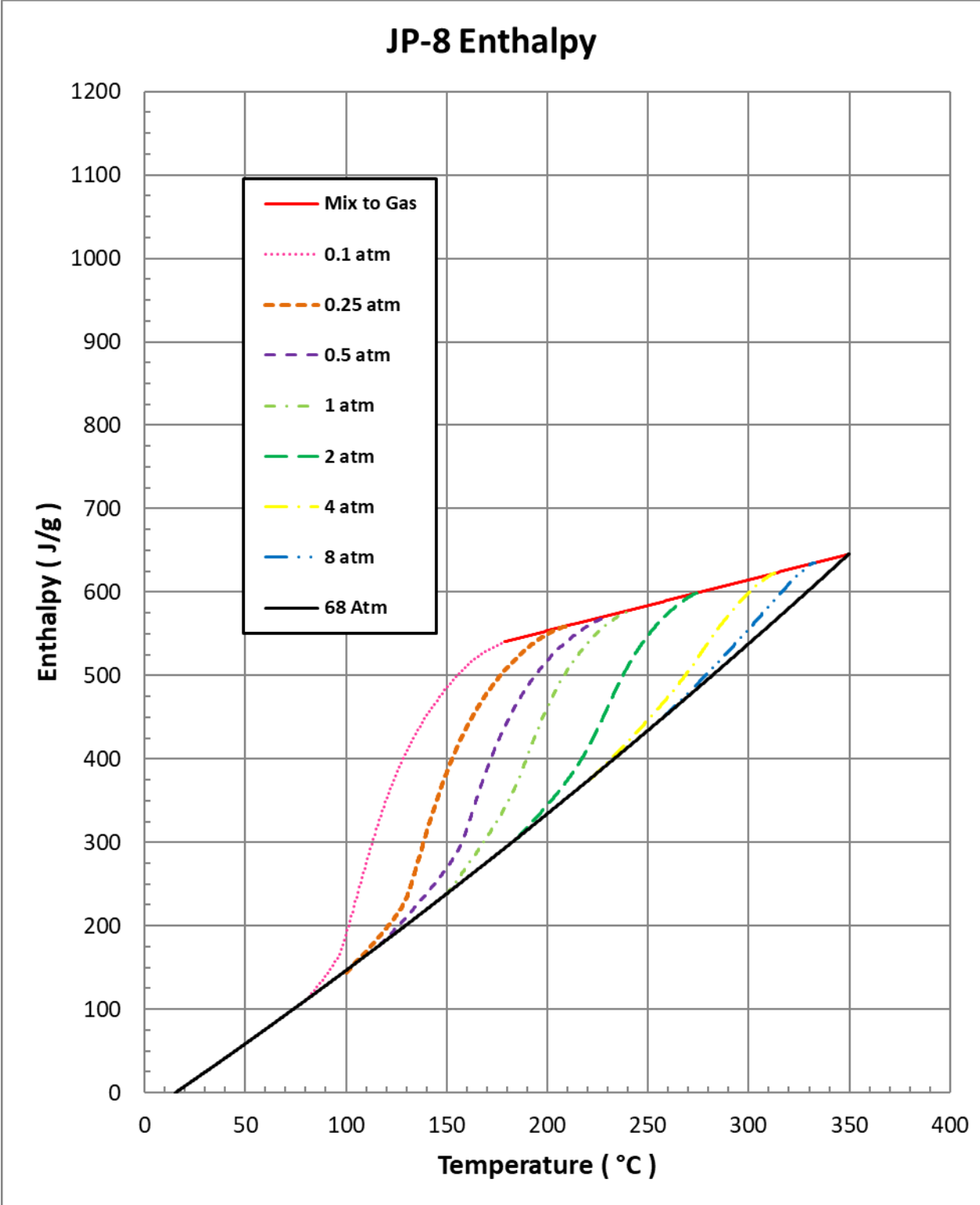


Figure 48: Enthalpy diagram for jet fuel JP-8 (WPAFB, OH, USA).

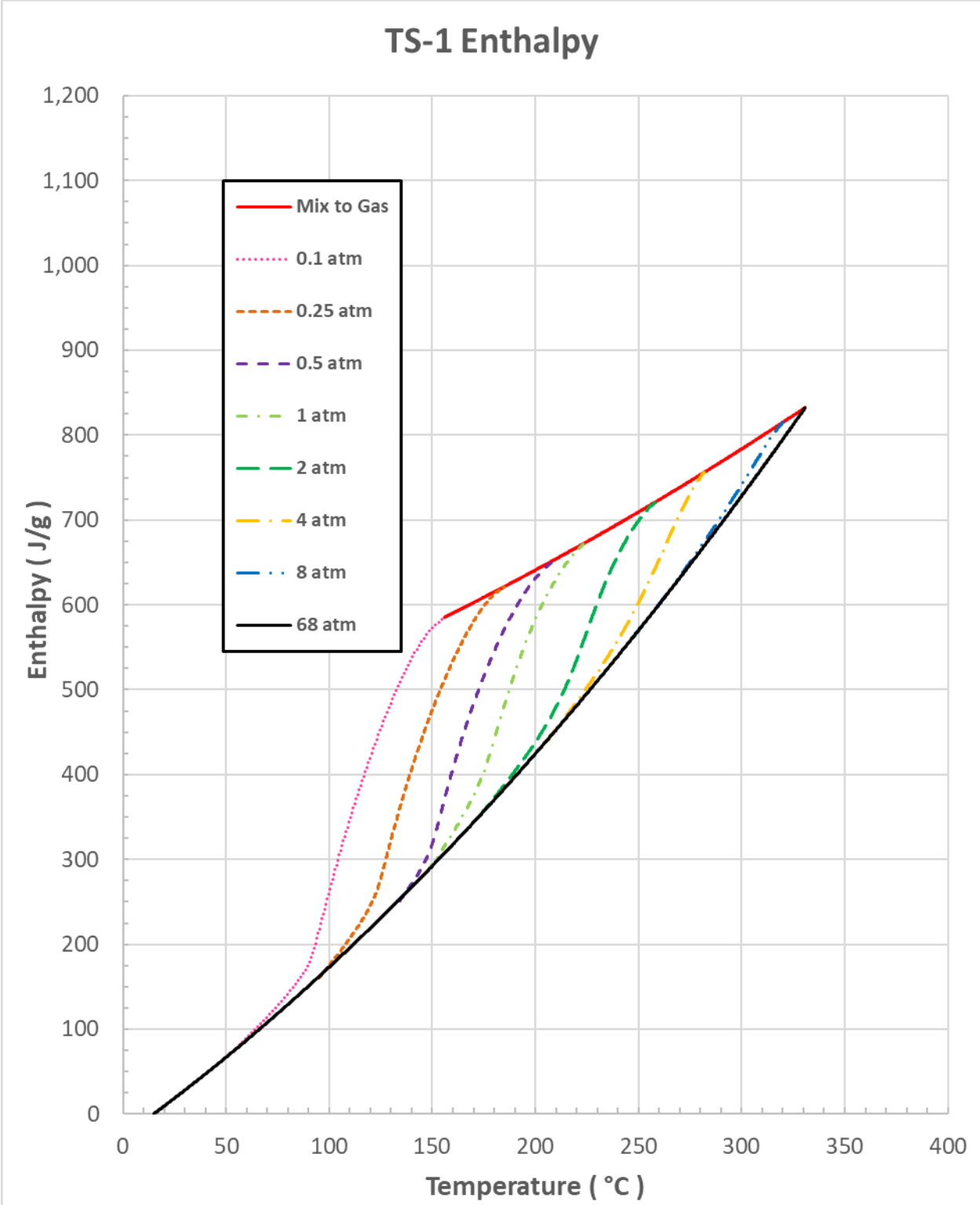


Figure 49: Enthalpy diagram for jet fuel TS-1 (GOST, AirBP, Kent, UK).

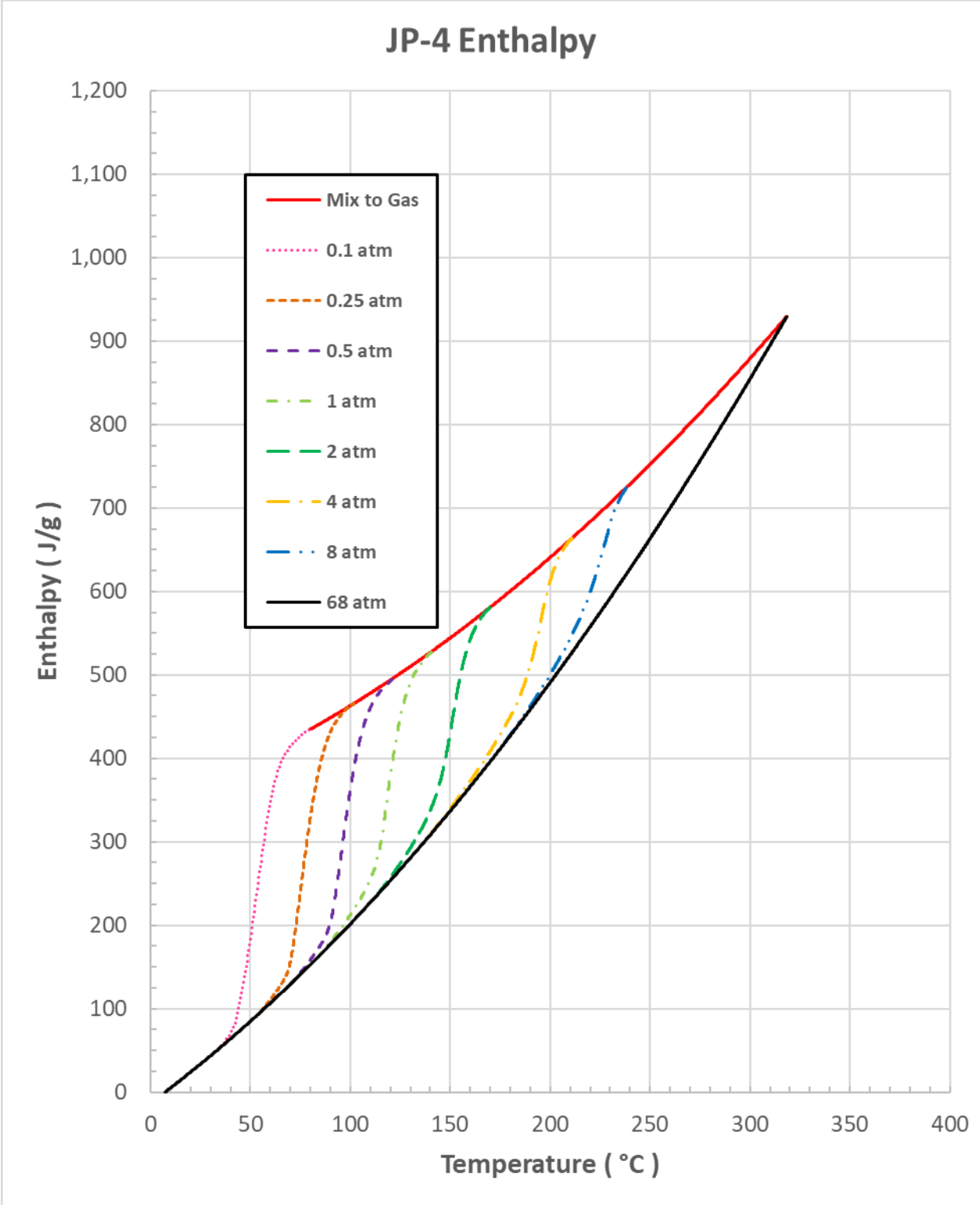


Figure 50: Enthalpy diagram for jet fuel JP-4 (Nova Research, VA, USA).

## 8.7. How to use Enthalpy Diagrams

### 8.7.1. Determining the HOV

First, select the enthalpy diagram that is the closest match to your JF. You will need to know the JF storage tank-pressure. In this case, we will assume the pressure is 120 psi. At this pressure, one will be using the 120 psi curve (blue dash-dot-dot line) in Figure 51. The starting temperature should be the temperature of the JF in the fuel tank. By example, the starting temperature will be 25 °C, red circle on Figure 51. The enthalpy at this starting point is 20 J/g.

When one assumes that the temperature at the nozzle is 350 °C. From Figure 52, one sees that the enthalpy at 350 °C is 815 J/g. So the total heat required to heat the Jet A from 25 to 350 °C is 795 J/g. Next one would like to calculate the wattage needed to heat the Jet A under actual conditions. We assume that the JF delivery rate is 10 g/s. The wattage is calculated from the following equation.

$$795 \text{ J/g} \times 10 \text{ g/s} = 7,950 \text{ J/s} = 7,950 \text{ Watts}$$

Of course, this is just one example. The flow rate needs to be correct for each engine and each throttle setting. Units can be converted to meet the end use requirements. If there is too much heating (wattage), the JF will start to evaporate before it gets to the nozzle. The excess temperature can cause the JF to decompose in the fuel line and leave deposits, which will reduce the fuel line inside diameter. Then if there is not enough heating, the JF will enter the combustion chamber as a liquid. This may slightly reduce the engine efficiency since the residual HOV will take away from the heat of combustion and reduce the amount of expansion work done during combustion.

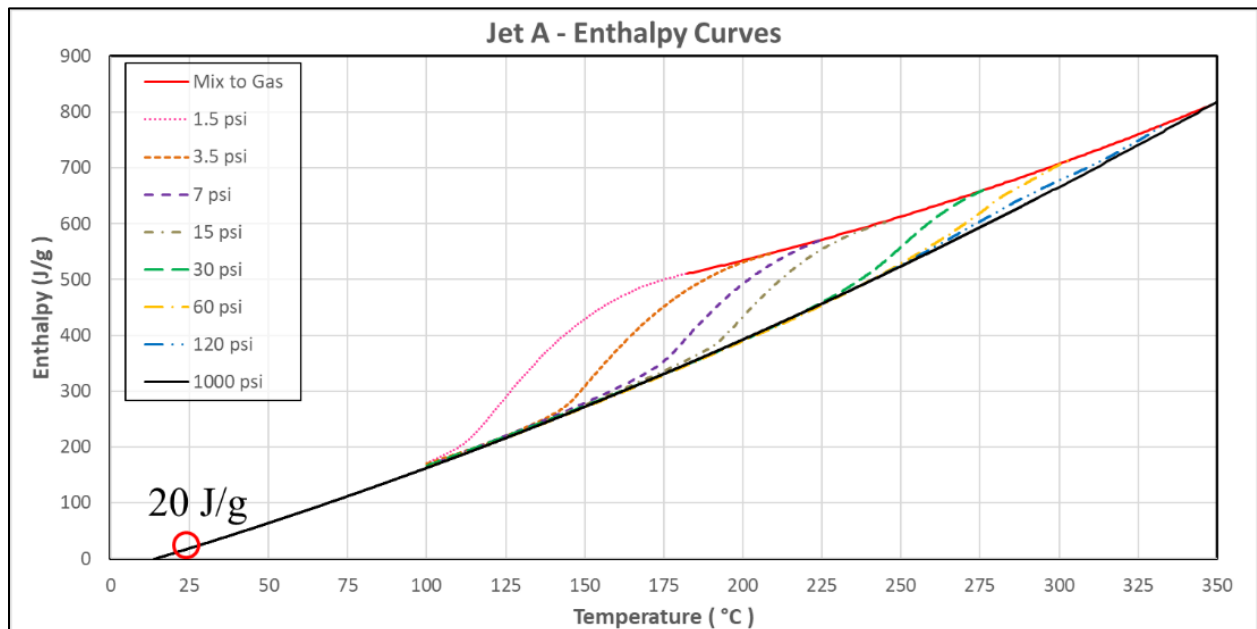


Figure 51: Jet A enthalpy at 25 °C is 20 J/g.

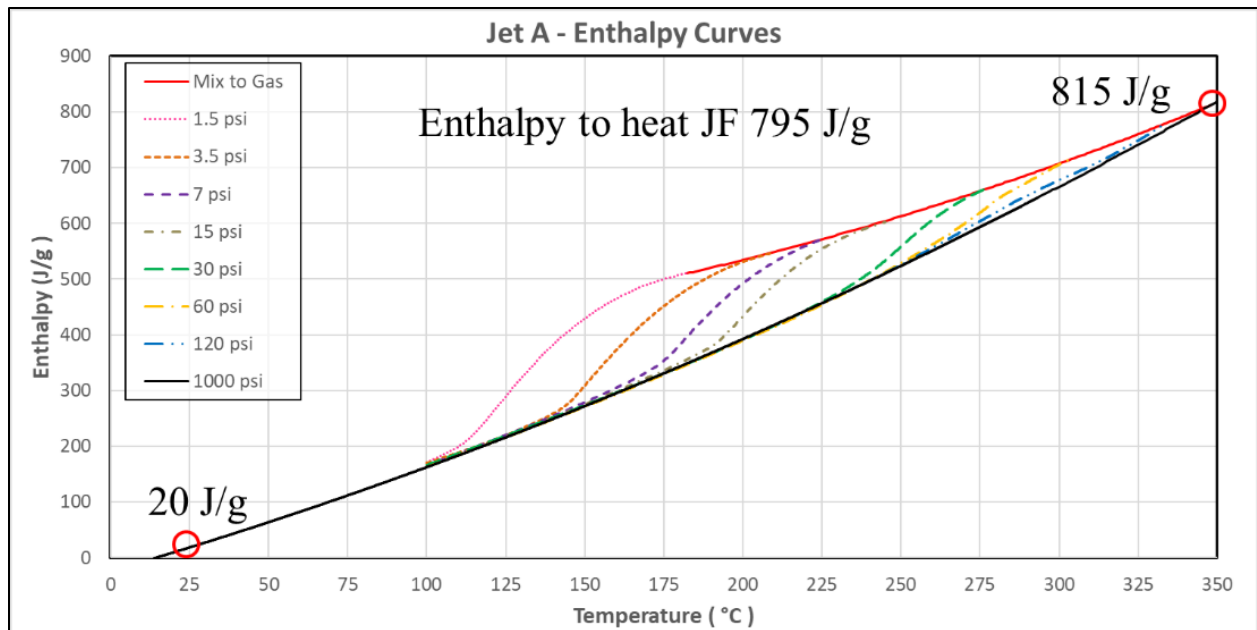


Figure 52: Jet A enthalpy at 350 °C is 815 J/g.

### 8.7.2. Optimal JF Pressure and Nozzle Temperature

Again, one must select the enthalpy diagram that is the closest match to your JF. The starting temperature should be the temperature of the JF in the fuel tank. By example, the starting temperature will be 25 °C, red circle on Figure 53. The enthalpy at this starting point is 20 J/g. You will need to know the JF delivery pressure. In this case, we will assume the pressure is 30 psi. At this pressure, one will be using the 30 psi curve (green dashed line) in Figure 54. Now one finds the intersection of the 30 psi curve (green dashed line) with the ‘Mix to Gas’ curve (red solid line) in Figure 55. The temperature at this intersection is 275 °C and the enthalpy is 657 J/g. So the total heat required to heat the Jet A from 25 to 275 °C is 637 J/g.

If the nozzle temperature is greater than 275 °C then JF will convert to vapor before it comes out of the nozzle. If the nozzle temperature is below/or equal to 275 °C, only liquid JF will be coming out of the nozzle and into the combustion chamber. In the design of jet fuel systems, it is better if the nozzle temperature is below 275 °C at all throttle positions. This ensures that the JF is always a liquid when it goes through the nozzle and the atomization of the JF will be consistent through all throttle positions.

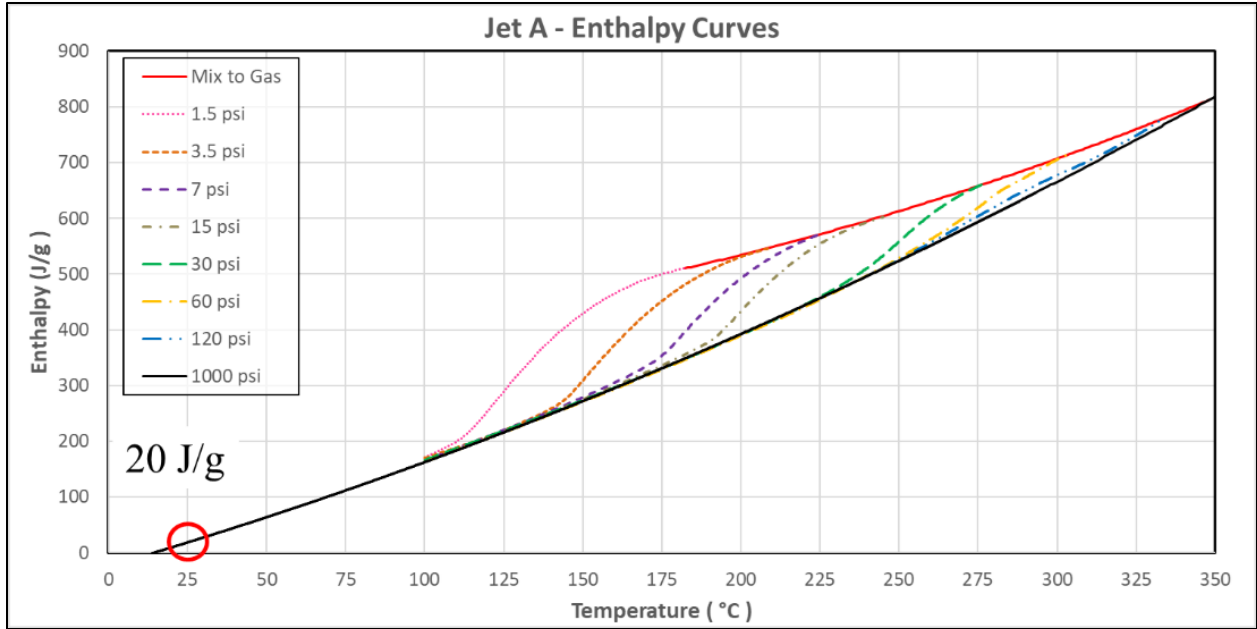


Figure 53: Jet A enthalpy at 25 °C is 20 J/g.

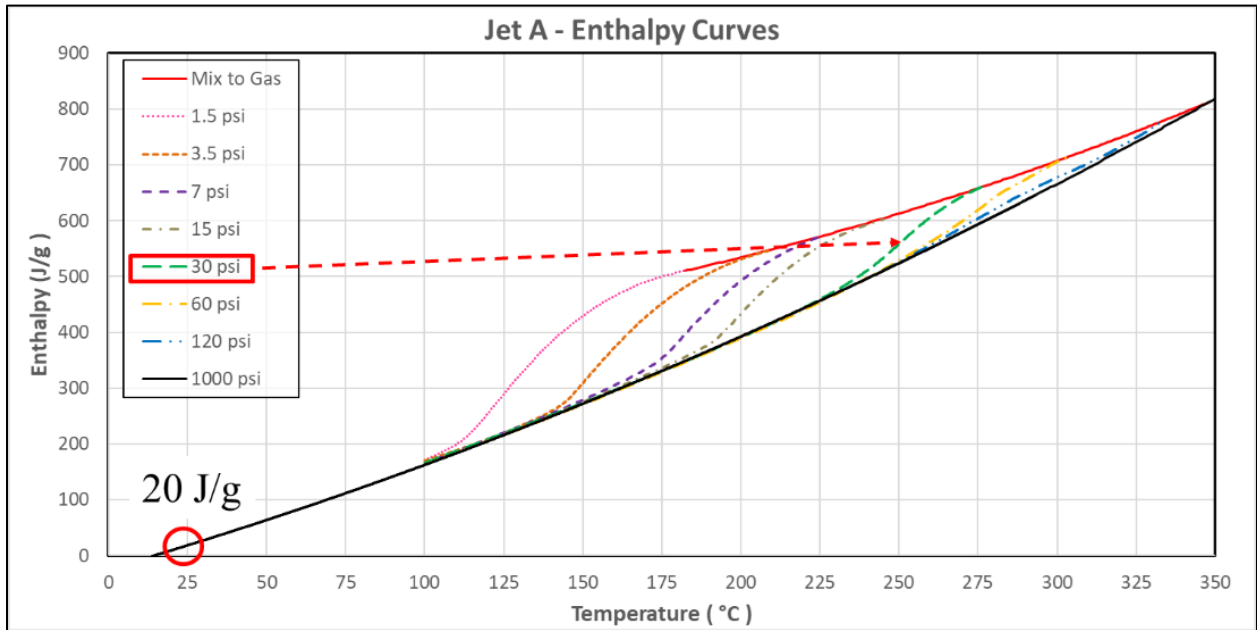


Figure 54: Enthalpy curve for Jet A. The 30 psi isobaric line is the green dashed line.

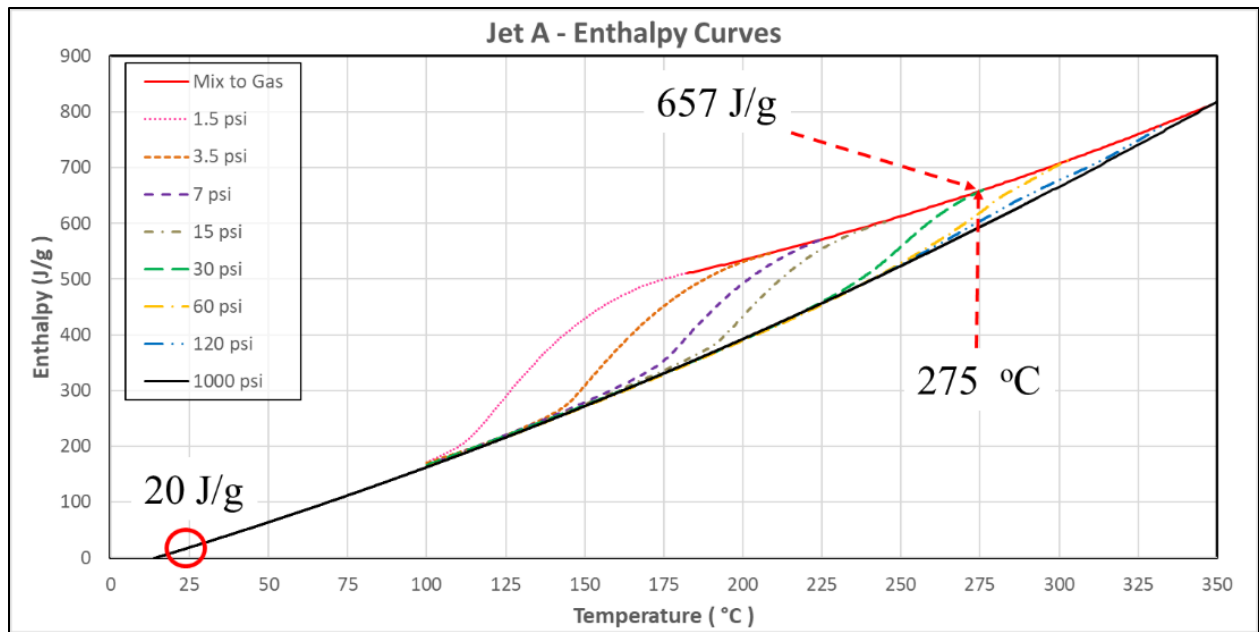


Figure 55: Enthalpy curve for Jet A. The Jet A is finished evaporating at 275 °C under 30 psi of pressure. The enthalpy at this point is 657 J/g.

## 9. Concluding Remarks

### 9.1. Heat of Vaporization (HOV)

Premature sample evaporation is a concern for this test. The correct HOV is dependent on the sample mass that is weighed before the experiment is the same as the sample mass at the beginning of the experiment. This error was minimized by weighing the sample after the crucible was sealed. Additionally, the crucible was sealed as soon as possible after the aliquot of sample was added to the crucible. Jet fuel is a petroleum distillate. As such the liquid evaporates over a range of temperatures. Some jet fuels evaporate as two separate endothermic peaks: JP-4 and JF#12 from WPAFB. The HOV is the total heat of vaporization over the entire evaporation process. The largest source of uncertainty is determining the baseline at the onset of vaporization. The best measure of standard deviation is from the multiple Jet A-1 samples which gave an average HOV of 308 J/g with +/- 9.6 J/g standard deviation, or about 3% error.

### 9.2. HOV Quasi-Isothermal

This test was the best way to measure the HOV versus temperature. The instrumental setup allows the JF to experience a constant ramp down in pressure. This gave very smooth heatflow curves from the HPDSC as the JF vaporized. The critical temperature,  $T_c$ , was also determined by extrapolating the temperature to zero HOV, the definition of the critical temperature. The critical temperatures are summarized in the Table 11, shown below. In all five of these jet fuels, the critical pressure,  $P_c$ , is equal or greater than 1000 psi. These jet fuels behave as a supercritical fluid when they are equal or greater than the  $T_c$  and equal or greater than the  $P_c$ .

**Table 11: Critical Temperature of Selected Jet Fuels**

Jet Fuel	Critical Temperature ( °C )
JP-4	320.2
TS-1	327.6
Jet A	346.5
JP-8	349.2
JP-5	379.2

### 9.3. Enthalpy Diagram

Premature sample evaporation is also a concern for energy diagrams, for the same reason as mentioned in section 9.1. In addition, care must be taken to be sure the sample does not evaporated during the pressurization (or evacuation) of the HPDSC cell prior to the test. A blank test must be run using the exact same reference and sample crucibles. The high pressure curve, 68 atm in these tests, is the standard curve where no sample evaporates. The data from all the other pressure curves must match the 68 atm curve at temperatures below the start of evaporation. High vapor pressure samples, such as JP-4, must be started at a low temperature, 15 °C in this case. This prevents early evaporation. The “mixture to vapor” line is a best fit third order polynomial fit to the HOV, as measured in quasi-isothermal HPDSC tests. The HPDSC provided high quality data for the construction of the Enthalpy Diagrams.

## 10. References

1. CRC Aviation Fuel Properties Handbook, 2014 Fourth Edition, CRC Report No. 663.
2. Clausius, R. (1850). "Ueber die bewegende Kraft der Wärme und die Gesetze, welche sich daraus für die Wärmelehre selbst ableiten lassen" [On the motive power of heat and the laws which can be deduced there from regarding the theory of heat]. *Annalen der Physik* (in German) **155**: 500–524 (1850).
3. Clapeyron, M. C. (1834). "Mémoire sur la puissance motrice de la chaleur". *Journal de l'École polytechnique* (in French) **23**: 153–190 (1834).
4. ASTM E2071, "Standard Practice for Calculating Heat of Vaporization or Sublimation from Vapor Pressure Data", 2000.
5. ASTM E1782, "Standard Test Method for Determining Vapor Pressure by Thermal Analysis".
6. Seyler, R.J., "Parameters affecting the determination of vapor pressure by differential thermal methods," *Thermochimica Acta.*, Vol 11, 1976, pp. 129-136.
7. Brozena, A., "Vapor Pressure of 1-octanol below 5 kPa using DSC," *Thermochimica Acta*, Vol 561, 2013, pp. 72—76.
8. Chappelow, C.C., "Density of Liquid n-Octane", *J. Chem. Eng.*, Vol 16, No. 4, 1971, pp 440-442.

# Appendices

## Appendix A: Enthalpy of Liquid Volumetric Change

The enthalpy due to the change of the liquid density as a function of temperature is caused by the work that the air pressure exerts against the liquid as the liquid density changes. The question to be answered is, "Is the enthalpy due to the liquid density change versus temperature and pressure significant enough that it needs to be considered?" The pure liquid n-Octane was selected as a model for this enthalpy. The density of n-octane was taken from Chappelow, et. al. [8].

**Table A1: Density of n-Octane and Enthalpy of JP-4**

Temperature ( °C )	n-Octane Density [8] ( g/mL )	JP-4 Enthalpy at 68 atm ( J/g )
26.103	0.69788	23.148
122.575	0.614554	210.3309
Delta Values	-0.08333	187.1829

The JP-4 was selected for this calculation because it has the lowest delta enthalpy of all the jet fuels. This makes it the worst case jet fuel with a delta enthalpy of 187.1829 J/g. It was also assumed that the jet fuel sample mass was 10 mg. This mass is larger than all the jet fuel samples tested. Again, this is a worst case scenario. The delta volume for a 10 mg sample is calculated in the equation below.

$$Vol = \left( \frac{mass}{\Delta density} \right) = \left( \frac{10 \text{ mg}}{-0.08333 \text{ g/mL}} \right) = -120 \mu\text{L} = -120 \text{ mm}^3 = -120 \times 10^{-9} \text{ m}^3$$

Volume change against a constant pressure work is in the units of energy, Joules, as shown below.

$$P \times V = \left( \frac{force}{area} \right) \times volume = \frac{N}{m^2} \times m^3 = N \cdot m = \text{Joules}$$

The largest work is done with the highest pressure. So 68 atms was selected for this calculation. The pressure is converted to Pascals, shown below.

$$68 \text{ atmos} = 68.901 \times 10^5 \text{ Pa}$$

The pressure times the delta volume gives the enthalpy, in Joules, for the decreasing volume of 10 mg of n-Octane over about a 100 °C range.

$$work = (68.901 \times 10^5 \text{ Pa}) \times (120 \times 10^{-9} \text{ m}^3) = 0.8268 \text{ Joules for 10 mg}$$

$$error = \left( \frac{0.8268}{187.18} \right) \times 100 = 0.44\% \text{ error}$$

This error is too small to be significant to the enthalpy diagrams generated in this work, and was ignored.

## Appendix B: Jet Fuel Enthalpy Equations

The equations for all the curves in the Enthalpy Diagrams are given below. Some of the lines are best fit to a 2<sup>nd</sup> order equation, but most are best fit to a 6<sup>th</sup> order equation shown here.

$$y = A * x^6 + B * x^5 + C * x^4 + D * x^3 + E * x^2 + F * x + G$$

Where:

X = temperature (°C)

Y = enthalpy (J/g)

**Table B1: Jet A Enthalpy Curve Equations**

Coefficients	A*X <sup>6</sup>	B*X <sup>5</sup>	C*X <sup>4</sup>	D*X <sup>3</sup>	E*X <sup>2</sup>	F *X	G	Temperature ( °C )	
								Start	End
Line									
Mix to Gas					-1.003811E-03	1.966122E+00	2.890430E+02	180.0	346.4
0.1 atm	-1.876693E-08	1.556853E-05	-5.310071E-03	9.513997E-01	-9.428265E+01	4.899176E+03	-1.042235E+05	90.0	180.0
0.25 atm	9.952192E-10	-5.903398E-07	8.839911E-05	1.092190E-02	-4.424364E+00	4.445478E+02	-1.490168E+04	100.0	211.0
0.5 atm	-1.132994E-08	1.351371E-05	-6.666677E-03	1.739981E+00	-2.532498E+02	1.948565E+04	-6.190075E+05	145.0	240.0
1 atm	-2.177274E-08	2.817081E-05	-1.510923E-02	4.298470E+00	-6.839452E+02	5.770205E+04	-2.016309E+06	170.0	256.0
2 atm	1.067156E-08	-1.534743E-05	9.153187E-03	-2.898051E+00	5.138549E+02	-4.838525E+04	1.890772E+06	205.0	287.0
4 atm	1.833616E-09	-2.866600E-06	1.855796E-03	-6.369606E-01	1.222856E+02	-1.245170E+04	5.257067E+05	222.0	314.0
8 atm					2.401582E-02	-1.173219E+01	2.060761E+03	303.0	338.0
68 atm					2.280039E-03	1.736222E+00	-2.542010E+01	14.4	346.4

**Table B2: JP-5 Enthalpy Curve Equations**

Coefficients	A*X <sup>6</sup>	B*X <sup>5</sup>	C*X <sup>4</sup>	D*X <sup>3</sup>	E*X <sup>2</sup>	F *X	G	Temperature ( °C )	
								Start	End
Line									
Mix to Gas					1.221325E-03	1.715016E+00	2.809821E+02	176.0	381.0
0.1 atm	-3.819284E-09	4.352679E-06	-1.926441E-03	4.311183E-01	-5.192467E+01	3.215110E+03	-8.027385E+04	99.0	176.0
0.25 atm	1.598759E-08	-1.534416E-05	6.049858E-03	-1.253786E+00	1.440317E+02	-8.692702E+03	2.153804E+05	128.0	210.0
0.5 atm	2.001654E-08	-2.242488E-05	1.037796E-02	-2.539302E+00	3.464797E+02	-2.499446E+04	7.448338E+05	160.0	231.0
1 atm	-1.174028E-07	1.604400E-04	-9.117482E-02	2.757529E+01	-4.680803E+03	4.227789E+05	-1.587278E+07	195.0	252.0
2 atm	5.348816E-08	-8.264087E-05	5.306341E-02	-1.812546E+01	3.473980E+03	-3.542524E+05	1.501664E+07	224.0	287.0
4 atm	-1.278040E-08	2.103060E-05	-1.437387E-02	5.222209E+00	-1.063491E+03	1.150811E+05	-5.168044E+06	258.0	322.0
8 atm					1.507716E-02	-5.441220E+00	1.058318E+03	311.0	362.0
68 atm					3.592181E-03	1.607851E+00	-2.303045E+01	14.0	381.0

**Table B3: JP-8 Enthalpy Curve Equations**

Coefficients	A*X <sup>6</sup>	B*X <sup>5</sup>	C*X <sup>4</sup>	D*X <sup>3</sup>	E*X <sup>2</sup>	F *X	G	Temperature ( °C )	
								Start	End
Line									
Mix to Gas					3.903300E-06	6.111130E-01	4.311041E+02	150.0	350.0
0.1 atm		-3.194423E-07	2.279597E-04	-6.420548E-02	8.862823E+00	-5.910334E+02	1.527381E+04	87.0	179.0
0.25 atm	-9.677213E-09	9.149585E-06	-3.552437E-03	7.238747E-01	-8.154080E+01	4.814692E+03	-1.163786E+05	104.0	201.0
0.5 atm	-4.202801E-09	4.628419E-06	-2.095827E-03	4.987069E-01	-6.568495E+01	4.540226E+03	-1.285746E+05	119.0	231.0
1 atm	-5.773134E-09	7.195068E-06	-3.704336E-03	1.007801E+00	-1.527405E+02	1.222791E+04	-4.039194E+05	152.0	242.0
2 atm	4.949408E-10	-3.063749E-07	-4.363201E-05	8.022504E-02	-2.500552E+01	3.274695E+03	-1.599993E+05	185.0	274.0
4 atm	2.681084E-09	-4.277935E-06	2.830964E-03	-9.946994E-01	1.957574E+02	-2.046123E+04	8.877541E+05	221.0	313.0
8 atm				-1.488641E-04	1.330275E-01	-3.692636E+01	3.681049E+03	258.0	333.0
68 atm					8.012991E-04	1.637700E+00	-2.526129E+01	15.0	350.0

**Table B4: TS-1 Enthalpy Curve Equations**

Coefficients Line	A*X <sup>6</sup>	B*X <sup>5</sup>	C*X <sup>4</sup>	D*X <sup>3</sup>	E*X <sup>2</sup>	F *X	G	Temperature ( °C )	
								Start	End
Mix to Gas					1.168861E-03	8.433773E-01	4.255899E+02	156.0	330.0
0.1 atm	-6.168142E-09	4.378708E-06	-1.263274E-03	1.881163E-01	-1.512445E+01	6.233344E+02	-1.023674E+04	75.0	156.0
0.25 atm	-1.942815E-08	1.679645E-05	-5.983948E-03	1.122757E+00	-1.168418E+02	6.392155E+03	-1.435178E+05	97.0	185.0
0.5 atm	-2.627817E-08	2.659309E-05	-1.112392E-02	2.459847E+00	-3.030320E+02	1.970932E+04	-5.284426E+05	133.0	209.0
1 atm	-1.754187E-08	2.062955E-05	-1.004667E-02	2.592100E+00	-3.735149E+02	2.849699E+04	-8.991231E+05	144.0	224.0
2 atm	1.365022E-08	-1.746226E-05	9.253474E-03	-2.600266E+00	4.087478E+02	-3.408513E+04	1.178427E+06	173.0	258.0
4 atm		-2.654881E-07	3.103240E-04	-1.445699E-01	3.357528E+01	-3.885931E+03	1.795983E+05	205.0	282.0
8 atm				-7.268141E-05	6.889589E-02	-1.792889E+01	1.882213E+03	247.0	320.0
68 atm					2.603396E-03	1.734519E+00	-2.627016E+01	15.0	330.0

**Table B5: JP4 Enthalpy Curve Equations**

Coefficients Line	A*X <sup>6</sup>	B*X <sup>5</sup>	C*X <sup>4</sup>	D*X <sup>3</sup>	E*X <sup>2</sup>	F *X	G	Temperature ( °C )	
								Start	End
Mix to Gas					3.034821E-03	8.666529E-01	3.460561E+02	80.0	319.0
0.1 atm	-1.016809E-06	3.650146E-04	-5.330811E-02	4.038423E+00	-1.668128E+02	3.564188E+03	-3.080007E+04	34.0	80.0
0.25 atm	-9.924691E-07	4.997876E-04	-1.035329E-01	1.127935E+01	-6.808981E+02	2.158774E+04	-2.808015E+05	63.0	102.0
0.5 atm	4.097645E-07	-2.121783E-04	4.471815E-02	-4.895570E+00	2.925398E+02	-8.994741E+03	1.102043E+05	71.0	119.0
1 atm	5.604652E-07	-3.768212E-04	1.046549E-01	-1.536943E+01	1.259054E+03	-5.456258E+04	9.776176E+05	84.0	143.0
2 atm	4.122329E-07	-3.533489E-04	1.255209E-01	-2.365440E+01	2.494375E+03	-1.395701E+05	3.237979E+06	114.0	172.0
4 atm	-1.459591E-08	1.325679E-05	-4.907608E-03	9.432850E-01	-9.850356E+01	5.229580E+03	-1.073092E+05	140.0	206.0
8 atm	-5.527939E-08	6.678765E-05	-3.354899E-02	8.969495E+00	-1.346231E+03	1.075601E+05	-3.574006E+06	177.0	240.0
68 atm					3.724737E-03	1.774588E+00	-1.308158E+01	7.0	319.0

## Appendix C: Instrumental Details

### C.1. HPDSC and Sample Preparation Details

Figures C1 through C17 show pictures for the 'step by step' process for preparing the jet fuel sample to be run in the HPDSC.



Figure C1: DSC pan resting on the crimping press lower die.

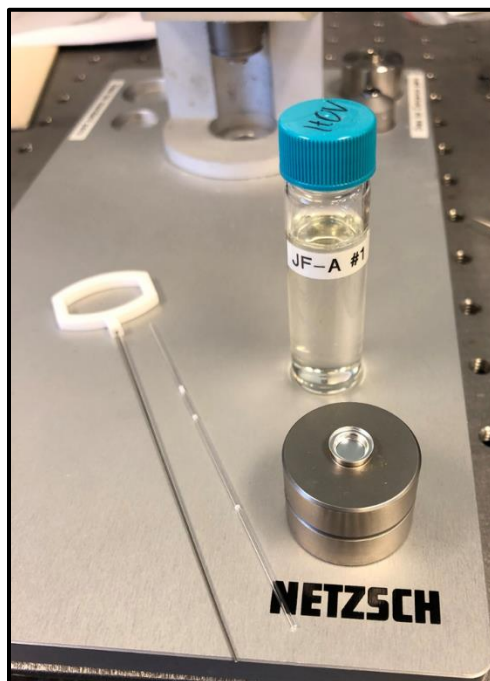


Figure C2: Micropipette and JF sample.

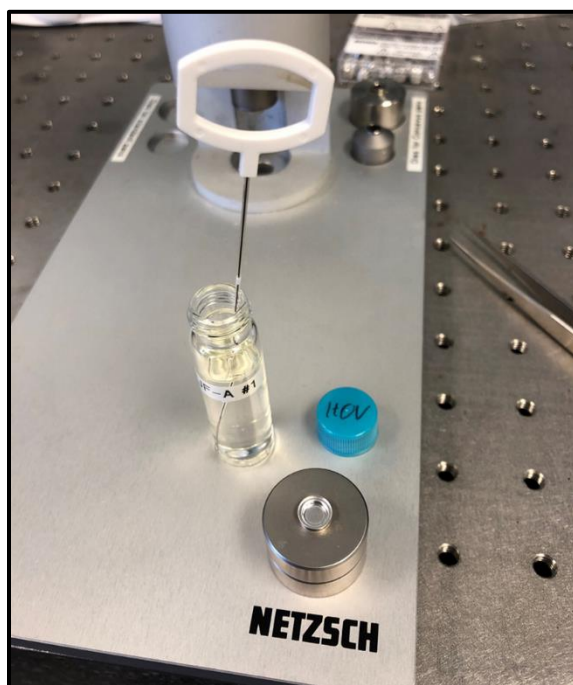


Figure C3: Micropipette in JF sample.

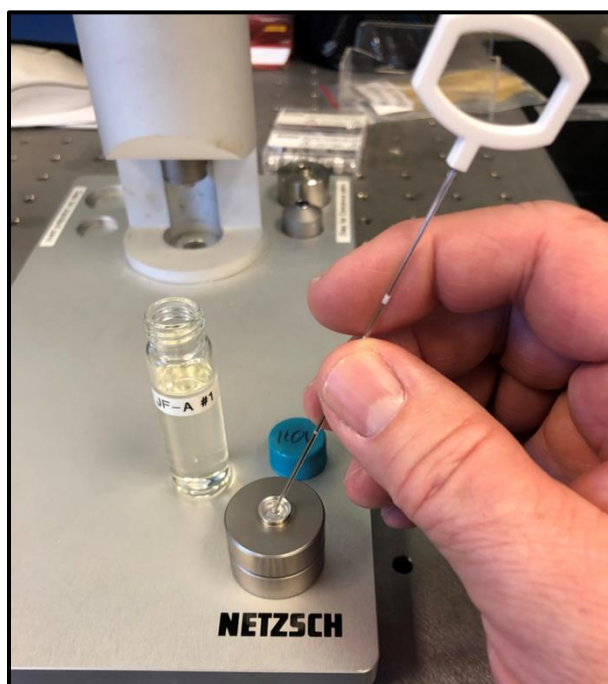


Figure C4: Micropipette depositing JF sample in DSC pan.

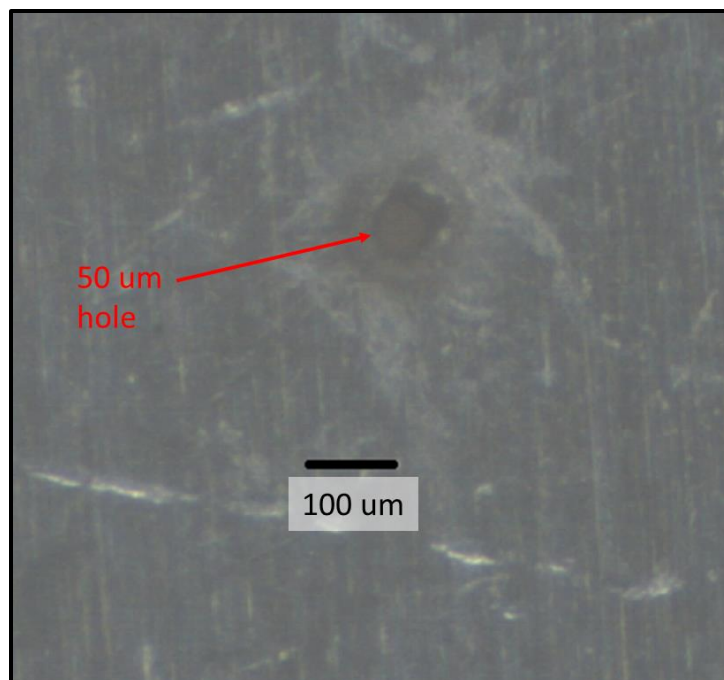


Figure C5: Microscope image of the 50 um laser-drilled hole in the DSC lid.



Figure C6: Laser-drilled lid placed on DSC pan.

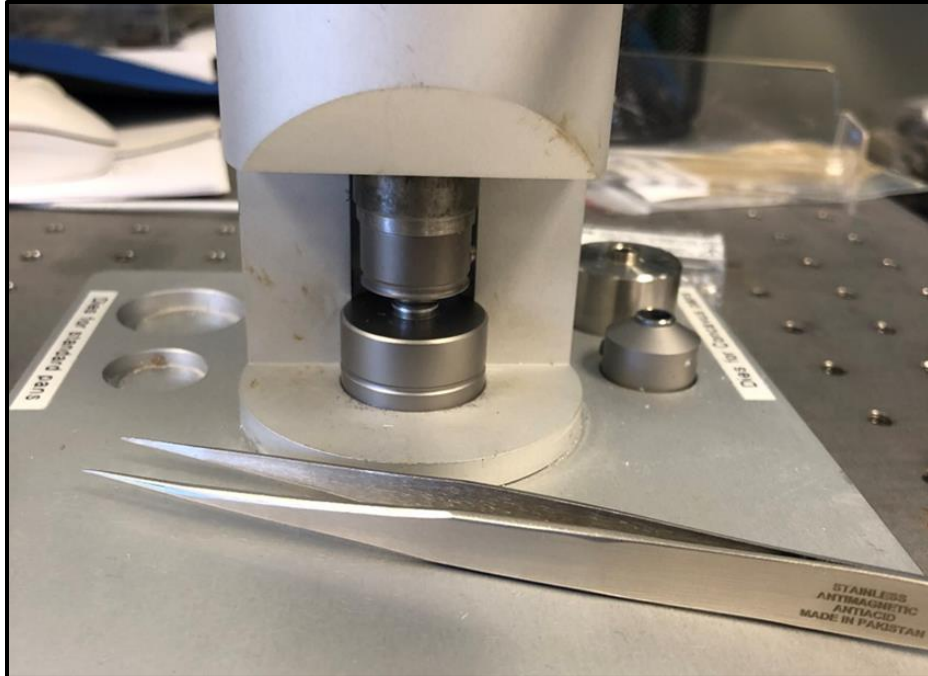


Figure C7: DSC pan/lid being pressed in the crimper. The pressing makes a hermetically sealed cold weld of the aluminum pan and lid. The only escape route for the JF is through the 50  $\mu\text{m}$  orifice.



Figure C8: DSC pan/lid after crimping



Figure C9: Inside of the HPDSC cell, with an empty pan/lid on the reference side of the HPDSC cell.



Figure C10: Inside of the HPDSC cell, with a JF sample on the sample side of the HPDSC cell.



Figure C11: Inside of the HPDSC cell, with the inner silver lid installed.



Figure C12: Inside of the HPDSC cell, with the outer silver lid installed.



Figure C13: The HPDSC cell, with the water-cooled SS lid.



Figure C14: The HPDSC cell, with the SS lid installed and retaining nuts tightened.

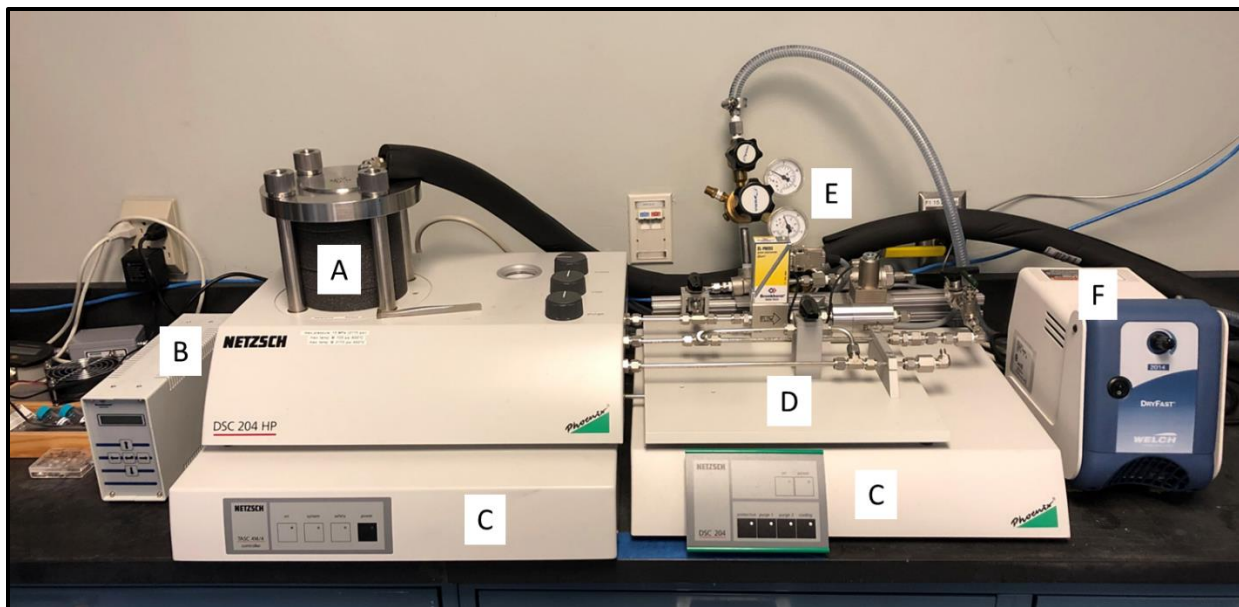


Figure C15: The complete HPDSC instrument setup. Parts included are A) the HPDSC cell, B) the pressure signal amplifier, C) the HPDSC electronics, D) the HP gas distribution connections, E) the QI regulator, F) the vacuum pump.

### C.2. QI HPDSC Setup

The HPDSC was setup differently so that the pressure inside the HPDSC was decreased linearly versus time. This is shown in Figure C16 and C17. The regulator was set so the high-pressure inlet faces the HPDSC and the low pressure outlet faces the vacuum pump. A 10  $\mu\text{m}$  orifice (E) was placed between the regulator (C) and vacuum pump (D) so that the pressure decrease rate is not too fast. The regulator is needed so that the rate of pressure change in the HPDSC is constant. The outlet pressure of the regulator controls the rate of pressure change. An outlet pressure of 5 psi gave a pressure change of about 1.75 atm/min, see figure C18. The vacuum pump is needed to get HOV data for low-temperature tests.

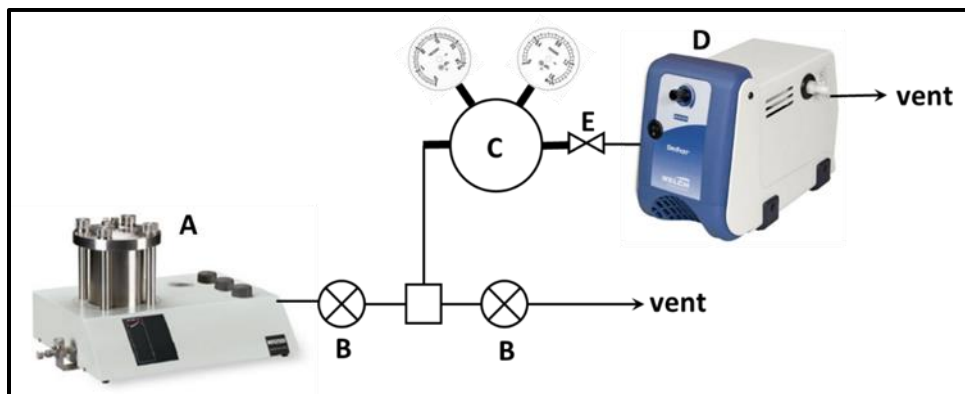


Figure C16: HOV QI HPDSC setup, where A is the HPDSC, B is a valve, C is a regulator set to 5 psi output, E is a 10  $\mu\text{m}$  orifice and D is the vacuum pump.

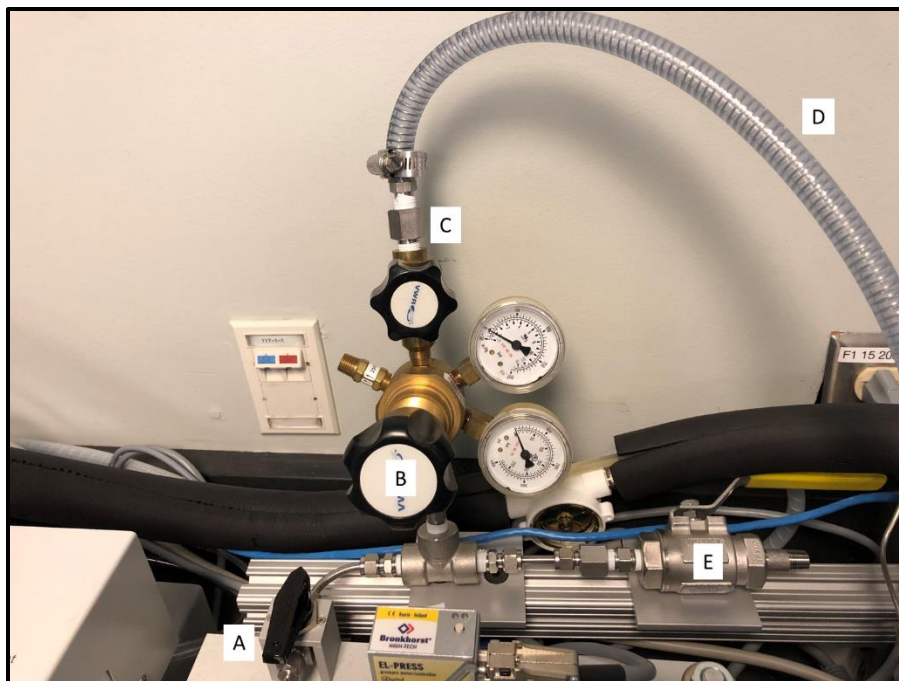


Figure C17: The QI DSC instrument setup. Parts included are A) outlet valve from the HPDSC cell, B) the QI regulator, C) the 10 μm diameter orifice, D) tubing to the vacuum pump, E) exhaust valve.

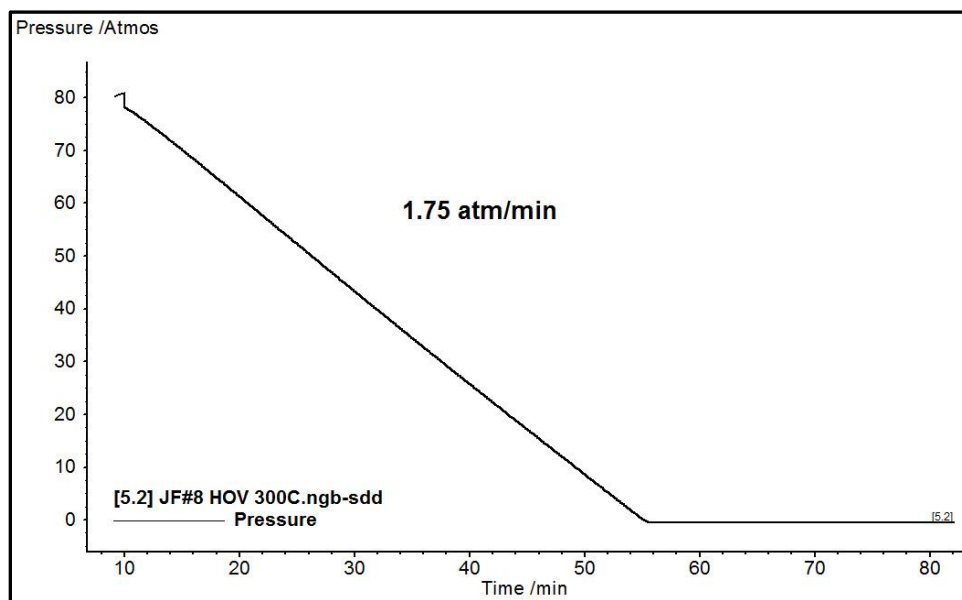


Figure C18: Typical pressure versus time for a HOV QI HPDSC experiment.